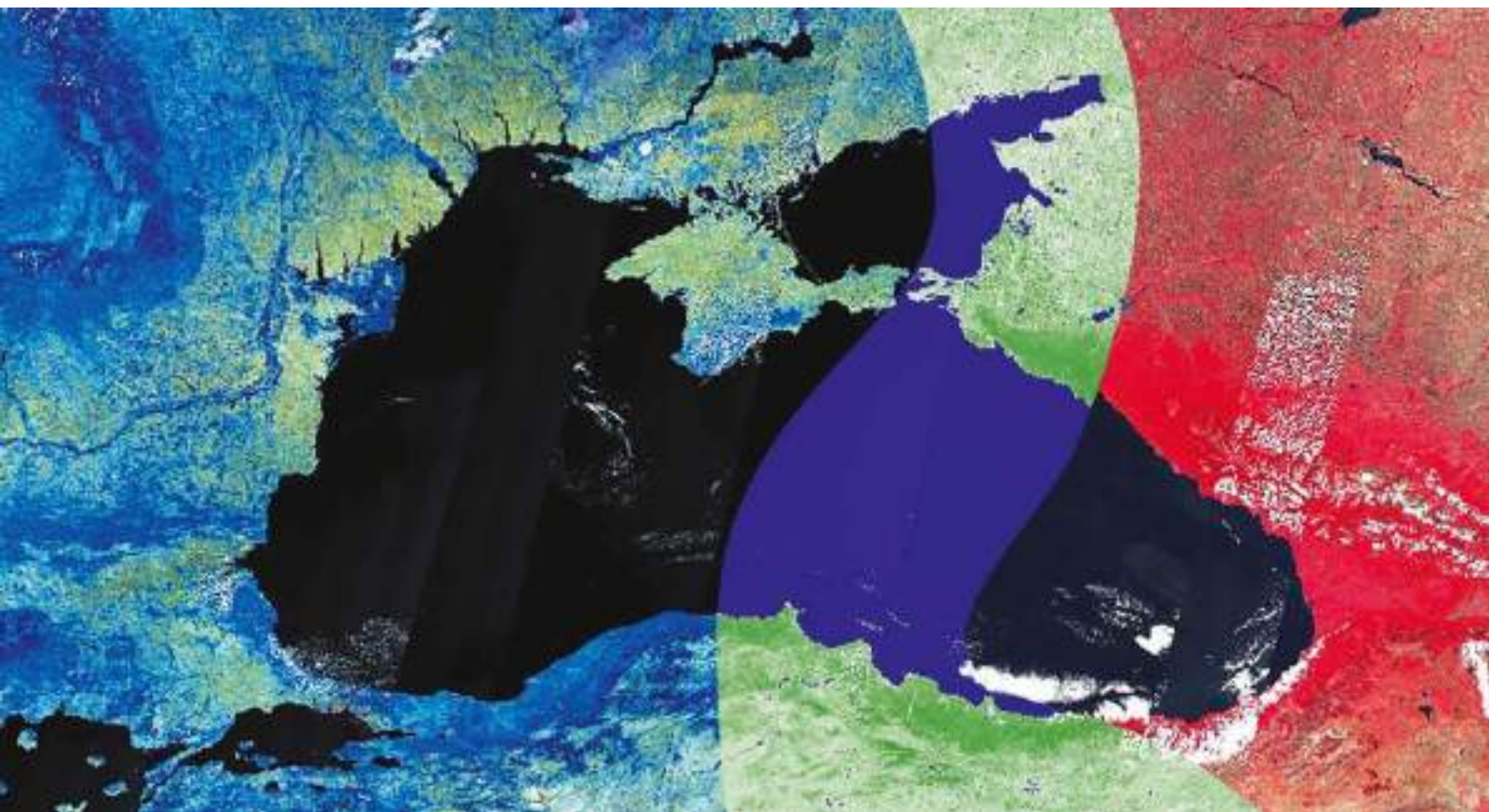




## Copernicus assisted environmental monitoring across the Black Sea Basin - PONTOS



# Report on Dynamics of Ukrainian Coastal Line Changes for 1980-2020

Deliverable D.T1.2.1

PONTOS - UA-1 (Ukraine)

Ukrainian coastal zone from Danube Delta to the Great  
Adzhalyk Estuary (Odessa bay)

Authors: Medinets V.I., Cherkez E.A., Pavlik T.V., Gazyetov Ye.I., Shatalin S.N.,  
Konareva O.P., Soltys I.E., Medinets S.V.



The Dniester water resources near the city Bendery at the catchment area of 66100 km<sup>2</sup> make (Main indicators..., 2000; Main indicators ..., 2003): norm – 10.7 km<sup>3</sup>; occurrence 50% - 10.4 km<sup>3</sup>; occurrence 75% - 8.64 km<sup>3</sup>; occurrence 90% - 7.17 km<sup>3</sup>; occurrence 95% - 6.56 km<sup>3</sup>.

According to the data (HYPE database, <https://hypeweb.smhi.se>), average value of the Dniester annual discharge for the period 1981-2010 made 8 km<sup>3</sup>/year with minimum of 3 (1990) and maximum of 14 (1981) km<sup>3</sup>/year (Table XXX.). According to the data of instrumental measurements at hydrological stations in 1950-2010 (IMB data, 2018), average annual Dniester discharge made 9.7 km<sup>3</sup>/year with minimum of 4.9 (1990) and maximum of 19.2 (1980) km<sup>3</sup>/year.

According to the data (Transboundary diagnostic study ..., 2005) for the long-term period, the Dniester River discharge is decreasing (observation since 1881), which is explained, first of all, by climatic changes. The tendency of atmospheric precipitation decrease is observed in the western part of Ukraine, which usually tells upon the flow characteristics. Certain impact on water quantity results from irrevocable water consumption from the river.

However, for the period of 1981-2010, positive linear trend was observed according to the data (IMB data, 2018): + 0.07 km<sup>3</sup>/year and the data (HYPE database, <https://hypeweb.smhi.se>): + 0.08 km<sup>3</sup>/year. According to the data (IMB data, 2018), the linear trend of annual discharge value in 1950-2010 was also positive and made + 0.02 km<sup>3</sup>/year.

According to spectral analysis(Gazyetov & Dyatlov, 2021), inter-annual fluctuations of the Dniester River discharge volume for the period of 1990-2010 contain 7 harmonic constituents with the periods 2.4, 3.6, 5.5, 10.3, 14.4, 24.0 and 36.0 years.

**Table 4.17.** Average annual Dniester River Discharges

Year	River Discharge (m <sup>3</sup> /s)				Total Runoff (10 <sup>6</sup> m <sup>3</sup> /y)
	Average	Minimum	Maximum	Standard deviation	
1981	448.931	176.018	1380.449	0.710	14157.503
1982	322.799	105.697	749.381	0.536	10179.795
1983	139.391	50.622	250.988	0.343	4395.829
1984	217.191	85.691	383.904	0.281	6868.096
1985	265.071	124.809	526.407	0.361	8359.270
1986	194.462	57.694	440.519	0.431	6132.542
1987	157.040	65.763	269.938	0.308	4952.413
1988	325.613	145.282	861.913	0.494	10296.677
1989	214.525	93.215	282.888	0.158	6765.259
1990	106.570	5.701	243.708	0.409	3360.807
1991	214.172	110.799	270.584	0.155	6754.133
1992	182.470	10.091	405.981	0.404	5770.147
1993	267.749	150.501	584.183	0.301	8443.721
1994	156.022	14.847	258.175	0.306	4920.321
1995	207.884	39.822	368.481	0.308	6555.829
1996	289.353	107.095	832.217	0.439	9150.047
1997	227.980	101.007	316.723	0.252	7189.589
1998	283.216	225.853	394.948	0.096	8931.492
1999	348.928	108.451	1481.578	0.829	11003.800
2000	305.723	111.016	996.055	0.618	9667.692
2001	268.907	139.136	444.025	0.190	8480.246

Year	River Discharge (m <sup>3</sup> /s)				Total Runoff (10 <sup>6</sup> m <sup>3</sup> /y)
	Average	Minimum	Maximum	Standard deviation	
2002	235.043	65.643	525.492	0.407	7412.328
2003	217.636	90.546	361.284	0.246	6863.367
2004	259.004	145.318	524.096	0.298	8190.341
2005	311.362	128.040	891.118	0.552	9819.106
2006	330.622	155.816	1052.920	0.583	10426.499
2007	192.067	26.752	343.966	0.373	6057.039
2008	308.946	219.062	503.328	0.199	9769.619
2009	287.661	78.292	731.178	0.517	9071.677
2010	411.181	236.212	1056.458	0.488	12966.995

### *The Southern Bug River*

The Southern Bug River (in Ukrainian – Pivdenniy Bug) is the only river whose entire catchment is in Ukraine (Figure 4.25).

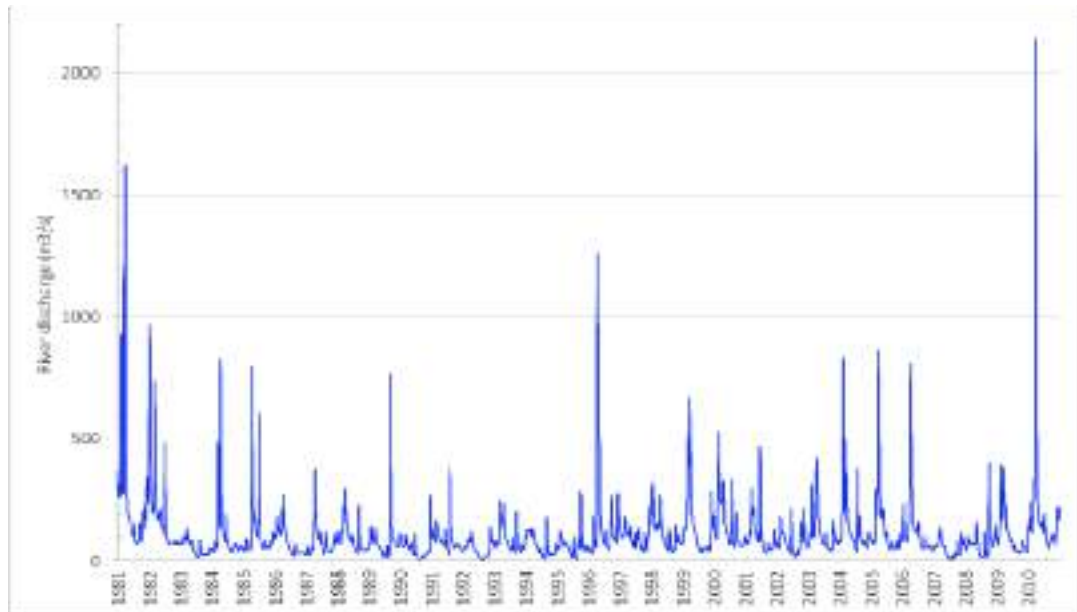
It starts from the Volyno-Podolsk Plateau in the village of Kholodets in Khmelnytsk Oblast and enters the Bug Estuary. Total length of the river is 813.6 km. Total area of the Southern Bug basin is 64300 km<sup>2</sup>. The Southern Bug basin is located in the territory of the following Ukrainian Oblasts (regions): Khmelnytsk, Vinnytsa, Kirovograd, Mykolaiv, Kyiv, Odesa and Cherkassy Oblasts.

The main tributaries of the Southern Bug are the rivers Bolshaya Vys, Gniloy Tikitch, Volk, Gornyi Tikitch, Zgar, Ingul, Kodyma, Mertvovod, Rov, Savranka, Sinyukha, Sob, Tchernyi Tashlyk, Chicheklya, Yatran.

There are a number of big water reservoirs on the Southern Bug River: Schedrivske, Ladyzhenske, Sabarovske, Glubochanske, Gaivoronivse, Pershotravneve and Oleksandrivske. Those are used mainly for power production. The Southern Bug does not have big tributaries. The biggest is the Sinyukha River (its catchment area is 16804 km<sup>2</sup> – 26% of the Southern Bug catchment); it is formed by confluence of the Tikitch and the Bolshaya Vys Rivers. The longest tributary is the Ingul, its length being 342 km.

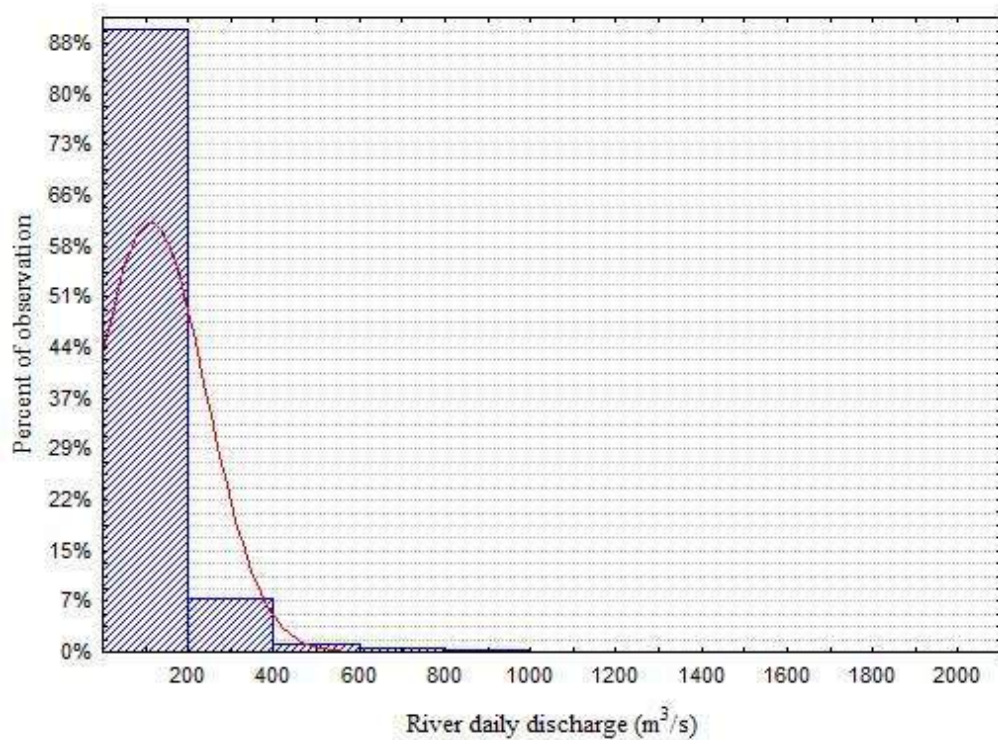
The Southern Bug River hydrology is characterized by significant seasonal changes in water quantity. It is fed mainly with snowmelt and rainfall, but also with groundwater. High water period is from late February to mid-April – early May, low water period is from June to February, floods are seldom. Spring high water period brings 50 to 80 % of discharge. In spring and winter the river is low. Slight rise of water level is observed in autumn, which is due to rainfall. It freezes over almost regularly in November (December) – February and becomes clear of ice by mid-March; ice regime is not permanent, ice melting and freezing is often observed in winter. In the lower reach does not freeze over in warm winters.

According to model data from the Swedish Hydrometeorological Institute (HYPE database, <https://hypeweb.smhi.se>), average daily flow of the Southern Bug River for the period of 1981-2010 made 1111 m<sup>3</sup>/sec with minimum of 2 (08.1992) and maximum of 2143 (28.10.2010) m<sup>3</sup>/sec (Figure 4.26).



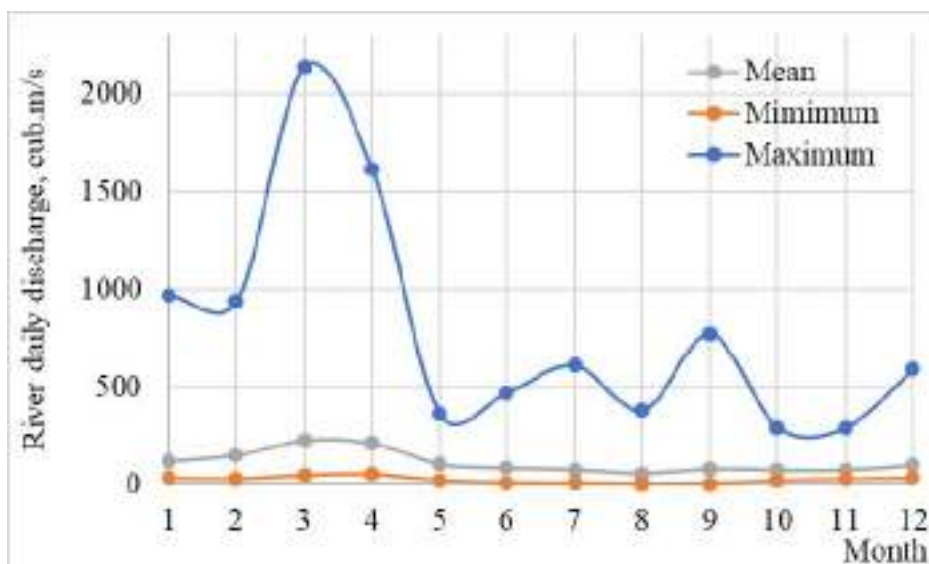
**Figure 4.26.** Temporal variability of daily discharge of the Southern Bug River (retrieved from HYPE database, 1981-2010, <https://hypeweb.smhi.se>)

About 90% of all the observations for the mentioned years have shown daily discharge less than 200 m<sup>3</sup>/sec (Figure 4.27).



**Figure 4.27.** Frequencies of the Southern Bug River daily discharges (retrieved from HYPE database, 1981-2010, <https://hypeweb.smhi.se>) (red line - Gaussian distribution)

According to the data (HYPE database, <https://hypeweb.smhi.se>), minimal water flow in the Southern Bug River seasonal variation for 1981-2010 was observed in average in May-December, maximal – in spring, from March to April (Figure 4.28).



**Figure 4.28.** Long-term average monthly, minimal and maximal values of the Southern Bug River daily discharges (retrieved from HYPE database, 1981-2010, <https://hypeweb.smhi.se>) (red line - Gaussian distribution)

According to the data (HYPE database, <https://hypeweb.smhi.se>), for the period of 1981-2010, average value of the Southern Bug River annual discharge made 4 km<sup>3</sup>/year with minimum of 2 (1983, 1986, 1987, 1990, 1992, 1994, 1995, 2007, 2008) and maximum of 9 (1981) km<sup>3</sup>/year (Table 4.18.). Average value of the Southern Bug annual discharge according to instrumental measurements at hydrological stations in 1977-2010 (IMB data, 2018) made 3.0 km<sup>3</sup>/year with minimum of 1.7 (1990) and maximum of 6.2 (1980) km<sup>3</sup>/year.

Negative linear trend for the period of 1981-2010 was observed in both sources: - 0.01 km<sup>3</sup>/year (IMB data, 2018) and - 0.003 km<sup>3</sup>/year (HYPE database, <https://hypeweb.smhi.se>). For the period of 1977-2010, according to the data (IMB data, 2018), the linear trend of annual discharge was also negative and made - 0.04 km<sup>3</sup>/year.

Inter-annual fluctuations of the Southern Bug River discharge volume for the period 1990-2010, according to spectral analysis results (Gazyetov & Dyatlov, 2021) contain 7 harmonic constituents with the periods 2.3, 4.2, 6.0, 8.4, 14.0, 21.0 and 42.0 years.

**Table 4.18.** Average annual Southern Bug Rivers Discharges

Year	River Discharge (m <sup>3</sup> /s)				Total Runoff (10 <sup>6</sup> m <sup>3</sup> /y)
	Average	Minimum	Maximum	Standard deviation	
1981	276.141	71.054	1624.518	0.903	8708.377
1982	198.174	72.651	969.604	0.683	6249.604
1983	57.184	16.201	134.757	0.203	1803.353
1984	110.043	40.102	832.975	0.626	3479.826
1985	122.454	43.661	800.399	0.575	3861.707
1986	78.478	25.719	277.806	0.315	2474.897

Year	River Discharge (m <sup>3</sup> /s)				Total Runoff (10 <sup>6</sup> m <sup>3</sup> /y)
	Average	Minimum	Maximum	Standard deviation	
1987	77.693	28.343	377.714	0.358	2450.124
1988	95.754	34.701	298.789	0.324	3027.960
1989	86.032	15.921	768.506	0.516	2713.120
1990	53.966	7.847	275.480	0.298	1701.885
1991	89.408	25.118	378.068	0.290	2819.567
1992	51.551	2.366	148.158	0.258	1630.181
1993	90.345	35.735	246.083	0.281	2849.115
1994	63.945	9.164	180.894	0.269	2016.574
1995	62.226	6.513	290.454	0.276	1962.358
1996	159.800	34.055	1263.635	0.897	5053.274
1997	100.240	41.688	224.982	0.210	3161.171
1998	112.122	38.098	321.031	0.310	3535.880
1999	138.853	37.411	673.299	0.582	4378.876
2000	148.559	56.426	529.255	0.420	4697.797
2001	101.530	33.457	472.538	0.364	3201.863
2002	81.324	23.276	218.178	0.261	2564.639
2003	118.514	44.937	422.851	0.408	3737.450
2004	139.488	40.707	836.643	0.536	4410.937
2005	139.839	46.038	865.000	0.630	4409.965
2006	134.484	43.686	813.471	0.612	4241.080
2007	53.910	8.557	142.516	0.233	1700.091
2008	78.745	13.530	405.506	0.342	2490.094
2009	105.448	35.840	400.248	0.443	3325.414
2010	208.974	56.939	2142.836	1.090	6590.205



## 4.6. Oceanography

As were indicated in part 4.5, the hydrophysical characteristics of marine environment are useful for assessment of coastal waters pressure on coastal zone changes. Temperature, salinity, waves, currents and sea level rise are the key indicators of climate change and help assess coastal erosion and accretion. Currents and waves play a crucial role in the determination of water circulation impact in shoreline dynamics.

Temperature and salinity determine the *values and distribution of density* of the Black Sea water. In the open areas, they are somewhat higher than in the coastal zone. In winter and autumn, the density of water at the surface is higher compared to spring and summer. Density grows with depth. Only near the bottom due to some heating of water because of geothermal flow of heat the density of water could be a little lower than in the layer above. In autumn at relatively weak stratification of surface layer and the layers below, strong durable winds stir the water from the surface down to horizons 15—20 m. The further deepening of the upper homogenous layer during late autumn happens due to convective-wind mixing. In spring and summer the freshened by river discharge waters are underlined by more saline water which creates stable stratification. Weak winds in these seasons stir only the upper 5—10-meters layer in which almost homogenous vertical distribution of characteristics is observed. Autumn process is more pronounced than the spring one, but even in cold seasons surface temperature is usually not less than 6—7°, that is why only thermal stage of density mixing develops here. Thermohaline convection takes place only in the zone of ice formation.

On the boundary of shelf zone in the western and northwestern parts of the sea density mixing expands to the horizons 170—175 m due to slipping down the slopes of the waters cooled in the northwestern shallow area, where convection penetrates down to the bottom. Results of volumetric statistical analysis enable us single out four water masses in the sea. The surface (upper) one takes 4.2% of the Black Sea water volume and spreads from the surface to the horizons 60—70 m in the central sea part, down to 100—125 m (in places down to 200 m) near the shores and in the coastal zone. Temperature of this water mass on the surface varies between 5—6° in winter and 24—26° in summer, at the lower boundary it equals to 7.5—8.0° all year round. Annual salinity trend lies between 17.5 and 18.6‰. The coastal water mass occupies about 0.2% of the Black Sea water volume. Its area is within the boundaries of isohaline 17‰. It covers significant areas in the western part of the sea and expands only 20—30 miles from the shore in the Prikerchenskiy area of the Black Sea where this water mass forms due to mixing of local waters with waters of the Azov Sea. The intermediate water mass occupies the biggest volume of water (50.2%) and lies between the horizons 100—150 and 800—1000 m. Its upper boundary is the layer of big density gradients often having dome shape. Temperatures here are 7.5—8.9°, salinity – 18.1—22.2‰. In the zone of transfer from the upper water mass to the intermediate one both oxygen and hydrogen sulphide occur. The deep water mass has somewhat smaller volume than the intermediate one (45.0%) and covers the entire layer of water from the horizon 1000 m to the bottom. Its temperature is 8.9—9.2°, salinity – 22.2—22.3‰. Hydrogen sulphide content increases with depth significantly. Judging from thermohaline characteristics on the lower horizons of the intermediate water mass and upper horizons of the deep water mass (800—1000 m), there is no significant boundary between them. It would be more correct to say that between horizons 150—200 m and 1500 m (upper boundary of bottom convection layer) there is the bottom water and from 1500 m to the seabed — bottom water mass. This subdivision accords well with dynamic processes in the Black Sea.

### 4.6.1. Temperature

Good warm-up of the Black Sea surface results at high average annual water temperature (8.9°). At that, average annual water temperature in the NWBS (in 1990-2005) made 15.23 °C (horizon 0 m) and 7.95 °C (horizon 30 m) [Hydrological and hydrochemical..., 2008]. In winter the most significant temperature changes from place to place happen in the shallow northwestern part. In the coldest month (February), it changes between –0.5—1.0° near the coast and +7° in the open part. In the deep areas water temperature at the surface equals



during this season to 7—8° and in the south-eastern corner - to 8.5°. In summer the surface layer temperature increases all over the water area reaching 25—26°. At that, spring monotony of temperature is violated. Usually the temperature increases from north-west to south-east. This increase is smoother and not as significant as in winter.

The temperature regime of the northwestern Black Sea where the UA1 pilot area is located is determined by the temperature regime of the atmosphere, shallowness and the influence of the big rivers discharge (Danube, Dnipro and Dniester). There are areas with maximal and minimal for the entire Black Sea annual cycle of temperature in the NWBS [Hydrometeorology..., 1991]. At that, in winter the temperature goes down to 2-4°C in the NWNS centre and to freezing temperature near the shores and in the Karkinitska Bay. Winter convection and cooling of the surface layer in the Danube coastal area are complicated due to high vertical gradients of salinity. Here, in the bottom layer under halocline temperature of 8 °C and higher can stay until February. The lowest water temperature is observed in the NWBS in February – unlike the rest of the sea where the minimal water temperature is registered in March [Hydrometeorology..., 1991]. In summer the average values of surface water temperature are the lowest in the NWBS due to often negative surges and upwelling of cold water from under the thermocline. The highest water temperature in the NWBS is registered in August. The spring water warming in the northwestern part of the sea becomes evident in March; by May a thermocline with gradient of 0.5°C/m and more is formed. However, spring field of water temperature in the near-surface layer has high spatial variability, as the thermocline located close to the surface is easily destroyed by wind, at that cold water from lower horizons get involved into the mixing process. The autumn cooling down of the NWBS water goes more intensively compared to other areas and begins from the north. The temperature goes below 10°C near the northern shores by the end of autumn. At the same time, it stays 3-4°C higher in the NWBS centre. In winter month temperature and salinity all over the NWBS water column are the same except for small areas near river mouths. In winter homothermal condition is observed down to 50 m depth, i.e. in the major NWBS part. In the rest of time the wave mixing form upper quasi-homogenous layer (UQL) with the depth rarely exceeding 10 m. Below the UQL and down to 25 m depth there is a single thermohalocline (alias the pycnocline), in forming of which thermal factor prevails in summer and salinity in winter and autumn [Blatov et al., 1984]. The structure of waters has its regional specific features. The upper Black Sea water mass (UBSWM) and the underlying cold intermediate layer (CIL) are pointed out as the structure elements of the open sea upper layer. The isosalinity line 18.6‰, which is up to 60-75 m deep in the coastal areas, is taken as the boundary between them [Hydrometeorology..., 1991]. The layer with maximal occurrence of the temperature of 7-8°C, which corresponds to the nucleus of the CIL, is located below this isosalinity line. Hence, as the NWBS is shallow, there is no CIL nucleus there. Inside the UBSWM, there is the shallow (coastal) Black Sea water mass (SBSWM), its properties being formed under influence of shallowness and river discharge. The criterion to single out the SBSWM is  $S < 17\text{‰}$ . From this it follows that the criterion for the UBSWM is  $17 < S < 18.6\text{‰}$ . So, the average annual SBSWM volume (280 km<sup>3</sup>) is 70 times lower than the average annual UBSWM volume (21586 km<sup>3</sup>) [Hydrometeorology..., 1991]. Not only salinity, but also other characteristics of the smaller water mass are changing under external factors influence faster and within broader limits. For example, average seasonal temperature of the SBSWM varies from 3.9 to 20.0°C, while that of the UBSWM — from 7.8 to 14.2°C. The SBSWM volume depends significantly on the volume of river discharge and respectively has significant seasonal fluctuations. Minimal volume in February and maximal in July differ 65-67% from the average value.

According to the Copernicus data (Figure 4.29), spatial distribution of temperature was studied to the fullest extent in the papers [Krivoguz D., Semenova A., Mal'ko S, 2021] , It has been shown that sea surface water temperature is an important environmental factor, determining both the location of ecosystems and their biodiversity. Water temperature can affect the metabolic rate of aquatic organisms and the rate of the photosynthesis reaction in aquatic plants and algae. Also, water temperature plays an important role in the formation of patterns of ocean circulation and distribution of nutrients.

According to this study, the temperature regime of the Black Sea in different periods of the year is determined by three main factors - the depth of the shelf zone, the influence of river runoff, and water circulation due to currents.



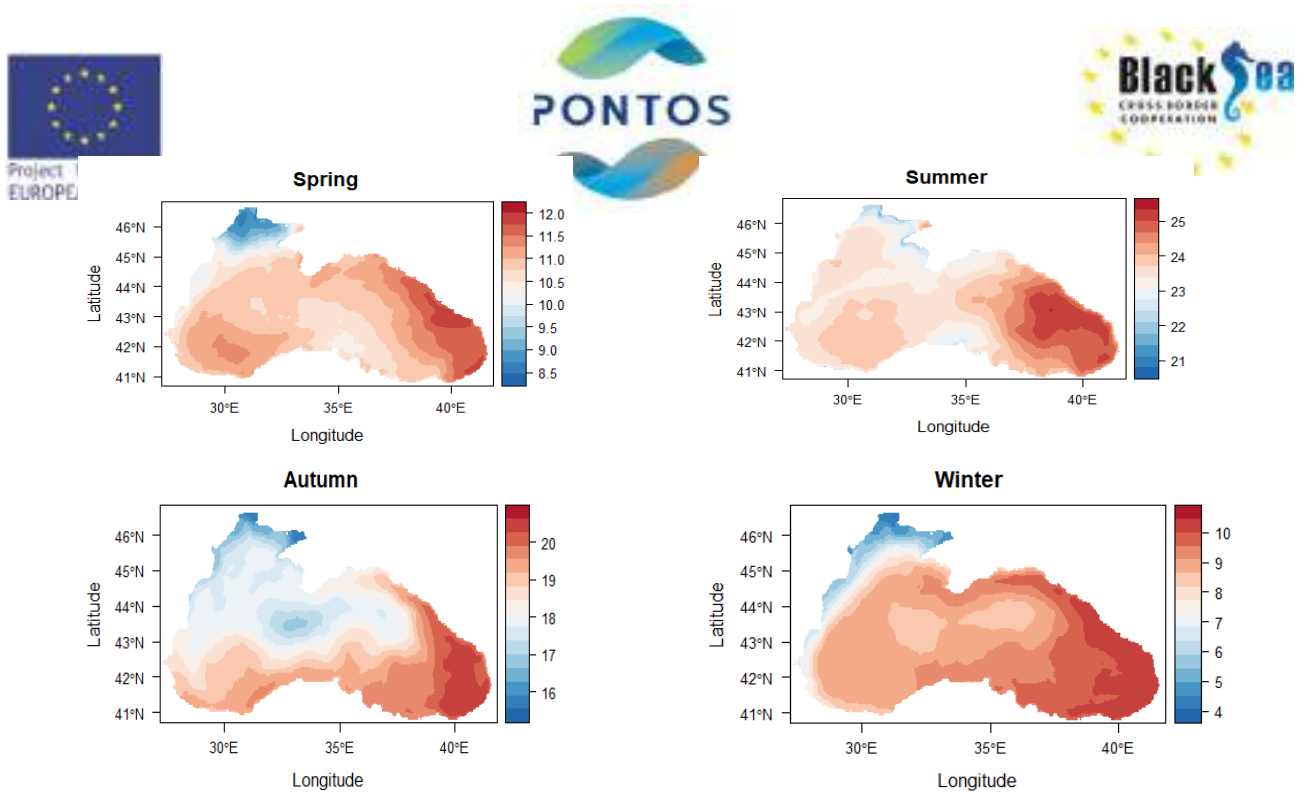


Figure 4.29. Distribution of sea surface temperature of the Black Sea in spring, summer, autumn and winter seasons 1992-2017

The Copernicus Database contains the ready product Black Sea sea surface temperature anomaly (Figure 4.30). Its analysis has shown the following.

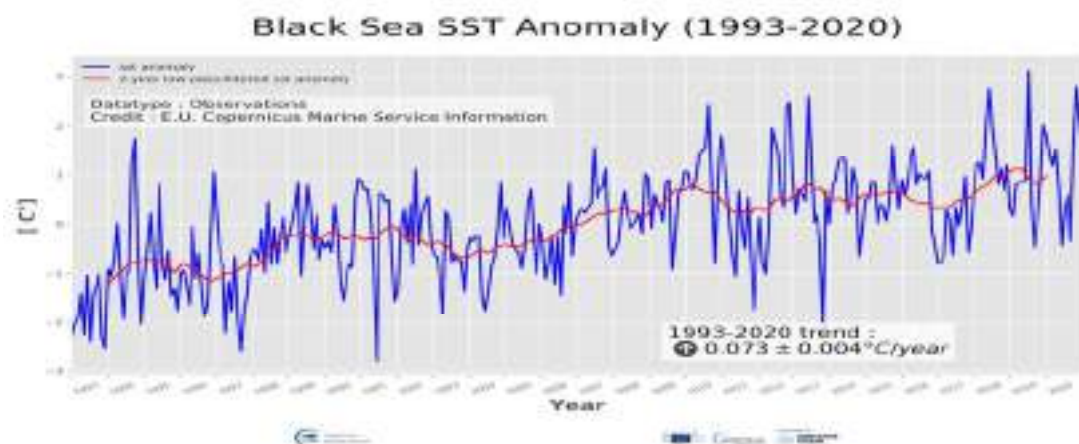


Figure 4.30 . **Black Sea Anomaly Time Series of Sea Surface Temperature (1993-2020)** (<https://marine.copernicus.eu/access-data/ocean-monitoring-indicators/black-sea-anomaly-time-series-sea-surface-temperature>) DOI (product): <https://doi.org/10.48670/moi-00217>

Time series of monthly mean (blue line) and 24-month filtered (red line) sea surface temperature anomalies in the Black Sea during the period 1993-2020. Anomalies are relative to the climatological period 1993-2014 and built from the CMEMS SST\_BS\_SST\_L4\_REP\_OBSERVATIONS\_010\_022 satellite product (see e.g. the OMI QUID, <http://marine.copernicus.eu/documents/QUID/CMEMS-OMI-QUID-BLKSEA-SST.pdf>). The sea surface temperature trend with its 95% confidence interval (shown in the box) is estimated by using the X-11 seasonal adjustment procedure (e.g. Pezzulli et al., 2005) and Sen's method [Sen 1968].

The reference for this OMI can be found in the first and second issue of the Copernicus Marine Service Ocean State Report (OSR), Section 1.1 [Roquet et al., 2016; Mulet et al., 2018].



The blksea\_omi\_tempsal\_sst\_area\_averaged\_anomalies product for 2020 includes unfiltered Sea Surface Temperature (SST) anomalies, given as monthly mean time series starting on 1993 and averaged over the Black Sea, and 24-month filtered SST anomalies, obtained by using the X11-seasonal adjustment procedure. This OMI is derived from the CMEMS Reprocessed Black Sea L4 SST satellite product (SST\_BS\_SST\_L4\_REP\_OBSERVATIONS\_010\_022, see e.g. the OMI QUID, <http://marine.copernicus.eu/documents/QUID/CMEMS-OMI-QUID-BLKSEA-SST.pdf>), which provided the SSTs used to compute the evolution of SST anomalies (unfiltered and filtered) over the Black Sea. This reprocessed product consists of daily (nighttime) optimally interpolated 0.05° grid resolution SST maps over the Black Sea built from the ESA Climate Change Initiative (CCI) [Merchant et al., 2019] and Copernicus Climate Change Service (C3S) initiatives, including also an adjusted version of the AVHRR Pathfinder dataset version 5.3 [Saha et al., 2018] to increase the input observation coverage. Anomalies are computed against the 1993-2014 reference period.

Sea surface temperature (SST) is a key climate variable due to its role for climate variability and change [Deser et al., 2010, IPCC, 2021]. On shorter timescales, SST anomalies become an essential indicator for extreme events, as e.g. marine heatwaves [Hobday et al., 2018]. In the last decades, since the availability of satellite data (beginning of 1980s), the Black Sea has experienced a warming trend in SST [Buongiorno Nardelli et al., 2010; Mulet et al., 2018].

On average, 2020 was a warm year characterized by high (well above 1 °C) positive anomalies with respect to the 1993-2014 reference climatology. This year, along with 2019 and 2018, maintains the peak record of almost 3 °C (namely, 2.99 °C) in anomaly, reached in October, over the whole period (1993-2020). With respect to 2019, 2020 was characterized by two negative anomalies, the first reached in May (-0.22 °C) and the second one in August (-0.13 °C). Over the period 1993-2020, the Black Sea SST has warmed at a rate of  $0.073 \pm 0.004$  °C/year, which corresponds to an average increase of about 2 °C during these last 28 years.

The next product of the Copernicus Database the Sea surface temperature cumulative trend over the period 1993-2020 in the Black Sea (Figure 4.31), evidences the influence of the global warming on the Black Sea region. (<https://marine.copernicus.eu/access-data/ocean-monitoring-indicators/black-sea-cumulative-trend-map-sea-surface-temperature>)

The blksea\_omi\_tempsal\_sst\_trend product includes the cumulative/net Sea Surface Temperature (SST) trend for the Black Sea over the period 1993-2020, i.e. the rate of change (°C/year) multiplied by the number years in the timeseries (28). This OMI is derived from the CMEMS Reprocessed Black Sea L4 SST satellite product (SST\_BS\_SST\_L4\_REP\_OBSERVATIONS\_010\_022, see e.g. the OMI QUID, <http://marine.copernicus.eu/documents/QUID/CMEMS-OMI-QUID-BLKSEA-SST.pdf>), which provided the SSTs used to compute the SST trend over the Black Sea. This reprocessed product consists of daily (nighttime) optimally interpolated 0.05° grid resolution SST maps over the Black Sea built from the ESA Climate Change Initiative (CCI) (Merchant et al., 2019) and Copernicus Climate Change Service (C3S) initiatives, including also an adjusted version of the AVHRR Pathfinder dataset version 5.3 [Saha et al., 2018] to increase the input observation coverage. Trend analysis has been performed by using the X-11 seasonal adjustment procedure [Pezzulli et al., 2005], which has the effect of filtering the input SST time series acting as a low bandpass filter for interannual variations.

Mann-Kendall test and Sens's method (Sen 1968) were applied to assess whether there was a monotonic upward or downward trend and to estimate the slope of the trend and its 95% confidence interval. The reference for this OMI can be found in the first and second issue of the Copernicus Marine Service Ocean State Report (OSR), Section 1.1 [Roquet et al., 2016; Mulet et al., 2018].

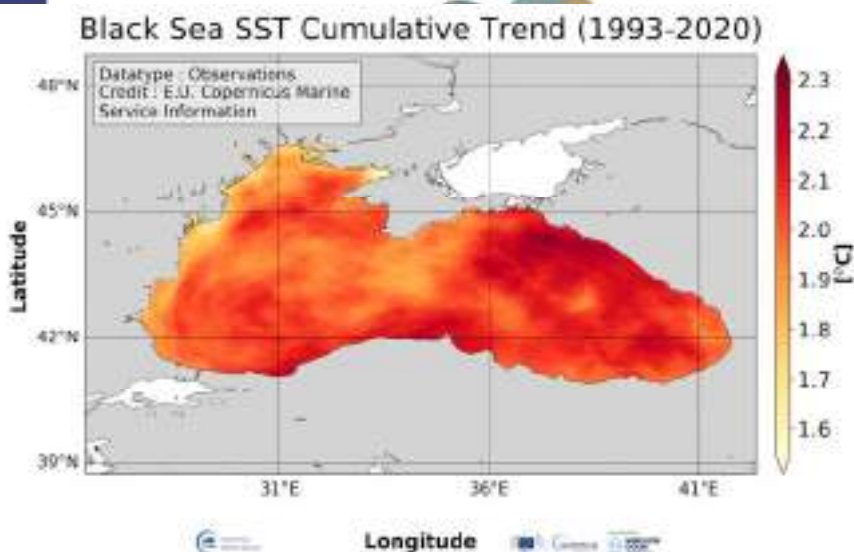


Figure 4.31. Sea surface temperature cumulative trend over the period 1993-2020 in the Black Sea. DOI (product): <https://doi.org/10.48670/moi-00218>

The spatial pattern of the Black Sea SST trend reveals a general warming tendency, ranging from 0.055 °C/year to 0.083 °C/year. Highest values characterize the Eastern area of the Black Sea, where the trend reaches the extreme value, while lower values are found close to the western coasts, in correspondence of main rivers inflow. This pattern seems to reveal an Eastward increasing trend intensity. Overall, the Black Sea SST trend shows the highest intensity among all the other European Seas. The Sea Surface Temperature is one of the Essential Ocean Variables, hence the monitoring of this variable is of key importance, since its variations can affect the ocean circulation, marine ecosystems, and ocean-atmosphere exchange processes. Particularly in the Black Sea, ocean-atmospheric processes together with its general cyclonic circulation (Rim Current) play an important role on the sea surface temperature variability [Capet et al. 2012]. As the oceans continuously interact with the atmosphere, trends of sea surface temperature can also have an effect on the global climate. The 99th mean percentile of sea surface temperature provides a worth information about the variability of the sea surface temperature and warming trends but has not been investigated with details in the Black Sea. While the global-averaged sea surface temperatures have increased since the beginning of the 20th century [Hartmann et al., 2013]. Recent studies indicated a warming trend of the sea surface temperature in the Black Sea in the latest years [Mulet et al., 2018; Sakali and Başusta, 2018]. A specific analysis on the interannual variability of the basin-averaged sea surface temperature revealed a higher positive trend in its eastern region [Ginzburg et al., 2004]. For the past three decades, [Sakali and Başusta, 2018] presented an increase in sea surface temperature that varied along both east–west and south–north directions in the Black Sea.

The CMEMS BLKSEA\_OMI\_tempsal\_extreme\_var\_temp\_mean\_and\_anomaly OMI indicator (Figure 4.32) is based on the computation of the annual 99th percentile of Sea Surface Temperature (SST) from model data. Two different CMEMS products are used to compute the indicator: The Iberia-Biscay-Ireland Multi Year Product (BLKSEA\_MULTIYEAR\_PHY\_007\_004) and the Analysis product (BLKSEA\_ANALYSIS\_FORECAST\_PHYS\_007\_001).

The mean annual 99th percentile in the period 1993–2019 exhibits values ranging from 25.50 to 26.50 °C in the western and central regions of the Black Sea. The values increase towards the east, exceeding 27.5 °C. This contrasting west-east pattern may be linked to the basin wide cyclonic circulation. There are regions showing lower values, below 25.75 °C, such as a small area west of Crimean Peninsula in the vicinity of the Sevastopol anticyclone, the Northern Ukraine region, in particular close to the Odessa and the Karkinytska Gulf due to the freshwaters from the land and a narrow area along the Turkish coastline in the south. Results for 2020 show negative anomalies in the area of influence of the Bosphorus and the Bulgarian offshore region up to the Crimean peninsula, while the North West shelf exhibits a positive anomaly as in the Eastern basin.



The highest positive value is occurring in the Eastern Turkish coastline nearest the Batumi gyre area. This may be related to the variously increase of sea surface temperature in such a way the southern regions have experienced a higher warming.

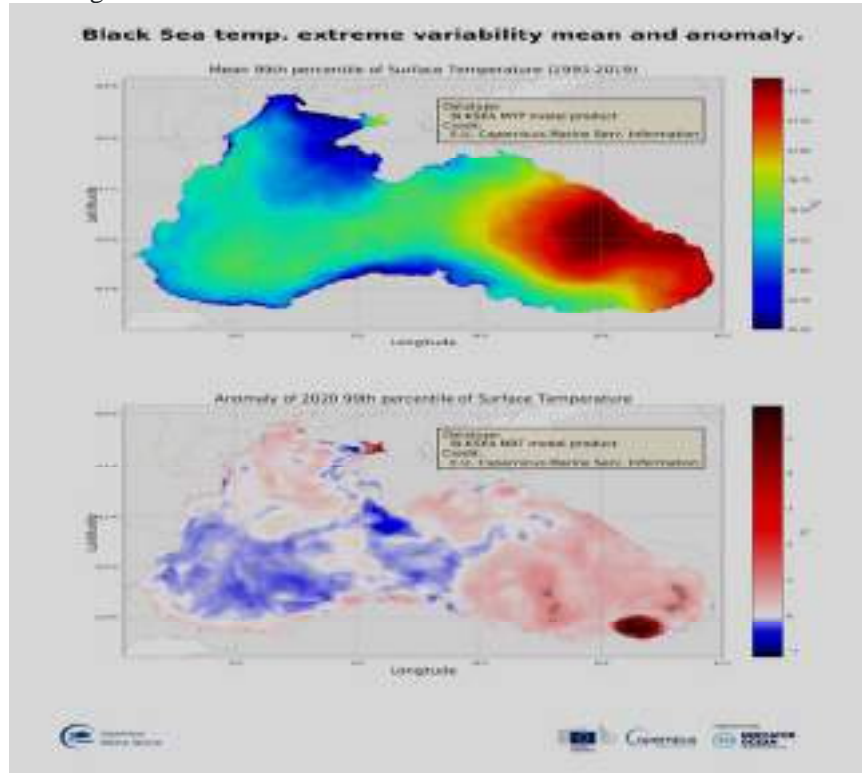
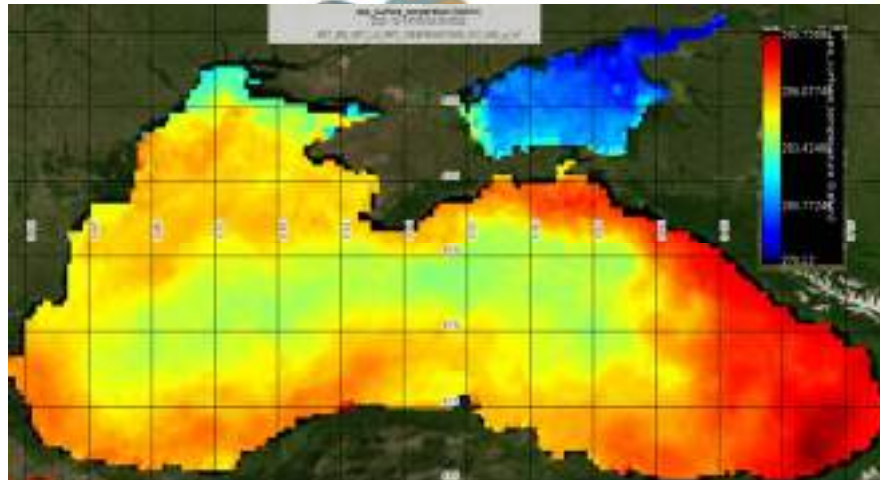


Figure 4.32. Black Sea Surface Temperature extreme variability: Map of the 99<sup>th</sup> mean percentile computed from the Multi Year Product (upper panel) and anomaly of the 99<sup>th</sup> percentile in 2018 computed from the Analysis product (bottom panel). Transparent grey areas represent regions where anomaly exceeds the climatic standard deviation (light grey) and twice the climatic standard deviation (dark grey). DOI (product): <https://doi.org/10.48670/moi-00216>, [https://resources.marine.copernicus.eu/product-detail/BLKSEA\\_OMI\\_TEMP\\_SAL\\_extreme\\_var\\_temp\\_mean\\_and\\_anomaly/INFORMATION](https://resources.marine.copernicus.eu/product-detail/BLKSEA_OMI_TEMP_SAL_extreme_var_temp_mean_and_anomaly/INFORMATION)

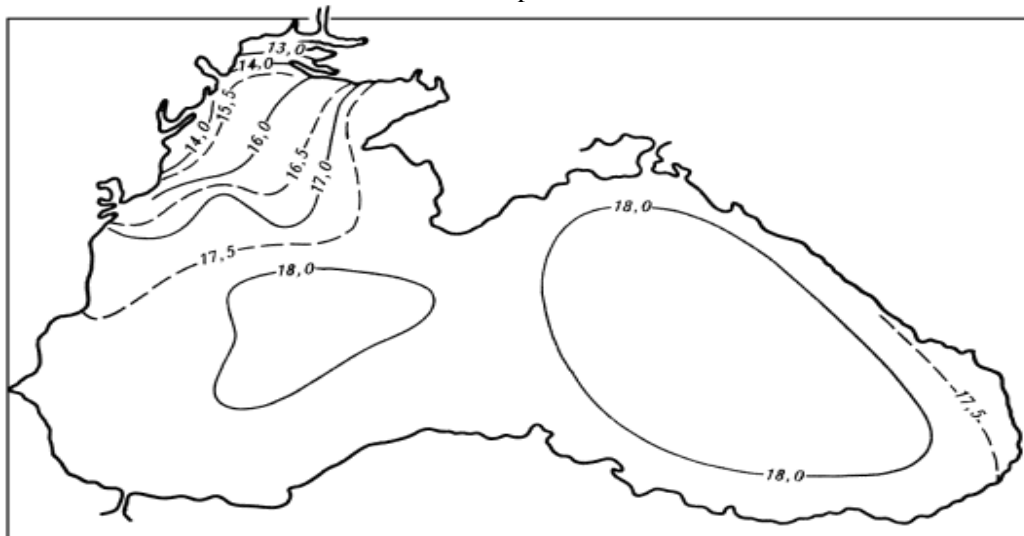
In case of a need to analyse specific data for specific dates for the purposes of the PONTOS Project, the daily data can be used. The figure 4.33 below shows an example for 14.12.2021



**Figure 4.33.** The sample of Sea Surface Temperature (SST) daily maps over the Black Sea from remotely-sensed L4 SST datasets for 14.12.2021 **Source:** The Copernicus Marine Service portal, version of 2021, <https://resources.marine.copernicus.eu>

#### 4.6.2. Salinity

Spatial distribution of salinity on the Black Sea surface, as one could see on the map (Figure 4.34), is as follows: the minimal salinity value 12-13‰ is observed in the NWBS and it increases gradually from north-west to south-east with maximal value 18,0 ‰ in central parts of the Black Sea .



**Figure 4.34 .** Salinity distribution on the Black Sea surface in summer [Dobrovolskiy and Zalogin, 1982]

This could be explained with the above mentioned influence of rivers flowing into the north-western part of the sea. Decreased to 5—10‰ salinity could also be registered in the narrow shore front near the mouths of big rivers. The values of surface salinity change with seasons, which is the most vivid in the freshened areas. In winter salinity is somewhat higher due to decrease of rivers discharge; in the northwestern part salinity is becomes even higher because of salinization due to ice storage.

In summer, freshening is supported by significant river discharge and sea currents distribute freshened water to the east and to the south-western coast of the Crimea.

Salinity increases with depth in the open part of the sea from 17—18‰ at the surface to 22.5‰ at the bottom. There is an important feature in the salinity vertical distribution: there is a permanent in time halocline between the horizons 100—150 m, where the salinity increases from 18.5 to 21.0‰.



Noticeable seasonal changes in salinity could be traced down to horizon 150 m in the western half of the sea and down to 100—120 m in its eastern half. Below these layers, vertical salinity trend is the same all over the sea.

The range of average monthly salinity values in the surface NWBS layer is maximal in the Danube Delta area and makes 3‰. It goes down gradually westward and equals to 0.75‰ near the Cape Tarkhankut and the Karkinitzka Bay. The month of maximal salinity also changes in westward direction from January to April; the month of minimal salinity – from May to September. The minimal salinity in the surface layer is connected with spring maximal river discharge. The forming halocline and at the same time spring warming of water restrict vertical mixing and contribute to horizontal distribution of freshened water. The maximum of salinity is connected with erosion of the upper halocline as the result of wind-wave water mixing and convection, which happen in autumn-winter period, when water that is more saline is involved into the UQL. Salinity seasonal changes in the upper layer are prominent in the western part of the NWBS. In the east, in the Kalamitska Bay and near the Cape Tarkhankut, salinity of 17.6-18.2‰ stays almost all year round and only in autumn, when the flow of freshened water reaches the eastern shore, goes down to 17.4-17.7‰. Seasonal changes of salinity are less pronounced on the 20 m horizon: their range in the west is 17.6-17.8, in the east - 18.0-18.2‰. In line with distribution of the freshening wave, the lowest salinity in the west is registered in spring, in the east – in autumn.

The transfer from fresh to salt water is non-uniform, but with forming of hydrofronts, zones with increased salinity gradients, which shape at such distance from the shore where river discharge influence becomes negligible – up to 10 km from a river mouth (Natural conditions..., 1999). Statistical processing of the results of observations at the seashore helped establish the stable maximums and minimums of occurrence of several salinity ranges. As frontal zones occupy small part of the water area compared to the water masses which they separate, the local minimums correspond to salinity ranges reflecting hydrofronts on histograms of occurrence. In line with the existing classification of surface water transformation zones near the Danube mouth [Natural conditions..., 1999], their boundaries are established depending on water salinity: 1) zone of primary transformation between the isosalinity lines 3 and 10‰, which includes the front of primary transformation (hydrofront); 2) zone of secondary transformation between the isosalinity lines 10 and 14‰, which includes the front of secondary transformation (isosalinity line 14‰); 3) zone of full transformation, its external boundary being the front of complete transformation (isosalinity line 17‰). The front, which corresponds to the isosalinity line 17‰, coincides with estimation of river waters transformation zone's external boundary according to V.S. Bolshakov [Bolshakov, 1970].

Spatial distribution of salinity in the surface layer according to Copernicus data (Figure 4.35) was the most fully studied in the paper [Krivoguz, Semenova and Mal'ko, 2021].

The average salinity of the Black Sea waters is 19 ‰, areas with lower salinity are located near the west shore, due to the flows from the largest rivers (Dnieper, Dniester, Danube) bringing a large amount of fresh water to the Black Sea. The area with higher salinity is located in the south-west due to the water exchange of the Black Sea with the saltier Sea of Marmara (~ 26 ‰) through the Bosphorus. The currents of the Black Sea pick up the salty water of the Sea of Marmara and slowly moving the water column against the clockwise, carry it across the entire Black Sea, thereby increasing its average salinity.

Thus, the salinity regime of the Black Sea is determined mainly due to the influence of river runoff, which brings a large amount of fresh water to the sea, and the circulation of water due to currents, which, in turn, are influenced by wind activity.

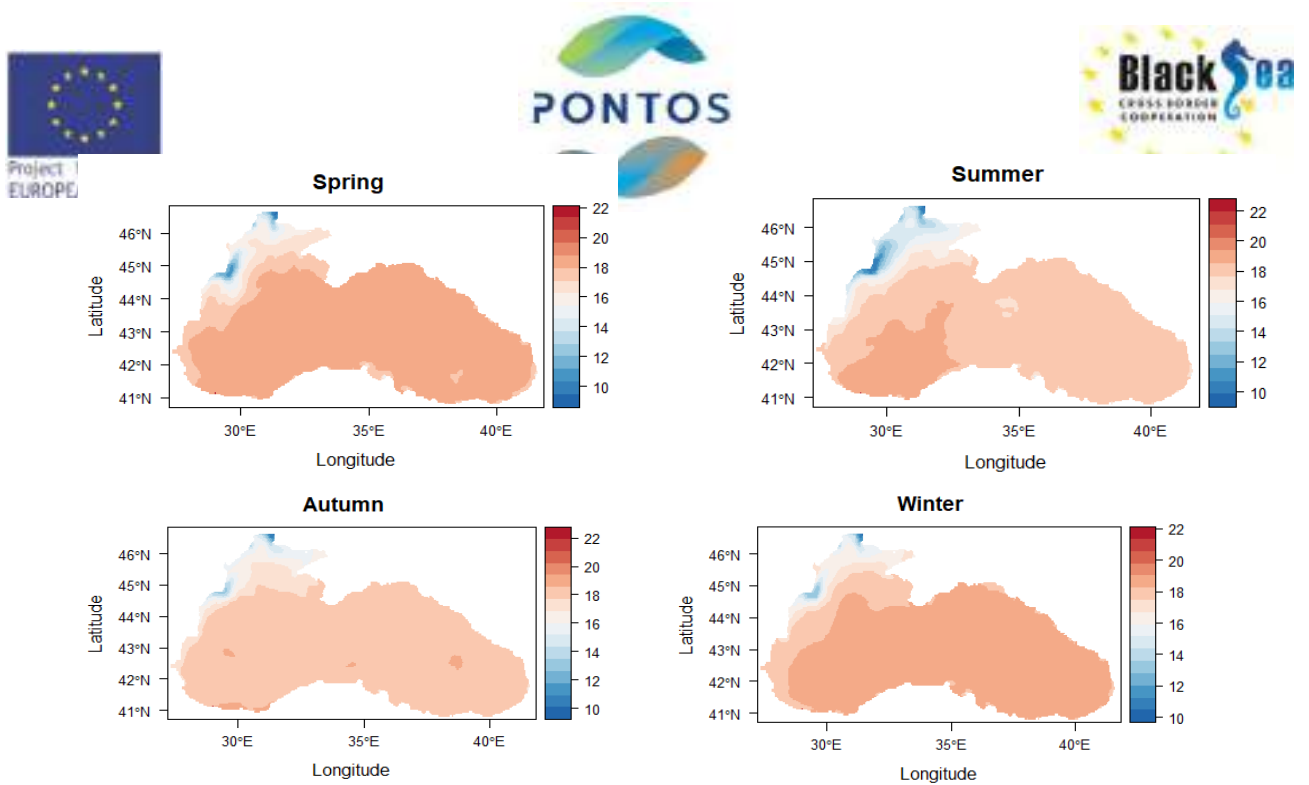


Figure 4.35. Distribution of sea surface salinity of the Black Sea in spring, summer, autumn and winter seasons 1992-2017.

Very important Copernicus database product characterising the features of the Black Sea salinity pattern is the Black Sea anomaly map of Sea Surface Salinity (Figure 4.36) (<https://marine.copernicus.eu/access-data/ocean-monitoring-indicators/black-sea-anomaly-map-sea-surface-salinity>) <https://sextant.ifremer.fr/Donnees/Catalogue#/metadata/78ea9bd9-ff76-42ae-a252-b254c4afbc53>, <https://sextant.ifremer.fr/Donnees/Catalogue#/search?keyword=black-sea>

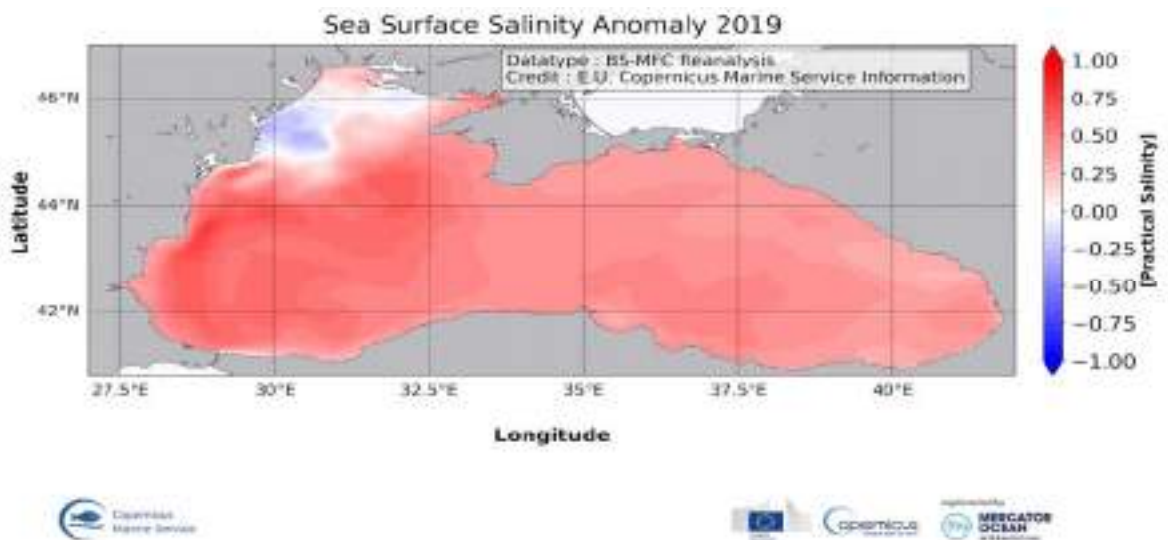


Figure 4.36. Black Sea anomaly map of Sea Surface Salinity in 2019

The sea surface salinity anomaly in 2019 (SSS') is the time average sea surface salinity (SSS) computed from the reanalysis results in 2019 minus the reference sea surface salinity (SSS). The map of sea surface salinity anomaly is derived from the results of the Black Sea reanalysis (product reference BLKSEA\_MULTIYEAR\_PHY\_007\_004).

The reference is the time-averaged SSS computed from 1993 to 2014 using the own reanalysis results. This OMI has been discussed in [Mulet et al., 2018].

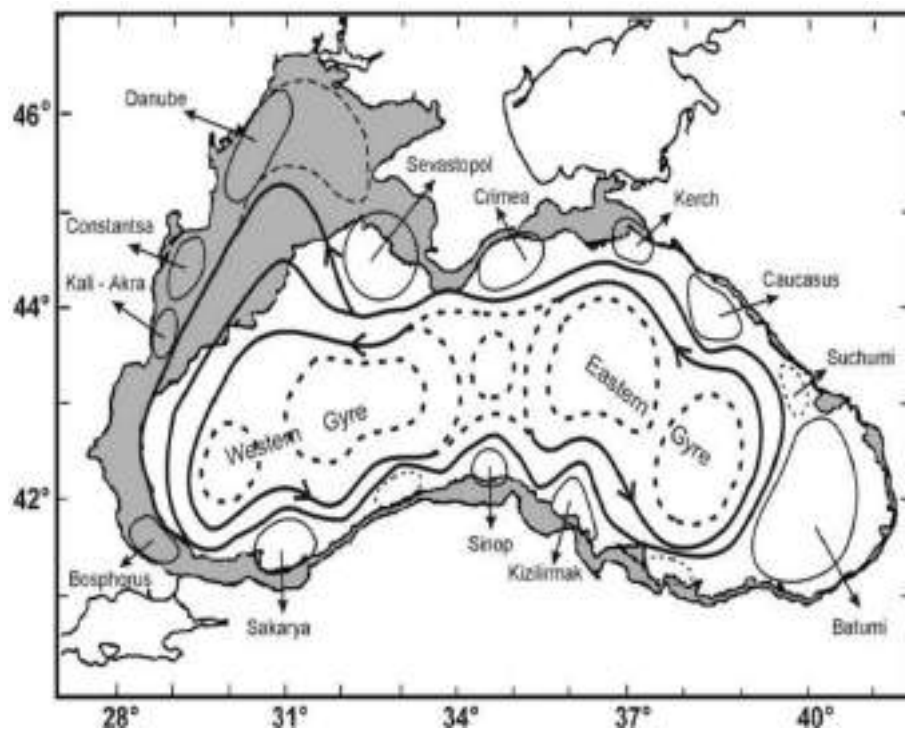
The Black Sea is a semi-enclosed basin with peculiar characteristics such as a positive net freshwater balance, which is mainly related to the outflow of some of the largest European rivers (e.g. Danube, Dniro) and high-rate of precipitation which in total exceeds the total evaporation most of the time over the basin [Kara et al., 2008]. In addition, an inflow of saltier water originates from the Mediterranean Sea, crosses the Marmara Sea and impacts the Black Sea circulation through the Bosphorus Strait [Stanev et al., 2001]. The sea surface salinity anomaly is a valuable metric to evaluate the impact of such external forcing on the Black Sea [Mulet et al., 2018]. A negative (positive) anomaly means that the sea surface salinity of the analyzed year is fresher (saltier) as compared to the reference period, which may be caused by larger continental runoff and/or precipitation (evaporation) fluxes. Moreover, sea surface salinity changes due to the local variations in ocean dynamics are also not negligible. For instance, the processes induced by the Rim Current and its inherent vortices can locally impact the thermohaline structure in the Black Sea [Kubryakov et al., 2018; Miladinova et al., 2017]. The salinity trends are still poorly studied in the Black Sea, although a more recent study by using model numerical simulations found different salinity trends in the water column: surface (negative), upper (weaker negative) and main halocline (positive) [Miladinova et al., 2017].

In 2019, the Black Sea shows a positive sea surface salinity anomaly over almost the entire basin.

The highest positive anomalies are found in the south-western basin such as near the coast and between 43°N and 44°N, where they exceed 0.75. On the contrary, negative anomalies are present in the northwestern shelf, which is under the influence of large continental runoff from important rivers: Dniester, Dniro and the northern branch of the Danube.

#### 4.6.3 Currents

The cyclonic currents that belt the entire sea near the shores is shown in the figure 4.37.



**Figure 4.37.** The Black Sea schematic currents pattern including features derived from the analysis of the altimeter data [Korotaev et al., 2003]





Inside this ring cyclonic circulations could be seen, their speed being up to 10 cm/sec in the central parts and up to 25 cm/sec in peripheral. The areas of contact between river and sea waters are specific frontal zones. Visible boundary between them is formed due to the difference in colours of those waters. The brightest frontal zones are observed in the northwestern part of the sea where significant river discharge is concentrated.

As were indicated in [Korotaev et al., 2003] seasonal, interannual, and mesoscale variability of the Black Sea upper layer circulation derived from altimeter data comprising the period from May 1992 to May 1999 were assimilated into a shallow water model for providing a dynamically consistent interpretation of the sea surface height variations and estimation of the temporal and spatial characteristics of the upper layer circulation in the Black Sea. The circulation possesses a distinct seasonal cycle whose major characteristic features repeat every year with some year-to-year variability. Understanding of the Black Sea circulation has significantly increased during the last decade through realization of several international programs. Analysing all the available data [Oguz et al., 1993] specified the building blocks of the upper layer circulation as the Rim Current system around the periphery, an interior cell composed by two or more cyclonic gyres, and a series of quasi-stable/recurrent anticyclonic eddies on the coastal side of the Rim Current. Construction of optimally interpolated and gridded (in both space and time) dynamical sea level data from altimetry recently provided a new resource for increasing our present level of knowledge on variability of the Black Sea circulation.

They described the methodology for reconstruction of the dynamical sea level data base for the period from May 1992 to November 1996, its validation by the available hydrographic survey data, and interpretation of the results by means of a simple two-layer analytical model of the wind-driven circulation in a rectangular basin.

The flow system within the northwestern shelf (NWS) is governed by both intrusions of the Rim Current and discharges from the Danube, Dnipro and Dniester Rivers; the discharge from the former is almost four times stronger than the sum of other two. The typical regional flow regime within the inner shelf is a southward coastal current system. The outer shelf, on the other hand, is characterized by highly dynamic and complicated interactions between the inner shelf and the Rim Current flow systems. The coastal fresh water-induced flow system includes some mesoscale anticyclonic eddies, one of which is located just outside the discharge zone of the Danube. We refer to this feature as the Danube anticyclonic eddy. The other eddy is located slightly south near Cape Kaliakra, in the narrowest part of the northwestern shelf (Figure ). The Kaliakra anticyclonic eddy also emerges during the late summer and autumn months, whereas it is embedded within the coastal current system during high-discharge periods. Another small anticyclonic eddy (the Constantsa eddy) is often present between the Danube and Kaliakra anticyclones.

Copernicus provides the opportunity to operatively receive daily maps of the Black Sea currents (Figure 4.38)

## Black Sea Sea Currents

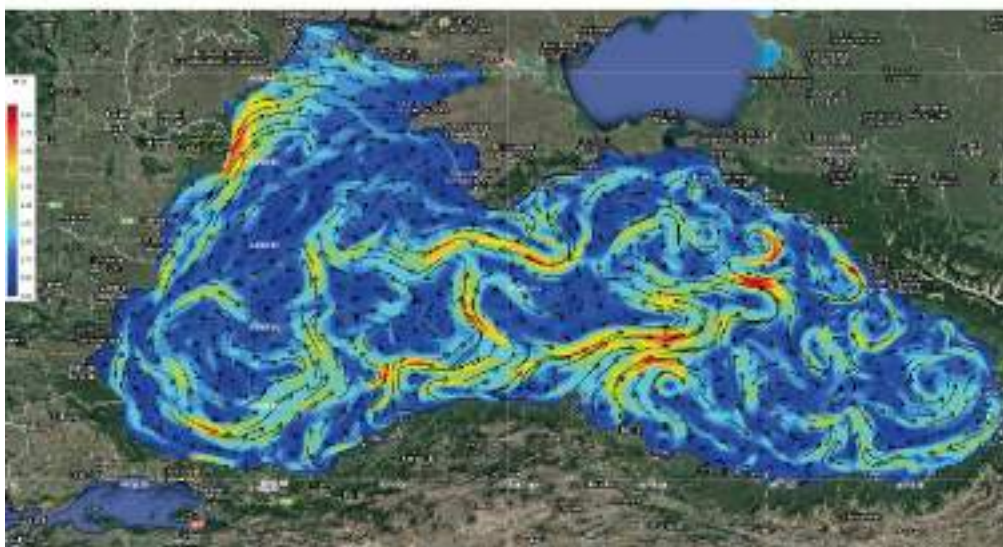


Figure 4.38. Example of currents map in the Black Sea dtd 15 May 2020  
(<https://marine.copernicus.eu/about/producers/bs-mfc>,  
<http://iswim.rmri.ro/index.shtml>,  
<http://iswim.rmri.ro/maps/maps1.shtml>)

### 4.6.4 Waves

In accordance with wind regime features, maximal intensity of wind-driven wave in the Black Sea [Ilyin et al., 2012] is observed during cold season, from October to March. At that, wind-driven wave intensity in the NWBS coastal zone is in general somewhat lower than in other areas, however severe storms happen there also, especially near the northern shore (Chornomorsk, Odesa, Pivdennyi), which is open to the winds of southern rhumbs. Repeatability of five-six points storms (waves higher than 2 m) in January-March in the NWBS is less than 2% (as a comparison, in the area of the Cape Khersones repeatability is 7-10, near Alushta - 3.0-5.5%). In summer, in the periods of rare storms, repeatability of such waves is minimal everywhere and makes less than 0.5 %. During last half-century period the highest waves in the NWBS were observed in Odesa (5 points – 216 times, 6 points – 2 times), near Cape Tarkhankut (5 points – 34 times, 6 points – 3 times, 7 points – once) and in Yevpatoriya area (5 points – 41 times, 6 points – 3 times). Waves 125 cm high and over can be observed any month in any area of Ukrainian coastal zone.

The prevailing directions of wave distribution are determined by the direction of the wind that caused wave, orientation of shores, influence of refraction in the shallows at diagonal approach of wave in relation to isobaths orientation, as well as by the diffraction phenomenon when a system of waves is bypassing obstacles like capes and shallow areas of the shelf. At the western shores of the NWBS, near Ust-Dunaisk port, waves of northern (18.1%), north-eastern (13.6%) and southern (13.5%) directions have the highest repeatability. According to the wave stations in Chornomorsk and Pivdennyi, the prevailing directions of dangerous waves distribution at the northern coast are southern (23-25%), south-eastern and eastern (8.7-9.4 %). South-eastern (18.1%), southern and eastern directions prevail in Odesa area. In the area of the Karkinitzka Bay waves of south-western (18%), south-eastern, northern (15.7-19.5%) and western (16.3%) directions have the highest reparability from the side of the sea. The highest repeatability of the most severe storms, up to 4-6 points, at the northwestern coast corresponds to north-eastern, eastern, south-eastern and southern directions. During the 28 years long period of observations wave height exceeding 2 m was registered at Ust-Dunaisk post 2 times only, near Chornomorsk port – 113 times for 48 years, near Odesa – 218 times during 60 years (in 2 cases out of them waves exceeded 3.5 m), near the Cape Tarkhankut – 38 times for 40 years.



The biggest part of these cases, as well as absolute registered maximums in Odesa were 5.1 m, near Tarkhankut - 8.0 m, near Cape Khersones - 7.3 m, observed during the periods of November storms. Repeatability of storm wave near Chornomorsk, Odesa and Pivdennyi is 1-3% of all observations. Due to the shape of the sea and typical wind fields over it, rough sea happens most often in the northwestern, north-eastern and central parts. Depending on wind speeds and fetch legislation the waves 1—3 m high prevail in the sea. In the open areas, maximal height of waves of 5% probability reaches 11 m and during very strong storms, this wave height could be exceeded. South-west and south-east of the sea are the most calm areas, which are rarely rough and waves higher than 3 m almost never happen. Waves of shallow sea are characteristic of coastal zone.

The CMEMS **Significant Wave Height** extreme variability indicator is aimed at monitoring the extremes of annual significant wave height and evaluate the spatio-temporal variability. The use of percentiles instead of annual maxima, makes these extremes study less affected by individual data. The sea state and its related spatio-temporal variability affect dramatically maritime activities and the physical connectivity between offshore waters and coastal ecosystems, affecting therefore the biodiversity of marine protected areas. Over the last decades, significant attention has been devoted to extreme wave height events since their destructive effects in both the shoreline environment and human infrastructures have prompted a wide range of adaptation strategies to deal with natural hazards in coastal areas [Hansom et al., 2015]. Significant Wave Height mean 99th percentile in the Black Sea region shows an east / west dependence, i.e. highest values of the average of annual 99th percentiles prevail in those areas where high winds and long fetch are simultaneously present. The largest values of the mean 99th percentile in the southwestern Black Sea are around 3.5 m, while in the eastern part of the basin they can amount to around 2.5 m [Staneva et al., 2019a and 2019b]. Significant Wave Height mean 99th percentile in the Black Sea region shows the typical east / west dependence with largest values in the southwestern Black Sea ranging up to 3.5 m, while the 99th percentile values in the eastern part of the basin are around 2.5 m.

The 99th mean percentile for 2002-2017 shows a similar pattern demonstrating that the highest values of the mean annual 99th percentile are in the western part of the basin [Akpınar et al., 2016 and Akpınar and Van Vledder, 2016]. The anomaly of the 99th percentile in 2018 is mostly negative with values down to ~-45 cm.

Figure 4.39 illustrated the Black Sea Significant Wave Height extreme variability for 2020:

### Black Sea wave height extreme variability mean and anomaly.

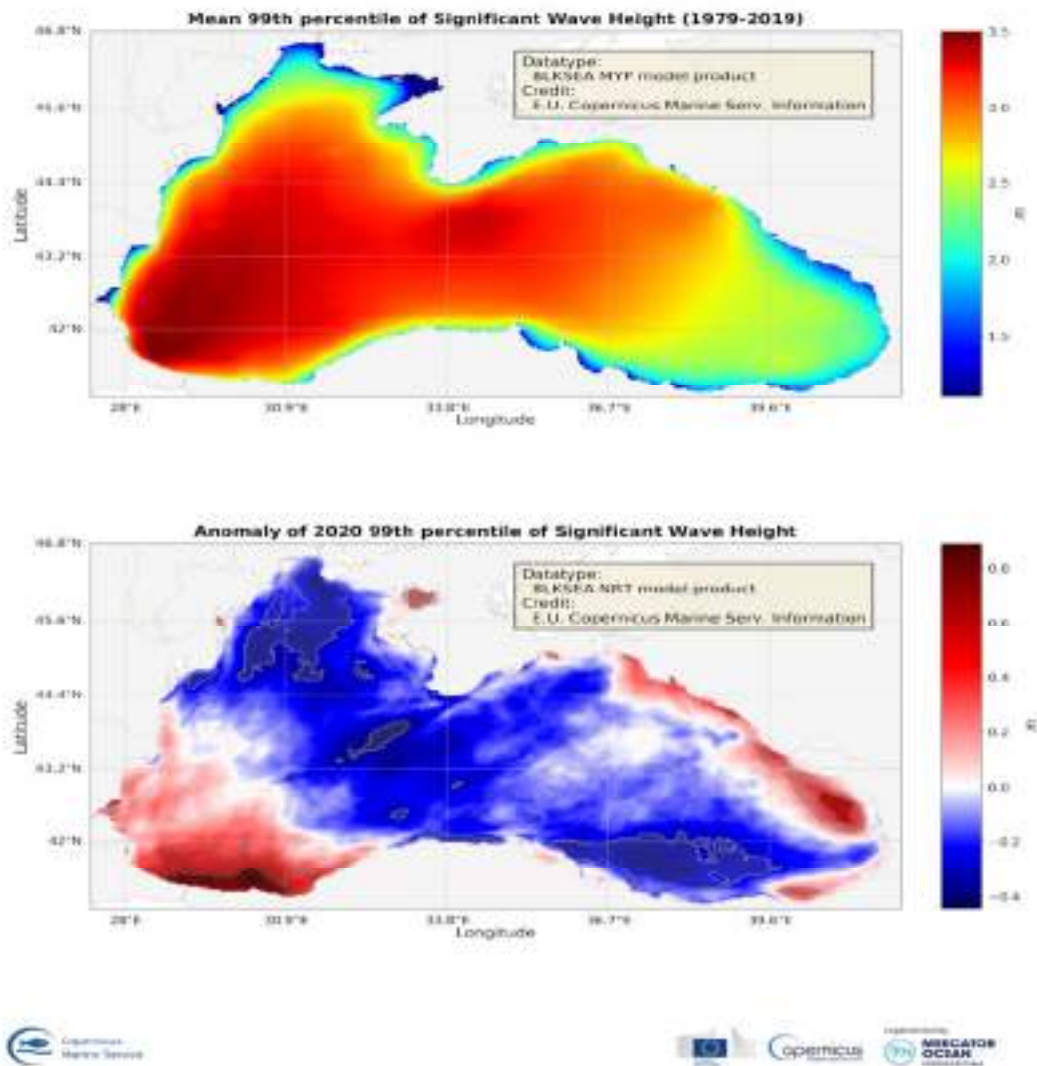


Figure 4.39. Black Sea Significant Wave Height extreme variability: Map of the 99th mean percentile computed from the Multi Year Product (upper panel) and anomaly of the 99th percentile in 2020 computed from the Analysis product (bottom panel). Transparent grey areas (if any) represent regions where anomaly exceeds the climatic standard deviation (light grey) and twice the climatic standard deviation (dark grey). <https://marine.copernicus.eu/access-data/ocean-monitoring-indicators/significant-wave-height-extreme-variability>. DOI: <https://doi.org/10.48670/moi-00214>

Significant Wave Height mean 99th percentile in the Black Sea region shows west-eastern dependence with largest values in the southwestern Black Sea, with values as high as 3.5 m, while the 99th percentile values in the eastern part of the basin are around 2.5 m. The 99th mean percentile for 2002-2019 shows a similar pattern demonstrating that the highest values of the mean annual 99th percentile are in the western Black Sea. This pattern is consistent with the previous studies, e.g. of [Akpınar and Kömürçü, 2012; and Akpınar et al., 2016]. The anomaly of the 99th percentile in 2020 is mostly negative with values down to ~-45 cm. The highest negative anomalies for 2020 are observed in the southeastern area where the multi-year mean 99th percentile is the lowest. The highest positive anomalies of the 99th percentile in 2020 are located in the southwestern Black Sea and along the eastern coast.

The map of anomalies for 2020, presenting alternate bands of positive and negative values depending on latitude, is consistent with the yearly west-east displacement of the tracks of the largest storms.

Besides, the Copernicus resources make wave height maps for specific dates accessible to users (Figure 4.40)

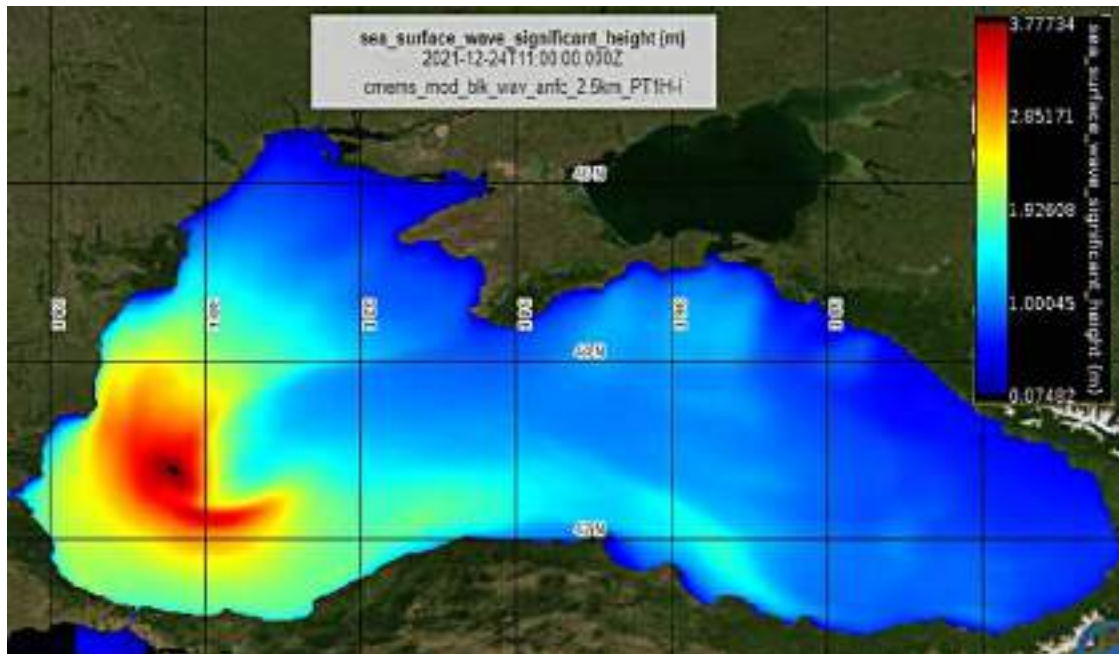


Figure 4.40 . The example of Sea surface wave significant height (SWH) daily maps over the Black Sea by the spectral wave model WAM (24.12.2021). Source: The Copernicus Marine Service portal, version of 2021, <https://resources.marine.copernicus.eu>

#### 4.6.5. Sea level

Sea level rise is a key indicator of climate change and helps to assess coastal erosion and accretion. Water level changes depending on season. Usually high level is observed in May-June and its drop — in October-November, at some places — in January-February. Difference between summer and winter level is 30—40 cm. These fluctuations of level mainly happen due to different river discharge in different seasons; that is why the fluctuations are the most pronounced in the areas suffering the rivers influence.

The significant in value non-periodical changes of level are wind-driven and connected with the development of certain atmospheric phenomena within a natural synoptic period, usually during 4—8 days. Wind-driven fluctuations of level differ between areas of the sea and seasons.

In the east, the biggest wind surges are caused by north-eastern and east-north-eastern winds, in the northwest — by the south-eastern. The biggest wind setdowns in the west and north-west are caused by west-north-western and northwestern winds.

The biggest wind-driven fluctuations of level (more than 30 cm) are observed in October—February in the western and northwestern parts of the sea. Seiches are well pronounced in the Black Sea level fluctuations, their period being from several minutes to 1—2 hours, their amplitude being usually up to 40—50 cm and a little more. Seiches of small (2—3 min) periods and amplitudes are mainly formed during waves in the open sea and at big waves' transformation in the coastal zone. Seiches of significant periods and amplitudes emerge at sharp fluctuations of atmospheric pressure and during passage of cyclones.

Construction of optimally interpolated and gridded (in both space and time) dynamical sea level data from altimetry [Korotaev et al., 2001] recently provided a new resource for increasing our present level of knowledge on variability of the Black Sea circulation.



They described the methodology for reconstruction of the dynamical sea level database for the period from May 1992 to November 1996, its validation by the available hydrographic survey data, and interpretation of the results by means of a simple two-layer analytical model of the wind-driven circulation in a rectangular basin.

According to the stations of northern coast, the average long-term Black Sea level for the period 1923-2005 is 477 cm [Ilyin et al., 2012]. The deviations from the average sea level make at some points from +7 to -2 cm. They are caused by the natural factors (water dynamics, features of up and down surges etc.), as well as by the peculiarities of level measurement methodology. The biggest positive deviations from the average level in the NWBS are observed in Odesa, Chornomorsk and Yevpatoriya (2, 7, 3 cm respectively), negative – in Khorly and Sevastopol (-2 and -3 cm). The difference in average annual values of level for the period 1875-2010 made 47 cm. The lowest level was registered in 1921 (450 cm), the highest – in 2010 (497 cm). Several cycles are pointed up in the longstanding level variability [Ilyin et al., 2012]. It is assumed, that since the beginning of observations in the Black Sea and until mid-20s of the 20<sup>th</sup> Century the sea level was relatively stable with slight tendency towards decrease, while since mid-20s of the 20<sup>th</sup> Century its increase showed itself distinctly [Byelokopytov, 2004]. At that, the longest sets of data for Constanta and Sulina show that the level was rising noticeably from 1858 until 1875. There are three visible cycles for the period, which is usually brought into correlation with the period of the World Ocean level rise in general: the first – almost continuing increase of the level (20s–60s of the 20<sup>th</sup> Century), the second – some stabilisation (70s-90s of the 20<sup>th</sup> Century), the third – the outlined in the 2000s new cycle in its growth. The tendency of the Black Sea level rise was pointed out for the first time in [Kubryakov et al., 2011], where it was estimated as 1.7 mm/year according to the data before 1970. The level rise due to eustatic factors minus the rate of vertical movements of the earth's crust was determined to be 1.7 mm/year. Later in [Oguz, et al., 1993] the intensity of the Black Sea level general rise was estimated to 1.83 mm/year. The most recent assessment of the trend value made for 5 stations of the Crimean coast for the period 1947-2006 gave a value of 2.3 mm/year with a trend span of about 14 cm. Comparison of altimetric and other data for the eastern part of Aegean Sea, Marmara and the part of the Black Sea adjacent to the Bosphorus has shown that the trend in the Black Sea is almost twice higher. So, it is unlikely that the current increase in the Black Sea level is due to the global rise of the World Ocean. In 2010 the Black Sea average level reached its historical maximum. The reasons are arguable. It is stated in [Bondar, 1989] that constant growth of the level during last decades did not depend on changes in water balance of the Black Sea basin rivers and was connected with general rise of the World Ocean level. In [Lappo et al., 1997] the magnitude of the Atlantic level trend was removed from the Black Sea data when they studied level variability in the Black and Caspian Seas. The authors came to the conclusion that both seas have similar character of level variability, which reveals itself in the level decrease from the beginning of the 20<sup>th</sup> Century till the 70s and increase from the 70s till 1985. According to them, short-period fluctuations in the Black Sea are caused by changes in the water balance constituents (mainly in river discharge), while the trend – by the long-period changes in the Atlantic Ocean level.

Presumably, the following main reasons could entail the long-term trend of the Black Sea relative level increase: general rise of the World Ocean level; increase of the positive constituent in the water balance; water density decrease (steric effect); increase in occurrence and amplitude of up and down surge; vertical movements of the earth's crust. Two last reasons can reveal themselves only in the data from coastal stations and are not described by altimetric observations. It is shown in [Goryachkin et al., 2006] that: the contribution of inter-annual changes in surge fluctuations cannot be responsible for the observed level increase; land subsidence prevails on the Black Sea coast, at an average rate close to 1 mm/year (except for the northwestern coast and the Kolkheti Lowland), which gives a seeming level increase of 1 mm/year and does not explain the magnitude of the observed trend. As for the first reason, the connection between the general rise in the level of the World Ocean and the Black Sea, which is often pointed out, is not so obvious.

Fluctuations of level in the NWBS happen at the background of its seeming rise as the result of real subsidence of the earth's crust. Odesa area is one of the parts of the coast where level rise rate due to this reason is close to the maximum for the Black Sea and makes 0.51 cm/year [Podprugina, 1972]. The eustatic fluctuations of the World Ocean level are smaller and do not exceed 0.2 cm/year.



The fluctuations of level with time intervals of decades are connected with fluctuations of water content in rivers [Goryachkin, Ivanov, 1996] in line with ending of atmospheric circulation epochs, which, in their turn, correspond to alternations in solar activity. Inter-annual and seasonal changes in sea level are determined by the ratio of water balance components: continental runoff; atmospheric precipitation; evaporation; water exchange of the Black Sea with the Azov and Marmara Seas. The levels exceeding the long-term average value 10-11 cm are observed in April-June. The biggest share of river discharge also falls on this period. Then river discharge decreases, while evaporation increases significantly, which brings to decrease of level 8-9 cm below the long-term average by autumn. The average long-term range of sea level seasonal changes in Odesa area is 19 cm. Maximal changes of sea level in the coastal zone are non-periodic and caused by strong, directionally stable and long-lasting surge winds. At negative and positive surges 30-40 cm changes of level are observed with the average speed of 2-6 cm/hour. Sometimes rises and drops in level are very intensive and their speed is 20-25 cm/hour. Maximal changes of level in Odesa Port were 100 cm at positive and 175 cm at negative surge. Along with surges, seiche variations of sea level are observed in Odesa Port and the Odesa Bay. These free oscillations happen at sharp changes of atmospheric pressure, wind speed or wind direction: water masses, previously unbalanced as the result of the influence of atmospheric pressure gradient forces and (or) shear wind stress, return to the equilibrium state through damper oscillations. One-knot seiche for the entire sea provides a 7-6 cm range of oscillation at the period of ca. 10 hours in the area of Odesa. Periods of seiches in different parts of the sea makes in Odesa area from 5 min to 2 hours; the range of oscillations of sea level reach 45 cm. The tides that form in the Black Sea itself are small but noticeable, especially in the NWBS. The semidiurnal tides are more pronounced. According to the literature data [Hydrometeorology..., 1991], the average tide is 14 cm, and in quadrature - about 3 cm. The maximum tide value is observed in the Odesa Bay, where it can reach 17 cm.

**Time series of mean sea level trends** over Black sea are derived from the DUACS delayed-time altimeter gridded maps of sea level anomalies based on a stable number of altimeters (two) in the satellite constellation. These products are distributed by the Copernicus Climate Change Service. The mean sea level evolution estimated in the Black Sea is derived from the average of the gridded sea level maps weighted by the cosine of the latitude. The annual and semi-annual periodic signals are adjusted and the time series is low-pass filtered. Mean sea level evolution has a direct impact on coastal areas and is a crucial index of climate change since it reflects both the amount of heat added in the ocean and the mass loss due to land ice melt [Dieng et al., 2017]. Long-term and inter-annual variations of the sea level are observed at global and regional scales. They are strongly related to the internal variability observed at basin scale and these variations can strongly affect population living in coastal areas. Using the latest reprocessed altimeter sea level products, it is possible to estimate the sea level rise in the Black Sea since 01/1993. The Black Sea is a relatively small semi-enclosed basin with shallow bathymetry, which explains the high level of inter annual variability observed in the sea level record compared to large, deeper and open ocean areas.

Mean sea level daily evolution Jan-1993 to Jun-2020 (Figure 4.41) can be used as a good example of using the daily sea level maps accumulated in the COPERNICUS database for the purposes of the PONTOS project.

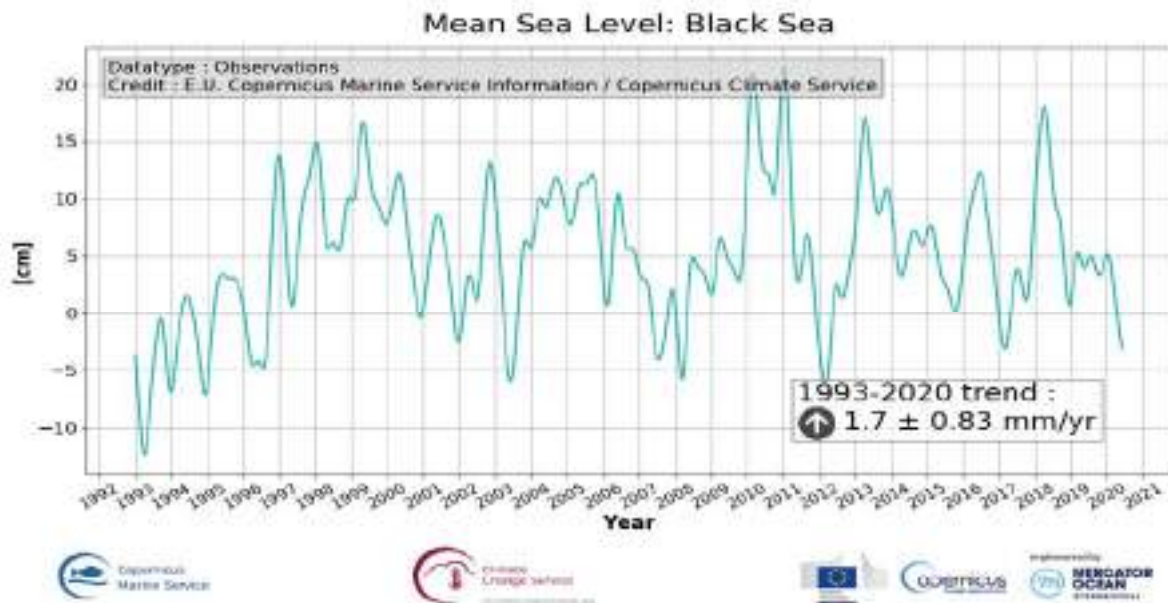


Figure 4.41. Mean sea level daily evolution Jan-1993 to Jun-2020 (in cm) from the satellite altimeter observations estimated in the Black Sea, derived from the average of the gridded sea level maps weighted by the cosine of the latitude. The timeseries is low-pass filtered, the annual and semi-annual periodic signals are adjusted (<https://marine.copernicus.eu/access-data/ocean-monitoring-indicators/time-series-mean-sea-level-trends-over-blacksea>) DOI (product): <https://doi.org/10.48670/moi-00215>

Mean sea level daily evolution since January 1993 (in cm) from the satellite altimeter observations estimated in the Black Sea, derived from the average of the gridded sea level maps weighted by the cosine of the latitude. The timeseries is low-pass filtered, the annual and semi-annual periodic signals are adjusted, and the curve is corrected for the GIA using the ICE5G-VM2 GIA model [Peltier, 2004]. Mean sea level evolution has a direct impact on coastal areas and is a crucial index of climate change since it reflects both the amount of heat added in the ocean and the mass loss due to land ice melt [IPCC, 2013; Dieng et al., 2017]. Long-term and inter-annual variations of the sea level are observed at global and regional scales. They are strongly related to the internal variability observed at basin scale and these variations can strongly affect population living in coastal areas. Using the latest reprocessed altimeter sea level products, it is possible to estimate the sea level rise in the Black Sea since 01/1993 (see the proposed figure of the indicator for the updated trend value). The associated uncertainty is provided in a 90% confidence interval and only errors related to the altimeter observation system have been considered in the sea level trend uncertainty [Prandi et al., 2021]. The uncertainty due to the sea level internal variability of the observed ocean is not included and should be considered additionally. The Black Sea is a relatively small semi-enclosed basin with shallow bathymetry, which explains the high level of inter annual variability observed in the sea level record compared to large, deeper and open ocean areas as North West Shelf.

#### 4.7 Coastal Zone of North-western part of the Black Sea (NWBS)

The information about abrasion and accretion processes in coastal zone of the NWBS we used from national historical data and from EMODNET sources.

##### 4.7.1 NWBS Coasts abrasion and accretion

The Black Sea coast is formed under the influence of many factors and under different conditions, which caused the diversity of the coasts. There are 14 main types of coasts in the north-western Black Sea illustrated in Figure 4.42 [Atlas, 2006].



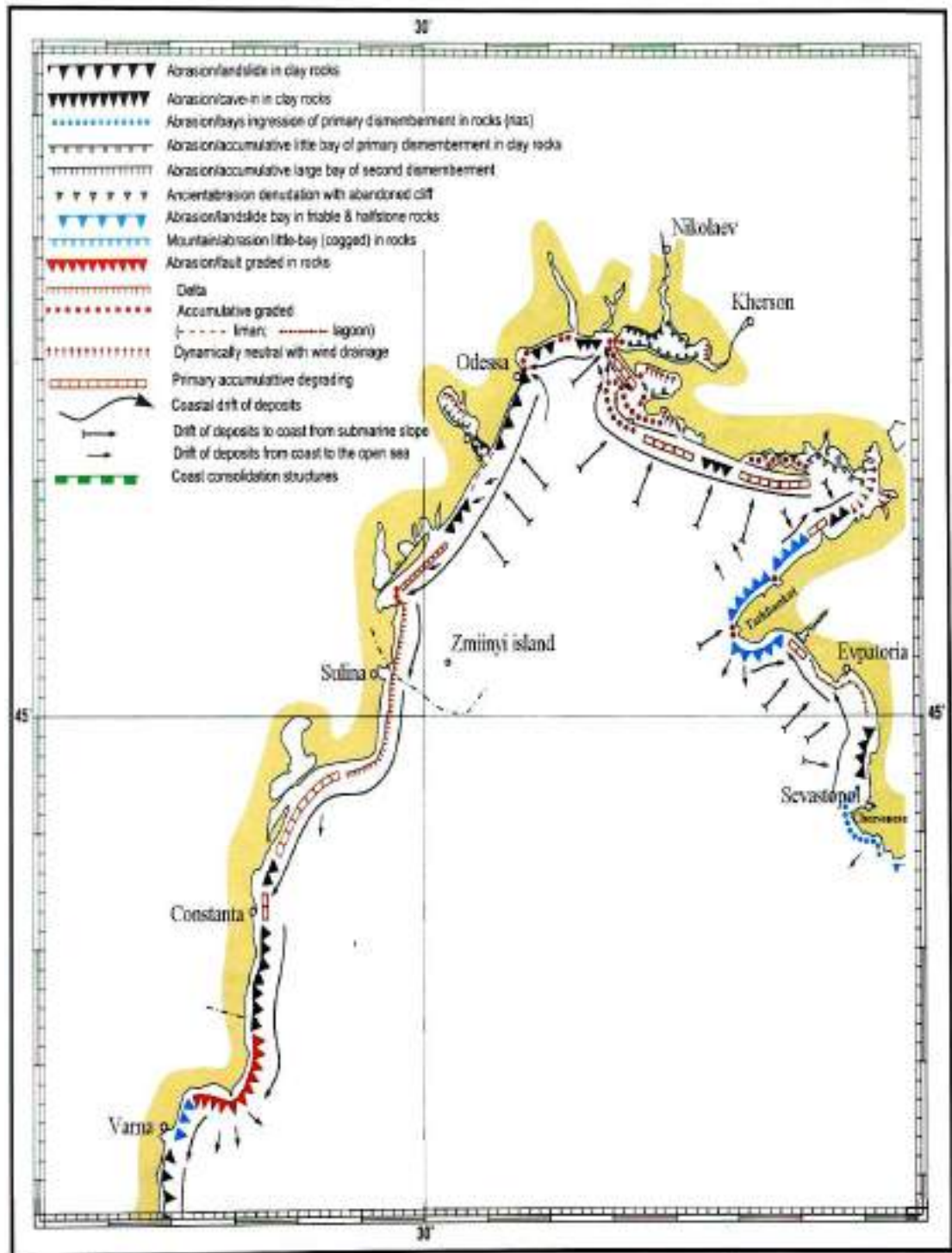








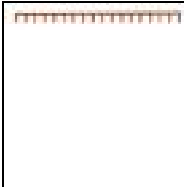
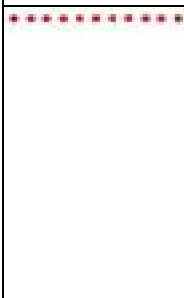
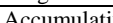
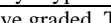

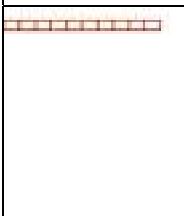



Figure 4.42. NWBS types of Coasts [Atlas, 2006]

**Table 4.21. Description of main types of coasts in the north-western Black Sea**

Legend	Coasts Types
	Abrasion/landslide in clay rocks. Their height exceeds 20 m, they are built mainly of Quarternary, sometimes Paleogene – Neogene muddy massif material interbedded by half-rock and rock. Gradient of underwater slope on such segments is 0,01 to 0,05. Speed of coastline recession is 0,1 – 2,0 m/year. Development of such coasts takes place under deficit of sediments (Atlas, 2006; Shuiskiy, 2000).
	Abrasion/cave-in in clay rocks. One of the most wide-spread abrasion forms of relief in the north-western Black Sea. Intensity of wave processing of this coast type is regulated by accumulation of sediments, geological construction, gradient of underwater slope and form of coastline. Speed of coastal regression varies within broad range – from 0,5-0,6 m/year (height of cliff seldom exceeds 20 m) to 70-80 m in elevated and mountainous areas. Speed of bench deepening on underwater slopes is 0,010 to 0,059 m/year [Atlas, 2006; Shuiskiy, 2000].
	Abrasion/bays ingression of primary dismemberment in rocks rias (Atlas, 2006). This is a result of erosion-tectonic dissection of the western side (flank) of the Mountainous Crimea anticlinorium [Geology of the USSR, 1969] and the Tarkhankut Elevation. Active cliffs and alluvial terraces on protruding corner parts of raises are characteristic of such coasts. The cliffs are up to 50 m high, often 5-7, at some segments of the coasts slopes submerge completely. Coastal slopes are stable, of rock (mainly of chalkstones). Speed of cliff abrasion is 0,05-0,15 m/year, maximum 0,5 m/year (Figure 8). Steepness of underwater slope down to the depth of 7 m is 0,03 to 0,09. Average speed of bottom abrasion is up to 0,02 m/year [Shuiskiy, 2000].
	Abrasion/accumulative little bay of primary dismemberment in clay rocks [Atlas, 2006]. This is characteristic of segments of coasts of limans (estuaries), bays and lagoons. Coastal processes develop weakly, under conditions of underwater slope small steepness (<0,007), low wave energy potential and significant influence of wind-induced oscillations of sea level. Sharp deficit of sediments prevails; there are practically no flows of sediments along the coast. Non-wave processes of coastal zone development and stable forms of relief dominate. Cliffs have small length; they are semiactive and interchange with denudation slopes, alluvial terraces and “pocket” beaches at relatively straight contour of coastline. Speed of abrasion is less than 0,7 m/year and of benches – less than 0,015 m/year within very narrow alongshore stripe [Shuiskiy, 2000].
	Abrasion/accumulative large bay of second dismemberment. These are mainly upper reaches of the Dnister Liman (Estuary), segments between the Dnipro-Bug Liman (Estuary) and the Perekop Bay. This type of coast is represented by two groups of relief forms: a) abrasion-avalanche abrasion-landslip of different height and steepness formed in rocks, clayey and sandy material; b) accumulative spites and terraces. There also are transitional forms of non-wave origin in the form of alongshore flows and transverse migration of sediments of different capacity. This type of coast is the most complicated compared to other types. In general, it has unified genetic and morphological & dynamic properties, however, its separate constituents have significant differences. For example, interchanges of rock and sandy-clayey matter in transect along the coast cause selective abrasion. As the result, secondary forms of dissection form because of different speeds of abrasion [Shuiskiy, 2000].
	Ancient abrasion denudation with abandoned cliff. This is pervasive in the form of short segments (less than 10 km). Faded cliffs and wave-built alluvial terraces that frame cliff foot (width exceeding 100 m) are characteristic forms of relief. Height of a faded cliff usually less than 20 m. This type of coast is often a constituent of other types of coast.
	Abrasion/landslide bay in friable & halfstone rocks. These are formed in damaged, clastic, weak rocks and sedimentary rocks. Dominant element is high cliff (higher than 25 m). Widespread are landslide amphitheatres and circuses with pronounced landslide terraces, small “pocket” beaches. Most often a cliff is formed in deluvium of clay loam and fragmentary material (rotted rock). Medium speed of abrasion varies from 0,01 m/year in clay rock of Tauric type to 2,9 m/year in deluvium formed by clay loam. Volume of washed off fragmentary material is 0,3 – 35,8 m <sup>3</sup> /m-year [Shuiskiy, 2000].
	Mountain/abrasion little-bay (cogged) in rocks. This type is widespread in strong abrasion resistant rock (chalk and Paleogene - Neogene chalky clay, limestone, greenstone, sandstone). Active cliffs over 100 m high are characteristic of this type. Abrasion speed is less than 0,01-0,02 m/year, in places there is no abrasion at all. Practically no accumulative forms of relief could be found with this type of coast.

	Delta. Deltaic type of coast is widespread along sea marginalia of the delta of the Danube, the Dnipro, the Dnister and small rivers. It develops as the result of interaction between river and sea hydrogenous factors. Wave energy is incapable to process the entire mass of river sediments, as the result alluvial cones of river delta appear [Korotaev, 1991; Mikhailov et al., 1977; Mikhailov et al., 1986], accumulation of fragmentary material takes place up to 2-3 m/year, in some segments of the Danube Delta – up to hundreds m/year. The share of river sediments in general denudation discharge of sedimentary material is not big and influences the development of coastal zone insignificantly. Typical forms of relief are underwater and overwater spites, wave-cut and fore-estuarine bars.
	Accumulative graded. There are two types:  liman (estuarine);  lagoon. Those make ½ of all the accumulative coasts. Limans and lagoons are the basic constituents of this type of coast. The main elements are bars, barrier beaches, spits, cliffs, benches, terraces and other linear alluvial forms. Forming of limans and lagoons is closely connected with the beginning and further development of Holocene transgression. Formation of primary contour of shoreline took place with subsequent transformation into ingressive bays that were later cut off from the sea by barrier beaches (spites, bars). This type of coast goes along destructive way of development due to which significant part of abrasion shelf was reformed [Zenkevich, 1958; Nevevskiy, 1967; Shuiskiy and Vykhoanets, 1989]. Speed of recession of abrasion and accumulative coastlines is 0,003 to 0,1 m/year within the depth 0-5 m. In the north-western part of the coast a classical liman type of shore has formed [Zenkevich, 1958; Zenkevich, 1962; Leontiev, 1961; Mikhailov et al., 1977; Mikhailov et al., 1986].
	Dynamically neutral with wind drainage. These are developed in the shallow part of the Dnipro-Karkinitzkiy area of the Black Sea. They are characterized by increased amplitudes of wind-induced oscillations of sea level. Wind-induced events up to 2,83 m are typical for the area. The main elements of relief of this coast type are pits and channels for wind-driven water, small spites and terraces of sandy and shelly material, low-level cliffs and benches. Mean height of a cliff is 1-2 m, maximum 15,2 m. Speed of abrasion of cliffs is 0,2-0,4 m/year (maximum up to 1,8 m/year in some years).
	Primary accumulative degrading. These include complexes of different separate forms subdued to active reformation in the direction of dynamic equilibrium. Intensive washing-out takes place with coastline recession. These forms accumulated in the past on the coast and underwater slope, seaward movement of coastline took place. Forming of sediments deficit in the coastal zone happened during last several hundred years [Zenkevich, 1958; Zenkevich, 1962; Shuiskiy, 1986; Shuiskiy and Vykhoanets, 1989]. Accumulative forms have lost their properties of real concentration and now are being washed out. Often they are strongly degraded. They are represented by spites, bars, barrier beaches and terraces which often interchange with cliffs, benches, Aeolian and biogenic forms. Speed of abrasion in different makes 0,9- 3,1 m/year to 5,5 m/year.
	Abrasion/fault graded in rocks. They are formed by tectonic processes, weakly subject to the influence of sea, developed in other rocks resistant to abrasion. The continental slope is corbelled out and abrupt. The height of cliff is up to 15-20 m. Abrasion speed is 0,1-0,2 m/year.

#### 4.7.2. Black Sea Coastal behavior from EMODNET

1 The EMODNET portal is a very important source of information on the types of coasts and shoreline migration. It contains information about coastal behaviour (<https://www.emodnet-geology.eu/data-products/coastal-behavior>), which refers to the movement of the coastline in a landward (through submergence or erosion) or seaward (through emergence or accretion) direction. EMODnet Geology provides two pan-European maps, one based on field monitoring and comparison of aerial photographs, and the other based on satellite data - ([https://emodnet.ec.europa.eu/sites/emodnet.ec.europa.eu/files/public/PDF/20210318-EMODnet\\_Geology-Coastal\\_Erosion-Press\\_Release\\_FINAL.pdf](https://emodnet.ec.europa.eu/sites/emodnet.ec.europa.eu/files/public/PDF/20210318-EMODnet_Geology-Coastal_Erosion-Press_Release_FINAL.pdf) ; New EMODnet Geology map on coastal type - Increased coverage for the 2004 pan-European shoreline-migration map. NEWS ARTICLE | 27 May 2021 - <https://emodnet.ec.europa.eu/en/new-emodnet-geology-map-coastal-type-increased-coverage-2004-pan-european-shoreline-migration-map>)

Using the information from the above-mentioned portal, we built the maps of coastal types and shoreline migration for the north-western Black Sea.

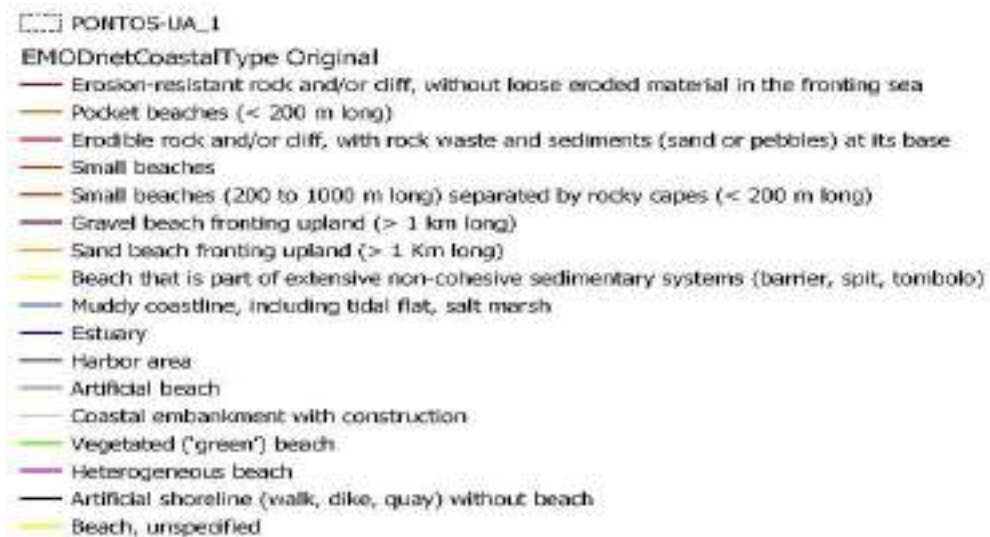
##### 4.7.2.1 NWBS Coastal type map

The NWBS coastal type map is build on the base of the EUROSION [Lenôtre et al. 2004] map of coastal type released almost twenty years ago (Figure 4.43) It gives a first-order indication of vulnerability and resilience for policy makers, identifying areas of potentially irreversible future change.

This important data product allows users to visualise coastal type at different spatial scales and to distinguish areas marked by rocky coasts, (pocket) beaches of sand and gravel, muddy tidal basins and estuaries, and man-made coastlines such as harbours and dams.



**Figure 4.43.** Coastal type map of the northwestern part of the Black Sea. **Source:** The EMODnet-Geology coastal type map, version of 2021, <https://www.emodnet-geology.eu/data-products/>



Analysis of the Fig. 4.43 has shown that the following coastal types prevail (83%) in the NWBS (Table 4.19):

- Heterogeneous beach;
- Beach that is part of extensive non-cohesive sedimentary systems (barrier, spit, tombolo);
- Muddy coastline, including tidal flat, salt marsh;
- Sand beach fronting upland.

Table 4.19. Types and lengths of shores in the northwestern part of the Black Sea and in the PONTOS-UA\_1 pilot site

Coastal type	NWBS, Lengths, km	NWBS, Lengths, %	PONTOS- UA_1, Lengths, km	PONTOS- UA_1, Lengths, %
Heterogeneous beach	607.0	28.2	39.5	15.4
Beach that is part of extensive non-cohesive sedimentary systems (barrier, spit, tombolo)	504.1	23.5	70.0	27.3
Muddy coastline, including tidal flat, salt marsh	390.3	18.2	1.5	0.6
Sand beach fronting upland (> 1 Km long)	288.4	13.4	38.9	15.2
Estuary	117.0	5.4	64.5	25.2
Erosion-resistant rock and/or cliff, without loose eroded material in the fronting sea	86.9	4.0		
Erodible rock and/or cliff, with rock waste and sediments (sand or pebbles) at its base	44.5	2.1		
Vegetated (green) beach	41.3	1.9	0.6	0.2
Harbor area	23.6	1.1	23.1	9.0
Artificial shoreline (walk, dike, quay) without beach	20.8	1.0	12.9	5.0
Small beaches (200 to 1000 m long) separated by rocky capes (< 200 m long)	15.9	0.7	1.9	0.7
Gravel beach fronting upland (> 1 km long)	6.1	0.3	1.5	0.6
Artificial beach	3.9	0.2	1.8	0.7

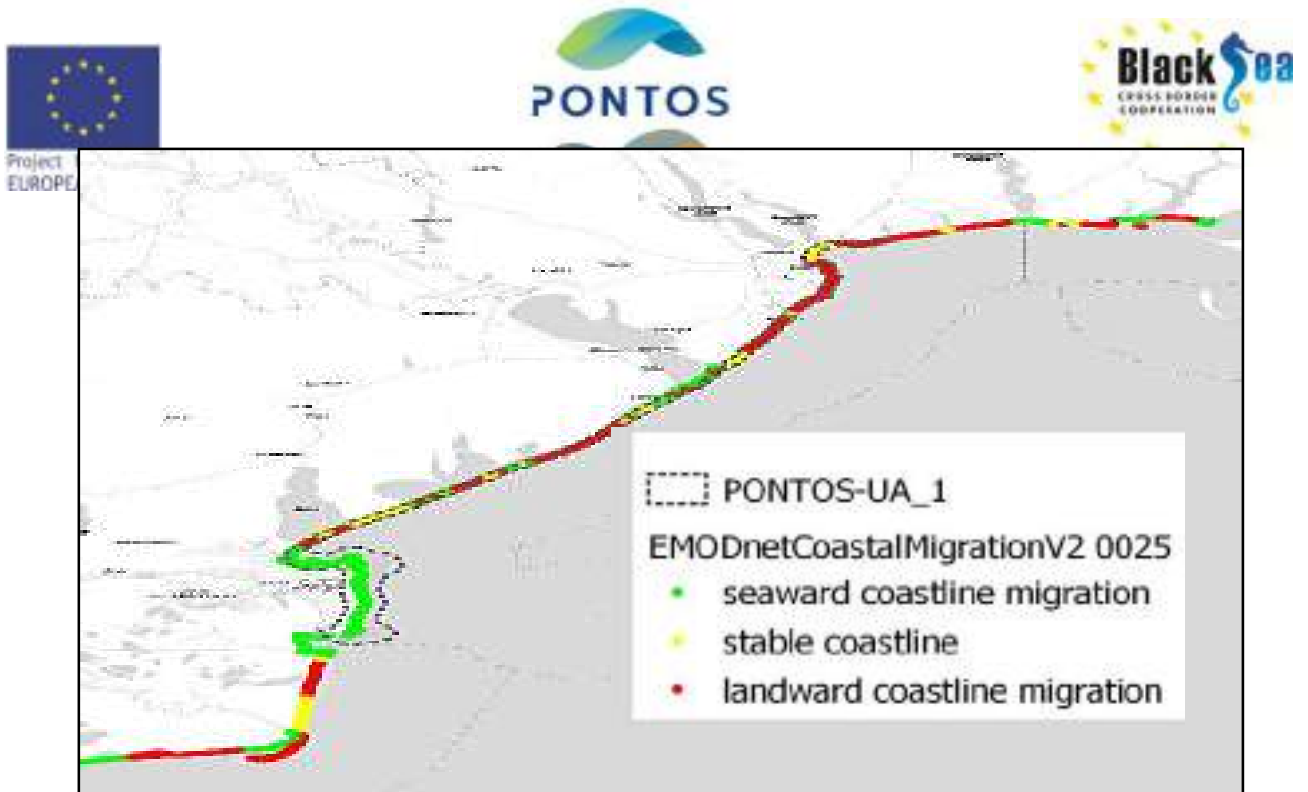
The prevailing within the PONTOS-UA\_1 pilot site (92%) coastal types are:

- Beach that is part of extensive non-cohesive sedimentary systems (barrier, spit, tombolo);
- Estuary;
- Heterogeneous beach;
- Sand beach fronting upland;
- Harbor area.

At that, one of the main characteristic features of the Ukrainian pilot site is significant input of the big rivers' estuaries. There the length of different beach types makes ca. 60% compared to 68% for the entire NWBS. At the same time percentage of coastline containing port infrastructure in the PONTOS-UA\_1 site grows significantly (by 8%).

#### 4.7.2.2 NWBS Shoreline migration map

This shoreline-migration map (Figure 4.44) allows policy and decision makers to assess large-scale coastal behavior and identify areas of significant erosion. It is based on field measurements and aerial photography, and covers time periods up to decades. The map is particularly valuable for cliffs, which are prevalent along European coastlines, since state-of-the-art satellite-monitoring methods aren't yet suitable for imaging erosion of non-sandy types of coastline.



**Figure 4.44.** Coastline migration map of the northwestern part of the Black Sea  
**Source:** The EMODnet-Geology coastline-migration map, version of 2021, <https://www.emodnet-geology.eu/data-products/>

Analysis of the map presented (Fig. 4.44) has shown that landward coastline migration (erosion) type prevails in the NWBS – 57% (Table 4.20), while within the PONTOS-UA\_1 pilot site seaward coastline migration (accretion) type is prevailing (49%) in the coastline migration, i.e. accumulative processes dominate in the PONTOS-UA\_1 site.

Table 4.20. Coastline migration types and lengths in the northwestern part of the Black Sea and in the PONTOS-UA\_1 pilot site

Coastline migration type	NWBS, Length, km	NWBS, Length, %	PONTOS-UA_1, Length, km	PONTOS-UA_1, Length, %
Stable coastline	74,6	14,6	36,0	15,6
Landward coastline migration (erosion)	291,3	57,1	81,3	35,3
Seaward coastline migration (accretion)	143,7	28,2	113,0	49,1

#### 4.7.2.3 NWBS Coastal behavior from satellite data

The shoreline is a highly dynamic land-sea interface that provides important services such as ecology, flood protection and recreation. It is constantly modified by wind, waves and tides, and impacted by human activity. Hence, the decadal change of shorelines reflect natural processes as well as human influence, whether positive or negative. Climatic-driven changes such as sea level rise, higher waves and changes in wind direction put increasing pressure on many of Europe’s shorelines. The EMODnet Geology shoreline-migration map (Figure 4.45). , based on satellite data, allows users to visualise pan-European coastal behaviour for 2007-2017 at different spatial scales.

The underlying, downloadable satellite-based dataset offers additional information on annual values and uncertainty. Thanks to the public availability of satellite data (optical imagery of ESA Sentinel 2 and NASA Landsat 5, 7 & 8 with pixel resolutions of 10-30 metres and a revisit time of 1 to 2 weeks) and new analytical tools for processing big data (such as the Google Earth Engine). The EMODnet Geology team in collaboration with Deltares and TNO (Geological Survey of the Netherlands) were able to quantify shoreline migration in a new way. Scripts for automated detection of the land-water boundary were used to separate land from water in annual image composites for the period 2007-2017. During this process, shorelines positions were determined for half a million transects every 500 metres along the European shoreline. These positions were then averaged by year and analysed for a decadal period. As part of EMODnet-Geology, Gerben Hagenaars at Deltares performed an analysis for tens of thousands of transects with a spacing of 500 meters, giving a map resolution of 1:1,000,000.

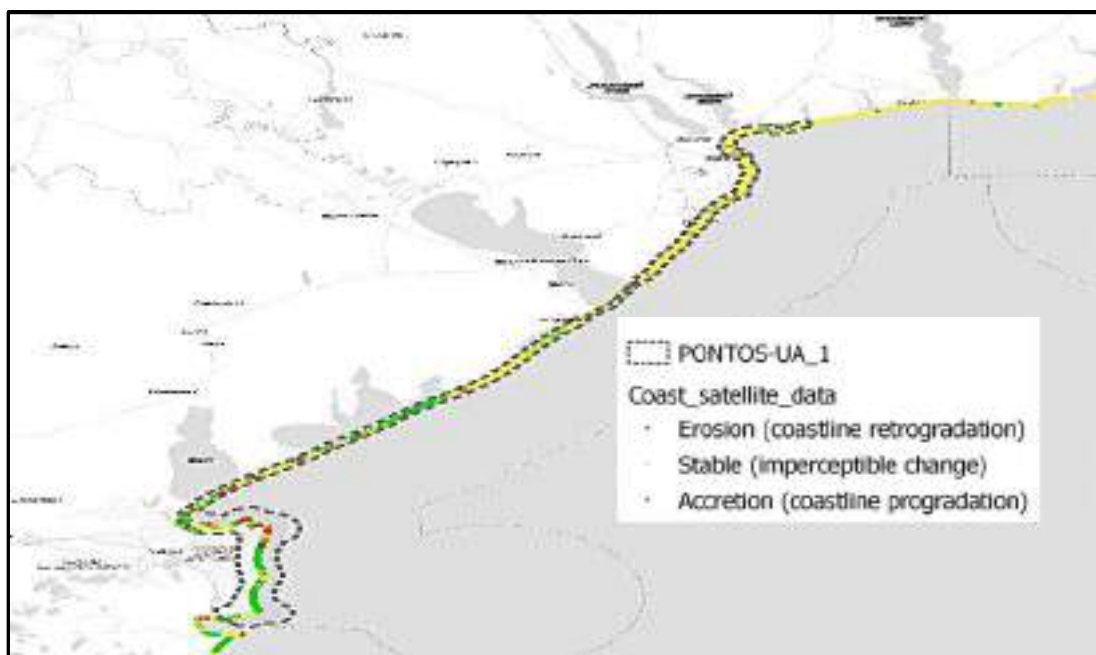


Figure 4.45. Coastal behavior from satellite data map of the northwestern part of the Black Sea. Source: The EMODnet-Geology coastal behavior from satellite data, version of 2021, <https://www.emodnet-geology.eu/data-products/>

Analysis of the map presented (Fig. 18) has shown that stable coastline type (70%) prevails in the NWBS (Table 4.21). Within the PONTOS-UA\_1 pilot site this coastline type stays dominant, however decreases to 61%.

Table 4.21. Coastline migration types and lengths from satellite data map in the northwestern part of the Black Sea and in the PONTOS-UA\_1 pilot site

Coastline migration type	NWBS, Length, km	NWBS, Length, %	PONTOS-UA_1, Length, km	PONTOS-UA_1, Length, %
Stable coastline	879.1	69.8	125.4	61.1
Landward coastline migration (erosion)	221.2	17.6	18.8	9.2
Seaward coastline migration (accretion)	159.7	12.7	61.0	29.7

## 5. Results of Coastal Erosion and Accretion Analysis

### 5.1. Coastal Erosion Analysis

The methodology applied to assess and define the coastal erosion activity and identify the coastal erosion “hotspots” along the coastal Zone in Ukrainian pilot area PONTOS UA1 (total length approximately 270 m) was based on the shoreline movement analysis by processing historical satellite images, using remote sensing techniques using DSAS [Himmelstoss et al, 2021] and ARCGIS software. The analysis was applied for the time period (1980-2020), analyzing historical satellite products (Landsat and Sentinel imagery) with a different spatial resolution (30 and 10 m, respectively).

The **shoreline movement analysis covers a 40 years period (1980 to 2020)** in a 5-year time step. For this analysis, satellite images from Landsat 3 MSS, Landsat 4-5 TM, Landsat 7 ETM+ and Sentinel 2 collection databases were used. The spatial resolution of the Landsat satellite image bands Green and NIR is 30 m, and they retrieved from the Earth Explorer (USGS database) and the spatial resolution of the Sentinel 2 satellite image bands Green and NIR is 10 m, and they retrieved from the Copernicus Open Access Hub database. The results of the coastal erosion analysis are presented according to the geographical sub-areas (Figure 5.1): UA1-1: Danube Delta area; UA1-2: Sasyk estuary area; UA1-3: Sasyk estuary – Budakskiy estuary area; UA1-4: Budakskiy estuary – Sukhiy estuary area; UA1-5: Sukhiy estuary – Great Adzhalyk estuary (Odessa bay) area



**Figure 5.1.**

Ukrainian sub-areas as divided along the PONTOS UA1 pilot area.

1.- UA1-1: Danube Delta area; 2.- UA1-2: Sasyk estuary area; 3.- UA1-3: Sasyk estuary – Budakskiy estuary area; 4.- UA1-4: Budakskiy estuary – Sukhiy estuary area; 5.- UA1-5: Sukhiy estuary – Great Adzhalyk estuary (Odessa bay) area

The main statistical parameters which we used for designation the shoreline movement Using DSAS software [Himmelstoss et al, 2021]:

- The **Shoreline Change Envelope (SCE)** represents the greatest distance among all the shorelines that intersect a given transect (units are in meters).

- The **Net Shoreline Movement (NSM)** represents the distance between the oldest and the youngest shorelines for each transect (units are in meters).

- The **Weighted Linear Regression (WLR)** represents a weighted linear regression applied on the most reliable data placing greater emphasis or weight towards determining a best-fit line. In the computation of rate-of-change statistics for shorelines, greater emphasis is placed on data points for which the position uncertainty is smaller (units are in meters/year).

Additionally, the **estimation of the land change** (in km<sup>2</sup>), in all sub-areas, by the time elapsed between the oldest and the latest shoreline was estimated and presented in the following sections.



## 5.2. Subarea UA1-1 (Danube Delta)

Subarea UA1-1 (Danube Delta) covers the 72.3 km long shoreline in the Danube Delta (Fig. 5.1) that stretches from the border between Ukraine and Romania (the Limba Island) to the Zhebriians'ka Bay (Village Primors'ke). The Danube Delta area is characterised by the lowland wetlands – the reed beds with a dense network of the Danube arms, deltaic lakes and islands. The delta acreage is changing all the time due to sediments inflow from the basin and the shoreline in this area is constantly displacing seaward (eastwards). The maps of coastal area changes in the Danube Delta (UA1-1 subarea) and the distribution of the main statistical characteristics of the shoreline dynamics (WLR (m/year), SCE (m) and NSM (m)) for 1980-2020 are presented on Fig. 5.2. -5.4.

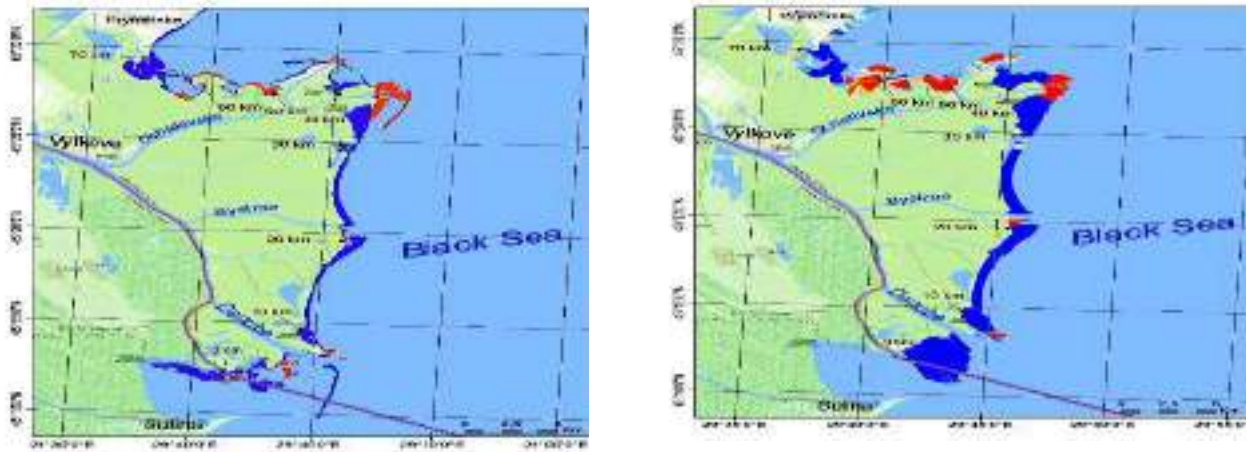


Figure 5.2. Maps of coastal area change in Danube Delta (UA1-1 subarea) .  $\rightarrow$  km distance,  $\equiv$  state borders. Left – Dynamics of shoreline for 1980-2020: ■ Erosion, ■ Accretion. Right – Distribution of WLR (Weighted Linear Regression Rate) for 1980-2020, m/year: ■ High Erosion ( $< -2$  m/year), ■ Medium Erosion( $-2 - -0,5$  m/year), ■ Stable Coastline( $-0,5 - 0,5$  m/year), ■ Medium Accretion( $0,5 - 2$  m/year), ■ High Accretion ( $>2$  m/year).

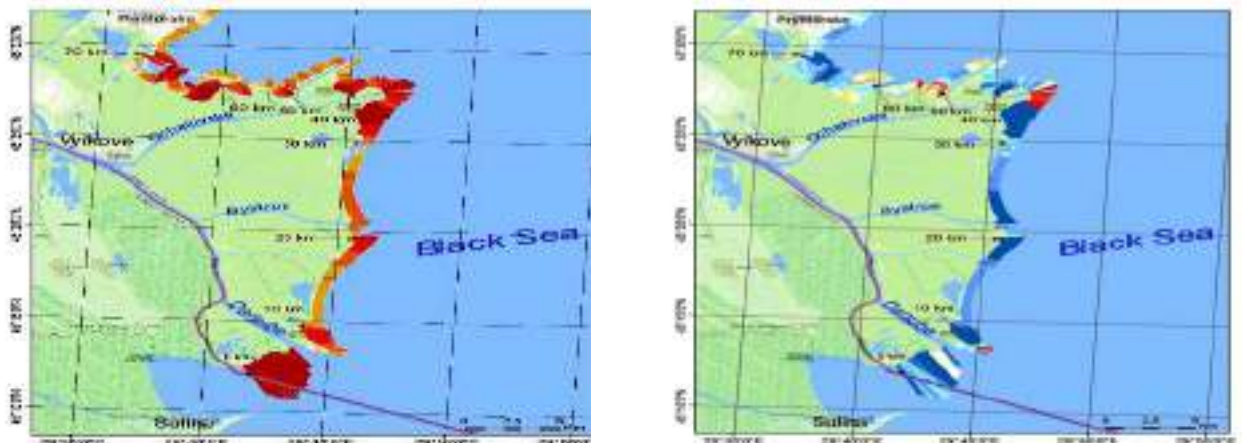


Figure 5.3. Distribution of statistical parameters (Left - SCE, Right – NSM) picture) by transects along the shoreline for Danube delta (UA1-1 subarea) for the period 1980-2020.  $\rightarrow$  km distance ,  $\equiv$  state borders. For SCE values: ■ 0- 20 m, ■ 20-50 m, ■ 50-100 m, ■ 100-250 m, ■ 250-500 m, ■ 500-1000 m, ■  $>1000$  m. For NSM values: ■  $< -250$  m, ■  $-250- -100$  m, ■  $-100$  m-  $-20$  m, ■  $-20- 20$  m, ■ 20- 100 m, ■ 100-250 m, ■  $>250$  m.

In Figure 5.4. presented the distribution of of the main statistical parameters (SCE, NSM, and WLR) results calculated by the DSAS tool to the shoreline transects.

Analysis of data on the mean position of the shoreline for the period 1980 - 2020 (Fig. 5.5), which was built using the data from the Fig. 5.4, has shown that in the period from 1980 to 2020 the averaged for every 5-year period values of the shoreline migration (accretion/erosion) intensity varied within the limits from -81.61 m (2010-2015) to 112.98 m (2005-2010) with the average for 1980-2020 value of 24.85 m.

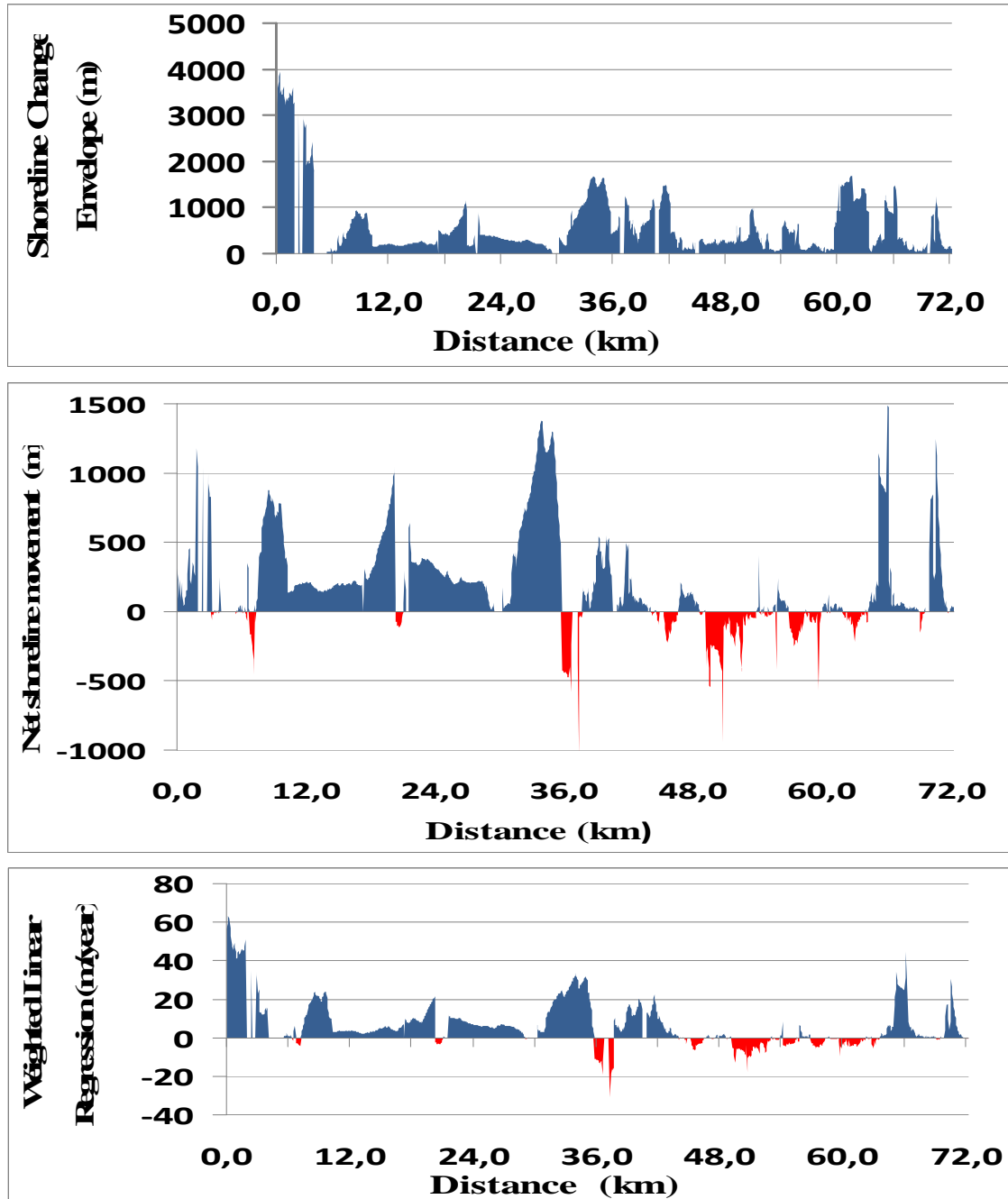


Figure 5.4. Spatial distribution of the estimated statistical parameters (SCE, NSM, and WLR) by transect along the shoreline for Danube delta area (UA1-1 subarea). : ■ Erosion, ■ Accretion.

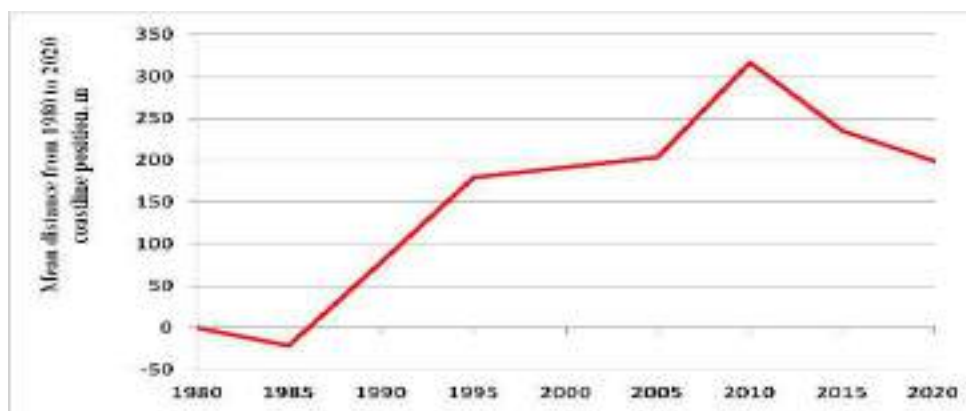


Figure 5.5. Temporal variability of the average (for every 5 years) shoreline position (m) in the Danube Delta (subarea UA1-1) from 1980 to 2020.

Table 5.1. presents the averaged for every 5-year period data on the annual mean change rate (m/year) received as the result of 1121 transects processing. We also calculated the values of increasing/decreasing coastal zone acreage and the new islands in the deltaic Black Sea area (Fig. 5.5 and 5.6). Their analyses have shown the following.

Table 5.1. Table of the annual mean shoreline change rate (m/year) covering 5-year periods

Class/time frame	No. of Transects	Average annual value of mean change rate, (m/year)	STD Error	Increase (+)/decrease (-) of the coastal zone area (km <sup>2</sup> )	Increase (+)/decrease (-) of the area of new islands in the Black Sea near the Danube Delta (km <sup>2</sup> )	Total (km <sup>2</sup> )
1980-1985	1121	-4,37	0,82	-1,581	0	-1,581
1985-1990	1121	20,19	1,73	+7,300	0	+7,300
1990-1995	1121	20,13	1,85	+7,265	0	+7,265
1995-2000	1121	2,49	2,29	+0,901	+1,452	+2,353
2000-2005	1121	2,42	2,31	+0,874	+0,560	+1,434
2005-2010	1121	22,60	2,66	+8,168	-0,076	+8,092
2010-2015	1121	-16,32	2,63	-5,901	+1,132	-4,769
2015-2020	1121	-7,34	1,32	-2,653	+0,551	-2,102
1980-2020	1121	4,97	1,95	+14,374	+3,619	+17,993

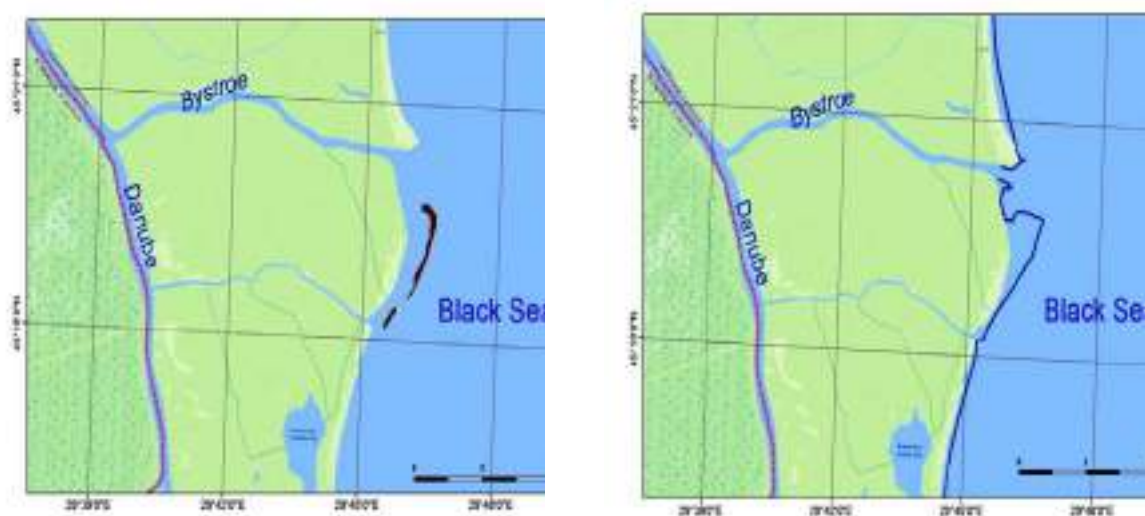


Fig. 5.6. Location of the Ptashyna Kosa Island in 2000 (left) and in 2020 (right)

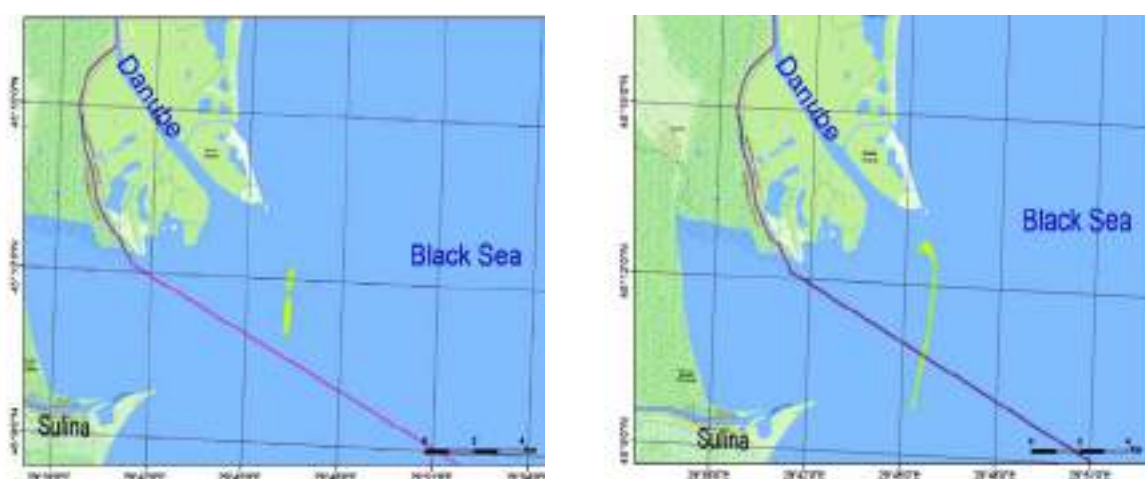


Fig. 5.7. Location of the Nova Zemlya Island in 1996 (left) and in 2020 (right)

Average annual values of the shoreline changes were within the limits from -16.32 m/year (2010-2015) to 22.60 m/year (2005-2010) at mean for 1980-2020 value of 4.97 m/year. At that the Danube Delta area grew 14.374 km<sup>2</sup> for 1980-2020. The acreage of the Nova Zemlya and the Ptashyna Kosa Islands (Fig. 5.6 and 5.7) also grew 3.619 km<sup>2</sup>. Thus the total terrain area in the Danube Delta has grown almost 18 km<sup>2</sup> for the period 1980-2020.

Analysis of the data on the mean shoreline position from 1980 to 2020 presented on Fig. 5.5 has shown that in that period the values of the shoreline migration intensity averaged for the 5-year periods (accretion/erosion) varied from -81.61 m (2010-2015) to 112.98 m (2005-2010) with the mean for 1980-2020 value of 24.85 m or from -4.37 (2010-2015) to 22.60 m/year (2005-2010) with the mean value of 4.97 m/year.

At that, we should point out that the range of the shoreline migrations averaged for 5-year periods made ca. 339 m with maximal deviation (+317.5 m) in 2005-2010 and minimal (-21.86 m) in 1980-1985, retaining the general tendency of the coastline migration toward the sea eastwards, which evidenced the predominant influence of accumulation processes and formation of the new land areas in the studied region.



Analysis of the data from figures 5.2-5.5 shows that through the 40-year period the coastal zone has changed, land retreat made around  $-5.17 \text{ km}^2$  and almost  $19.87 \text{ km}^2$  accumulated. Practically all over the UA1-1 Subarea the accumulation process dominates (Table 5.1 and Fig. 5.5) and only in the area of the Ochakivske Arm of the Danube and in the northern part of the delta (Zhebryianivska Bay) intensive erosion processes were observed for the 40-year period.

It should be noted that as the result of mutual influence of the river discharge, wind and wave action, as well as changes of the Danube Delta hydro-morphological characteristics, forming of new islands takes place in the adjacent Black Sea area. The biggest of them are the Ptashyna Kosa Island to the south from the Bystre Canal (Fig. 5.6), which appeared on the official maps in 1996, and the Nova Zemlya Island to the south from Starostambulske Arm of the Danube (Fig. 5.7), which appeared on the official maps in 2000 [<http://wikimapia.org/#lang=en&lat=45.338150&lon=29.693298&z=11&m=ys>]. We did not make a detailed analysis of the dynamics of the abovementioned islands location and acreage changes in this Assessment, however we should underline that increase in their area took place mainly due to suspended matter flows transport from the Danube Delta, as well as erosion processes in the coastal zone to the north of these islands. Average, minimum and maximum values of the main statistical parameters SCE (m), NSM (m), WLR (m/year) for the UA1-1 pilot subarea (Danube delta area) presented in Table 5.2

Table 5-2. Table with the average, minimum and maximum values of the main statistical parameters SCE (m), NSM (m), WLR (m/year) for the UA1-1 pilot subarea (Danube delta area)

Value	SCE,m	NSM,m	WLR, m/year
Average	603,57	198,80	6,62
Min value	26,39	-1033,71	-31,08
Max value	3950,40	1486,80	63,04

In total for 1980-2020 the Squares of the erosion and accretion areas in Danube delta ghtptned in Table 5.3.

Table 5.3. Table with the erosion and accretion areas in Danube delta

	Area in $\text{km}^2$
Net Area Movement	25,04
Erosion	-5,17
Accretion	19,87

In the course of processing and analysis of the data received using DSAS (Chapter 3.3) we have revealed some peculiarities and drawbacks in processing of the images of some areas, which were characterised by spatiotemporal non-uniformity and lead to significant errors in determination of the following characteristics: NSM (Net Shoreline Movement - represents the distance between the oldest and the youngest shorelines for each transect), SCE (Shoreline Change Envelope - represents the greatest distance among all the shorelines that intersect a given transect), WLR (Weighted Linear Regression). We tried to correct those errors, so further on we made the detailed analysis of the recalculated data for the Subarea UA1-1 for the period 1985-2020.

Statistical analysis of the shoreline dynamics indicators (Table 5.4) and their spatial distribution along the coast (Fig. 5.8) had shown that the highest values were observed near the place where the Danube enters the sea and on the segments of some river arms and channels where speed of shoreline displacement reached 30 - 40 m/year. In the intermediate areas of the delta frontal part the speed of the shoreline seaward movement makes 2 - 10 m/year. The most negative values of the shoreline dynamics, from -7.04 to -36.48 m/year, are observed in the Ochakivske Arm area in the segment from 35.8 km to 37.6 km.

Table 5.4. Statistical characteristics of shoreline displacements in the Subarea UA1-1.

Statistical characteristics	Shoreline Dynamics Indicators					
	Initial variant (1980-2020)			Corrected variant (1985-2020)		
	NSM (m)	SCE (m)	WLR (m/year)	NSM (m)	SCE (m)	WLR (m/year)
MEAN	201.97	603.57	6.62	194.55	435.14	5.15
MIN	-1033.70	26.39	-31.08	-1218.99	10.22	-36.48
MAX	1486.80	3950.40	63.04	1416.66	2418.28	40.16

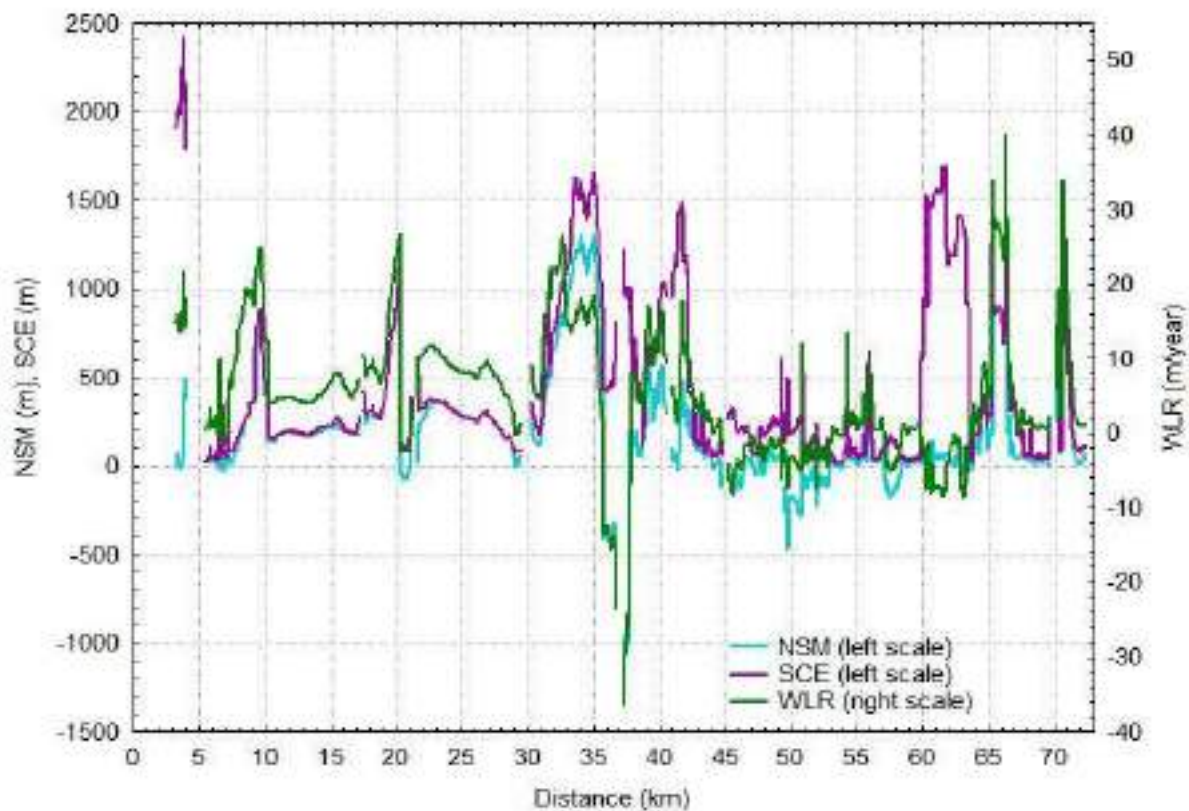


Fig.5.8. Spatial distribution of shoreline dynamics indicators in the coastal UA1-1 Subarea for the period 1985-2020.

Comparison between the data for different periods had shown that the results for 1985-2020 for the NSM (m), SCE (m) and WLR (m/year) were respectively 3.8%, 39% and 29% lower than those presented by us for the period 1980-2020 and, to our opinion, more reliable.

### 5.3. Subarea UA1-2 (Sasyk estuary area)

Subarea UA1-2 (Sasyk Estuary area) covers a 14 km long shoreline (Fig. 5.1), starting from Zhebriians'ka Bay (Village Prymors'ke) (72<sup>nd</sup> km of the shoreline) till the bank of the Sasyk Lake to the south from village Katranka (86<sup>th</sup> km of the shoreline). The 14 km long subarea UA1-2 is orientated from south-west to north-east. The subarea UA1-2 is a sand spit that separates the Sasyk Lake from the sea. The shoreline in the area mainly consists of sandy beaches formed at the boundary of the lake and the Black Sea. The shoreline change statistic parameters from 1980 to 2020 were estimated by 222 transects orientated vertically to the coastline. Figure 5.9 shows the average coastline change of the total sub-area from 1980 to 2020 in five-year time period.

From 1980 till 2000 accumulation has been observed (with average growth of 3.03 m/year from 1980 to 1985 and 3.87 m/year from 1990 to 1995), after which, in 2000 – 2005, erosion of the coastline averaging to - 3.57 m/year was registered and from 2005 to 2020 accumulative processes were observed again (average speed of accumulative movement of the shore in 2005 - 2010 made 5.31 m/year) (Table 5.5.).

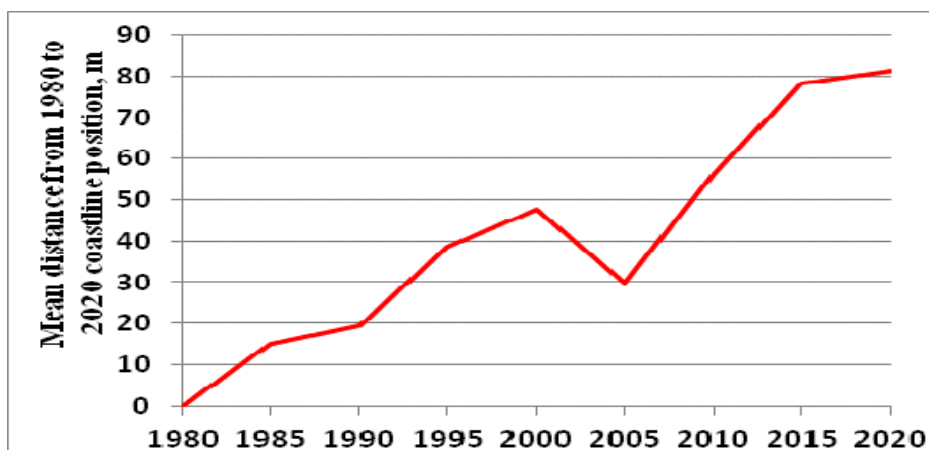


Figure 5.9.. Temporal variability of the average shoreline position (m) in UA1-2 subarea ( the Sasyk Estuary) from 1980 to 2020.

Table 5.5. Table of the mean shoreline change rate in periods

Class/time frame	No of Transects	Mean (m/year)	Std. Error
1980-1985	222	3,03	0,59
1985-1990	222	0,82	0,19
1990-1995	222	3,87	0,65
1995-2000	222	1,81	0,29
2000-2005	222	-3,57	0,41
2005-2010	222	5,31	0,60
2010-2015	222	4,40	0,41
2015-2020	222	0,57	0,47
1980-2020	222	2,03	0,45

It can thus be concluded that the UA1-2 Subarea is characterised as accumulative as the difference in the medium position of the oldest (1980) and the youngest (2020) shoreline makes ca. 81.19 m with average speed of movement seaward of about 2 m/year.

Fig. 5.10. - 5.12. present the maps of coastal area change in the Sasyk Estuary area (UA1-2 Subarea) and the distribution of the main statistical characteristics of shoreline dynamics: WLR (m/year), SCE (m) and NSM (m) for 1980-2020, the analysis of which has shown that the erosion processes are mainly observed in the northern part of the area (from 81 to 86 km), while in the rest of the area accumulation processes dominate.



Figure 5.10. Maps of coastal area change near Sasyk estuary (UA1-2 subarea) . Left – Dynamics of shoreline for 1980-2020: ■ Erosion, ■ Accretion. Right – Distribution of WLR (Weighted Linear Regression Rate) for 1980-2020, m/year: — High Erosion ( $< -2$  m/year), — Medium Erosion ( $-2 - -0,5$  m/year), — Stable Coastline ( $-0,5 - 0,5$  m/year), — Medium Accretion ( $0,5 - 2$  m/year), — High Accretion ( $>2$  m/year).



Figure 5.11. Statistical parameters (SCE – left picture, NSM – right picture) by transect along the shoreline for UA1-2 Sasyk Estuary subarea for the period 1980-2020. → km distance , For SCE: □ 0- 20 m, — 20-50 m, — 50-100 m, — 100-250 m, — 250-500 m, — 500-1000 m, —  $>1000$  m., For NSM: —  $< -250$  m, —  $-250 - -100$  m, —  $-100 - -20$  m, □  $-20 - 20$  m, —  $20 - 100$  m, —  $100 - 250$  m, —  $>250$  m.



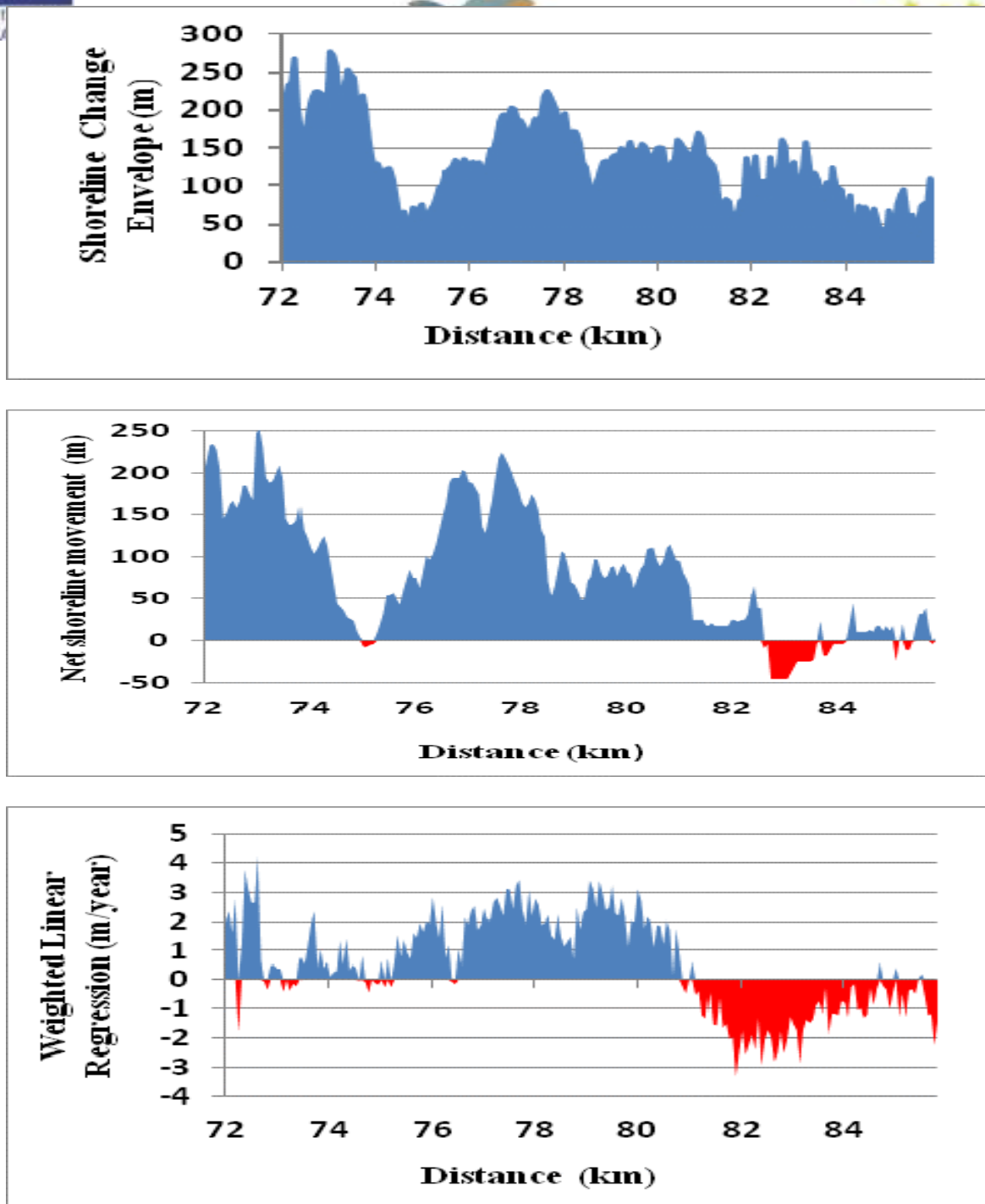


Figure 5.12. Spatial distribution of the estimated statistical parameters (SCE, NSM, and WLR) by transect along the shoreline for UA1-2 subarea (Sasyk Estuary) red – erosion, blue – accretion

Table 5.6 presents the average, minimum and maximum values of the main statistical parameters (SCE, NSM, and WLR) calculated by the vertical to the shoreline transects. The average shoreline change (SCE) estimate in the sub-area is about 132.55 m. The maximal SCE values in the **Subarea UA1-2** were observed near the Prymors'ke village and made from 200 m to 277 m in the area between the transects 17 and 36 or from the 72.9 km of the studied area to the 74.04 km. The second area where the SCE value exceeded 150 m was located in the segment from 76.74 km to 78.42 km (transects 81-109), where the SCE values were reaching 155 – 224 m.

Table 5.6. Average, minimum and maximum values of the main statistical parameters SCE (m), NSM (m), WLR (m/year) for the Sasyk Estuary (subarea UA1-2)

	SCE, m	NSM, m	WLR, m/year
Average	132,55	81,19	0,55
Min value	28,31	-46,02	-3,30
Max value	277,05	253,05	4,19

Through the 40-year period the coastal zone has changed; around  $-0.04 \text{ km}^2$  of land retreated and almost  $1.06 \text{ km}^2$  accumulated. The accumulation process is observed practically all over the UA1-2 Subarea (Table 5.7, Fig. 5.12).

Table 5.7 . Table with the erosion and accretion areas in the region 2

	Area in $\text{km}^2$
Net Area Movement	1,09
Erosion	0,04
Accretion	1,06

According to the results of shoreline dynamics' statistical characteristics calculation (Fig. 5.13), which was carried out using the corrected input data for 1985 – 2020, we found out that the highest values of the coastline seaward movement (4-5 m/year) were observed in the vicinity of the village Prymors'ke on the segment from 72 km to 74 km and in the area of the 78<sup>th</sup> km.

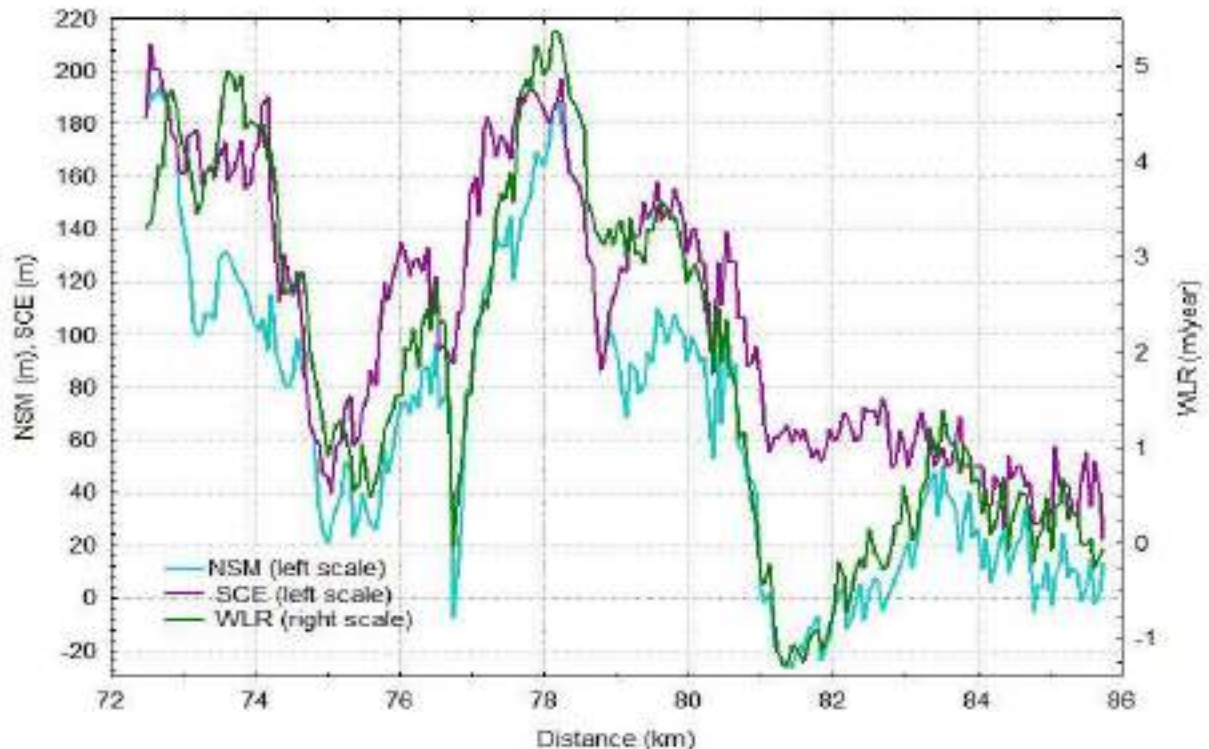


Fig. 5.13. Spatial distribution of the coastline movement indicators in the UA1-2 Subarea along the shore.

The NSM (m) and SCE (m) average values in 1985-2020 (Table 5.8) decreased 23% and 25% respectively compared to the period of 1980-2020 and the WLR (m/year) mean value grew 3.4 times.

Table 5.8. Statistical characteristics of the shoreline dynamics in the UA1-2 Subarea.

Statistical characteristics	Coastline dynamics indicators					
	Initial variant (1980-2020)			Corrected variant (1985-2020)		
	NSM (m)	SCE (m)	WLR (m/year)	NSM (m)	SCE (m)	WLR (m/year)
MEAN	81.19	132.55	0.55	66.05	106.13	1.89
MIN	-46.02	28.31	-3.30	-32.29	22.38	-1.29
MAX	253.05	277.05	4.19	193.29	209.79	5.35

#### 5.4. Subarea UA1-3 (Sasyk estuary – Budakskiy estuary)

The shoreline of Subarea UA1-3 (Fig. 5.1) is separating of the Tuzly group of estuaries from the Black Sea; it is an about 55 km long sand spit. The shoreline change statistic parameters from 1980 to 2020 were estimated by 905 vertical to the coastline transects (86 – 139 km). Figure 5.14 shows the average coastline change of the total sub-area from 1980 to 2020 in five-year time period. The erosion and accumulation processes during the 40-year period were abrupt: from 1980 to 1985 erosion was observed (in average -3.69 m/year), from 1985 to 1990 accumulation followed (in average 0.52 m/year), than from 1990 to 1995 erosion processes took place again (average speed -2.39 m/year), in the next 5 years from 1995 to 2000 accumulation processes were observed again (average speed 2.58 m/year).

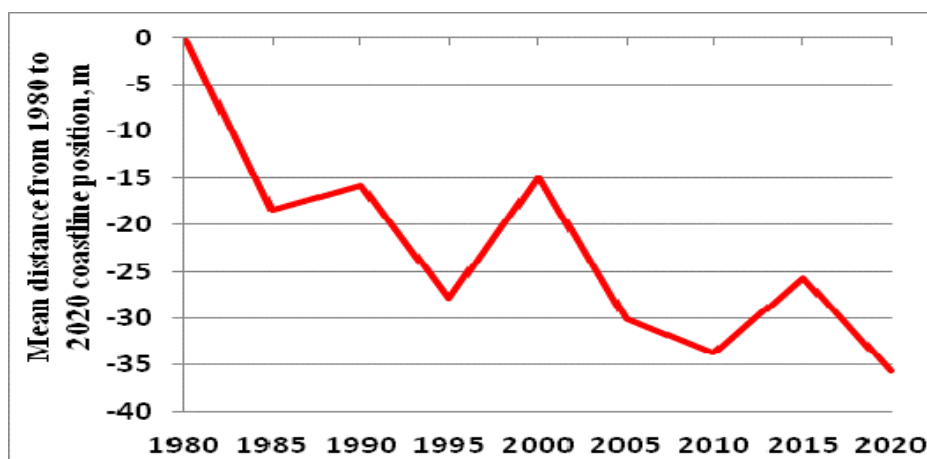


Figure 5.14. Temporal variability of the average shoreline position (m) in UA1-3subarea (Sasyk estuary – Budakskiy estuary) from 1980 to 2020.

In the next 10-year period from 2000 to 2010 erosion continued, after which the 5-year periods that followed were characterised by alternation of erosion and accumulation (Table 5.9). The difference between mean positions of the oldest (1980) and the youngest (2020) shoreline is -35.56 m. The area is in general erodible.

Table 5.9. Table of the mean shoreline change rate in 1980-2020

Class/time frame	No of Transects	Mean(m/year)	STD Error
1980-1985	905	-3,69	0,17
1985-1990	905	0,52	0,08
1990-1995	905	-2,39	0,16
1995-2000	905	2,58	0,08
2000-2005	905	-3,03	0,14
2005-2010	905	-0,73	0,13
2010-2015	905	1,61	0,13
2015-2020	905	-1,97	0,09
1980-2020	905	-0,89	0,12

Table 5.10 presents the average, minimum and maximum values of the main statistical parameters (SCE, NSM, and WLR) calculated by the vertical to the shoreline transects (Fig. 5.15-5.17). The average shoreline change (SCE) estimate in the subarea is about 82.96 m. the maximal SCE values (from 119.4 m to 280.2 m) in the subarea observed in the area from the border of the Dzhansey estuary (from 268th to 289 transects), from 87.96 to 89.16 km of the study area UA -1. The second ‘peak’ segment with high SCE value is from 102.3 km to 104.34 km (transects 508-545) where the SCE makes from 116.37 to 351.93 m for the period 1980-2020.

Table 5.10. Table with the average, minimum and maximum values of the main statistical parameters SCE (m), NSM (m), WLR (m/year) for the UA1-3 subarea (Sasyk estuary – Budakskiy estuary)

	SCE (m)	NSM (m)	WLR (m/year)
Average	82,96	-35,56	-1,62
Min value	23,60	-110,00	-4,77
Max value	351,93	60,13	0,65

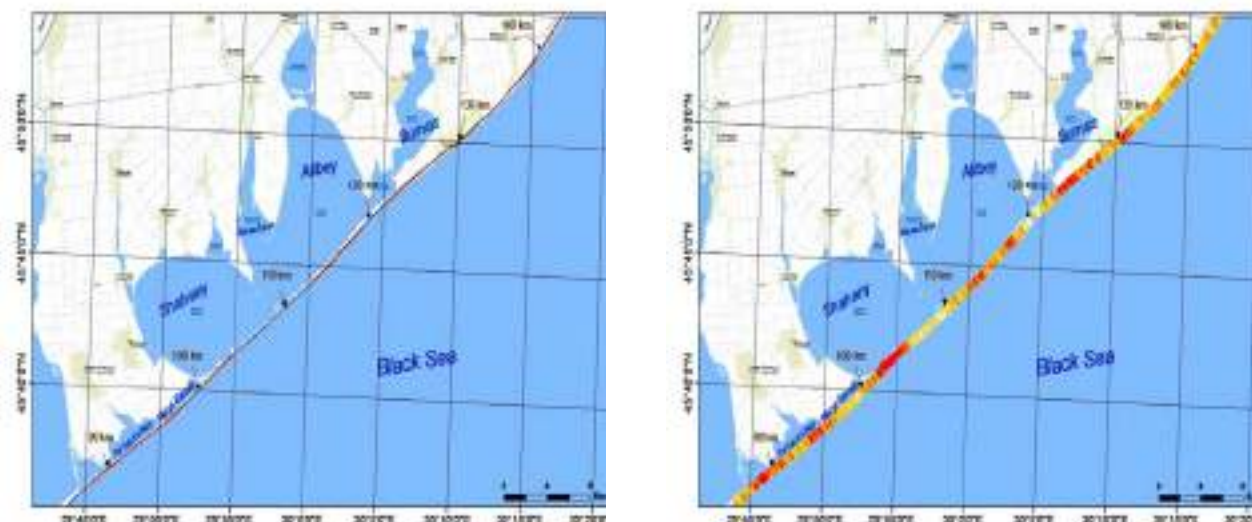


Figure 5.15. Maps of coastal area change in subarea UA1-3 (Sasyk estuary – Budakskiy estuary). Left – Dynamics of shoreline for 1980-2020: ■ Erosion, ■ Accretion. Right – Distribution of WLR (Weighted Linear Regression Rate) for 1980-2020, m/year: — High Erosion (< -2 m/year), — Medium Erosion(-2 - -0,5 m/year), — Stable Coastline(-0,5 – 0,5 m/year), — Medium Accretion(0,5 -2 m/year), — High Accretion (>2 m/year)



Figure 5.16. Statistical parameters SCE (left) and NSM (right) by transect along the shoreline for subarea UA1-3 (Sasyk estuary – Budakskiy estuary) for 1980-2020. → km distance

For SCE: □ 0- 20 m, □ 20-50 m, □ 50-100 m, □ 100-250 m, □ 250-500 m, □ 500-1000 m, □ >1000 m. For NSM: □ < -250 m, □ -250- -100 m, □ -100 m- -20 m, □ -20- 20 m, □ 20-100 m, □ 100-250 m, □ >250 m.

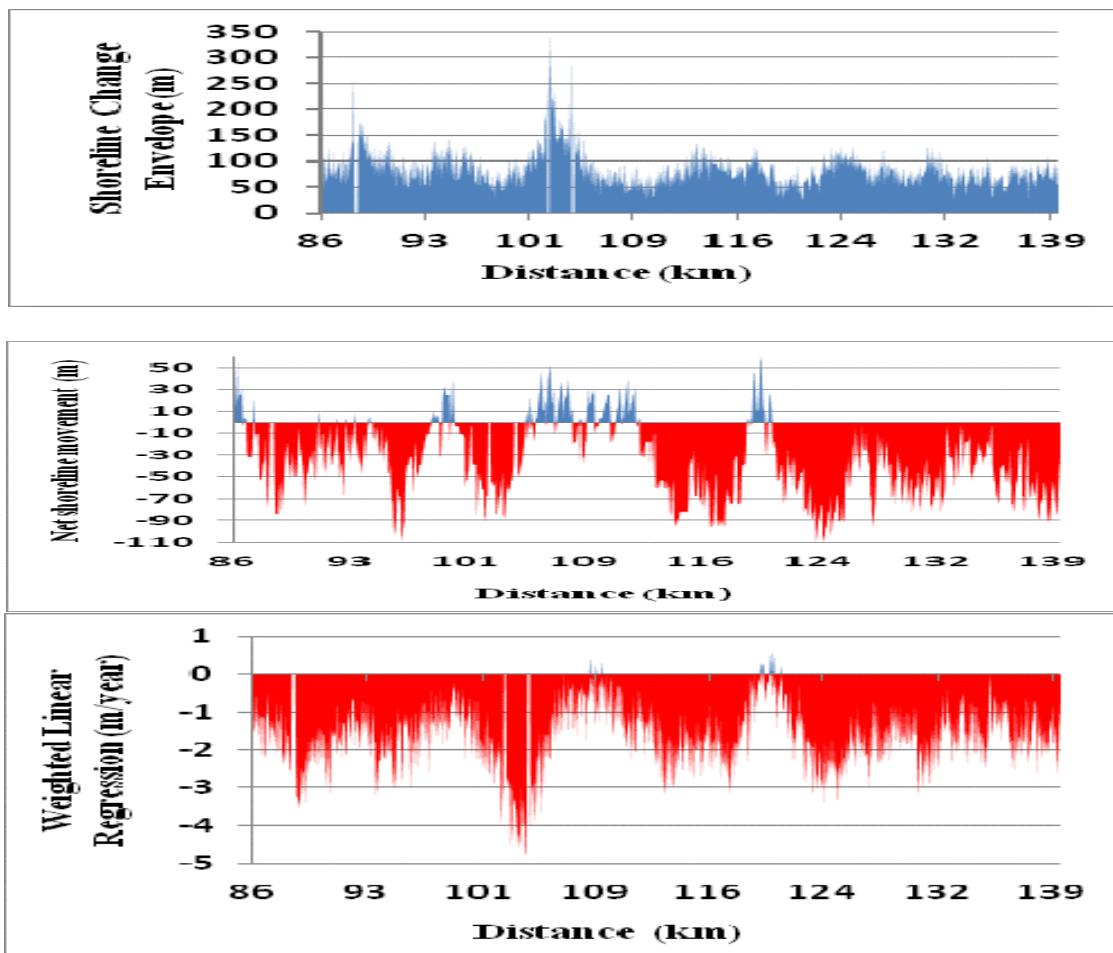


Figure 5.17. Spatial distribution of the estimated statistical parameters (SCE, NSM, and WLR) by transect along the shoreline for Subarea UA1-3 (Sasyk estuary – Budakskiy estuary). red – erosion, blue – accretion

Through the 40-year period the coastal zone has changed, around  $-2,18 \text{ km}^2$  of land retreated and almost  $0.17 \text{ km}^2$  accumulated. Domination of erosion processes is observed practically all over the UA1-3 Subarea (Table 5.11, Fig. 5.15).

Table 5.11. Table with the erosion and accretion areas in UA1-3 subarea (Sasyk estuary – Budakskiy estuary)

	Area in $\text{km}^2$
Net Area Movement	2,36
Erosion	2,18
Accretion	0,17

Statistical analysis of the shoreline dynamics indicators (Table 5.12, Fig. 5.18) performed by us using the corrected source data for 1985-2020 showed that the values of the shoreline displacement values varied within the limits from  $-3.32$  to  $1.73 \text{ m/year}$  with the mean value of  $-0.49 \text{ m/year}$ , which indicated the general tendency of the shoreline retreat, i.e. the erosion processes domination.

It should be pointed out that mean values of NSM (m), SCE (m) and WLR (m/year) for the period 1985-2020 decreased in comparison with the initial assessments of these characteristics for 1980-2020 respectively 2.1; 2.0 and 3.3 times. At that, the main tendencies of those characteristics' spatial distribution stayed the same.

Table 5.12. Statistical characteristics of the shoreline dynamics in the UA1-3 Subarea.

Statistical characteristics	Shoreline dynamics indicators					
	Initial variant (1980-2020)			Corrected variant (1985-2020)		
	NSM (m)	SCE (m)	WLR (m/year)	NSM (m)	SCE (m)	WLR (m/year)
MEAN	-35.56	82.96	-1.62	-17.06	41.03	-0.49
MIN	-110.00	23.60	-4.77	-104.21	7.08	-3.32
MAX	60.13	351.93	0.65	56.68	137.09	1.73

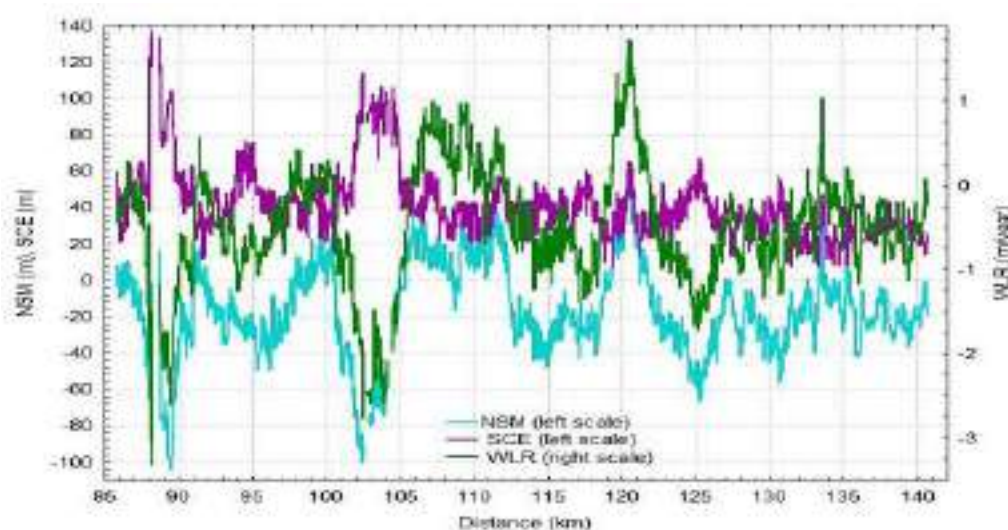


Fig. 5.18. Spatial distribution of shoreline dynamics indicators for the UA1-3 Subarea.

A feature of spatial distribution of the main shoreline dynamics indicators along the coast (Fig. 5.18) is their well-defined spatial periodicity, which according to the results of our spectral-harmonic analysis (Fourier transformation) is 6-7 – 10-11 km.

The maximal shoreline retreat rates towards the land are observed in the following segments: 88 km (-3.5 m/year), 102 km (-2.7 m/year) and 125 km (-1.8 m/year), where the width of the sand spit is reduced respectively. In the area of the village Lebedivka, where a transition from accumulative-erosive (sand spit) to abrasive-avalanchine (slope composed of loess rocks) type of coast starts, from 127<sup>th</sup> km onwards, the rate of erosion (shoreline retreat from the sea) is from 0 to -1.2 m/year. In the section from 118<sup>th</sup> km to 122<sup>nd</sup> km the shoreline is shifting seaward at a rate of up to 1.8 m/year

Beside the usual method using the Landsat images we also performed the pilot assessments of the shoreline dynamics using the high-resolution VHR space images for the period from 2005 to 2021 bought by the project from the Maxar Company (Tables 3.6 and 3.7). Below we show the preliminary results of the use of the VHR images from the satellites GeoEye-1, QuickBird-2, WorldView-2 and WorldView-3 in the shoreline dynamics assessment on the Black Sea coast in the site ‘Burnas Lake – Lebedivka village’ located in the north-eastern part of the **Subarea UA1-3** in the segment between the 125.75 km and 128.94 km. The images were processed using the DSAS software with the transects every 10 m. This part of the shoreline was chosen due to the differences in the geological conditions of adjacent areas where two types of coast were formed: accumulative-erosive (a part of the Tuzly Sand Spit, which separates the Burnas Estuary from the Black Sea) and abrasion-avalanchine (a steep coastal slope composed of loess rocks) (Fig. 5.19-5.21).



Fig. 5.19. Scheme of the shoreline segment near the Lebedivka village - pilot subarea UA1-3.



Fig. 5.20. Root area of the Tuzly Sand Spit – accumulative-erosive type of coast



Fig. 5.21. Abrasion-avalanchine type of coast in the north-eastern part of the area

Shoreline dynamics indicators were determined based on the results of the VHR (high-resolution) space images automatic processing (Table 3.6-3.7). The images were obtained for the following dates: 11.27.2005, 03.28.2007, 07.10.2009, 04.05.2013, 09.03.2015, 23.08.2016, 12.02.2017, 21.06.2019, 18.06.2021. Statistical analysis of shoreline dynamics indicators (Table 5.13, Fig. 5.21) shows that the values of the shoreline movement speed vary in the range from -2.55 to 0.73 m/year with average values of -0.81 m/year, which indicates the general trend of the shoreline displacement landward.

Table 5.13. Statistical characteristics of the shoreline dynamics near the village Lebedivka

Statistical characteristics	Shoreline dynamics indicators					
	Landsat (2005-2020)			VHR (Maxar) (2005-2021)		
	NSM (m)	SCE (v)	WLR (m/year)	NSM (m)	SCE (m)	WLR (m/year)
MEAN	-9.87	18.49	-0.40	-8.63	27.03	-0.81
MIN	-27.38	3.64	-1.50	-32.42	14.35	-2.55
MAX	18.68	39.68	1.69	25.88	49.96	0.73

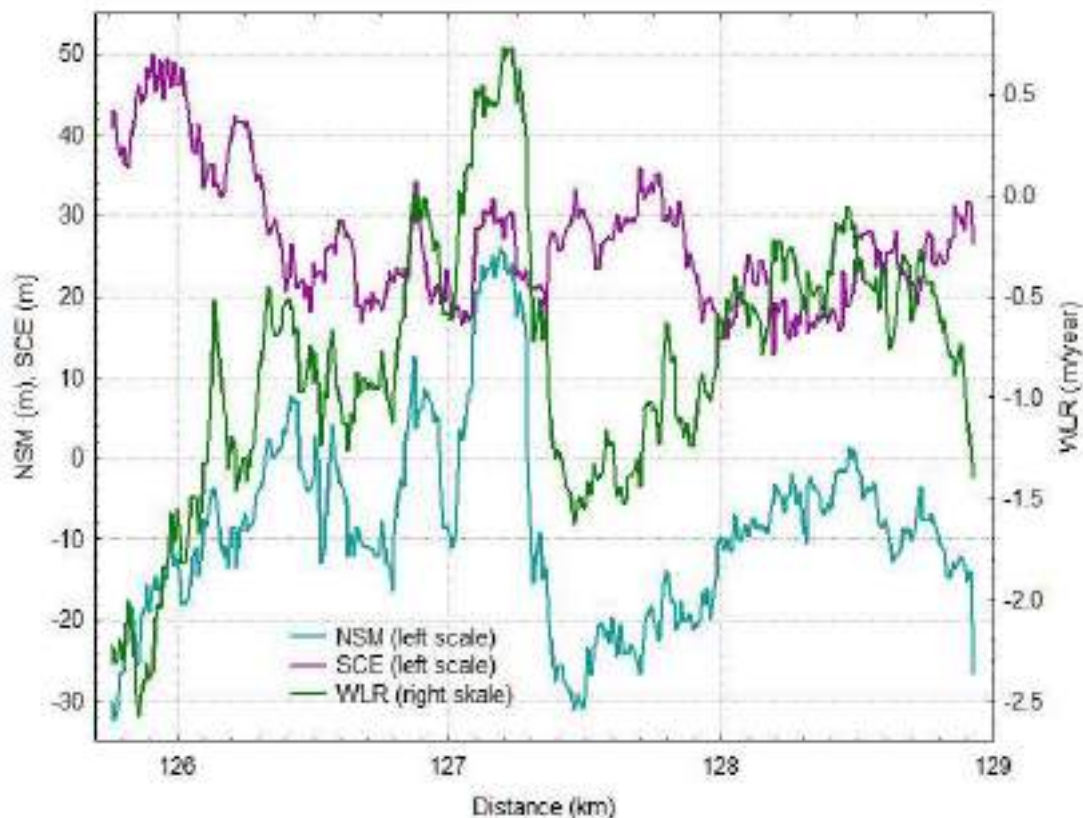


Fig. 5.21. Spatial distribution of shoreline dynamics indicators for the coastal area near Lebedivka village according to Maxar high-resolution satellite images.



It should be mentioned that the comparison between mean values of NSM (m), SCE (m) and WLR (m/year) assessed on the VHR using MAXAR (2005-2021) and Landsat (2005-2020) images has shown that the statistical characteristics according to the VHR images decreased for the NSM 14% and increased 46% and 100% for the SCE and WLR respectively – compared to the initial estimation of those characteristics, which were calculated using Landsat images for the period 2005-2020. At that, the main tendencies in spatial distribution of those characteristics stayed the same. It should be pointed out that precision and spatial resolution of the data received using the VHR images are more reliable and enable us take into account meandering of the shoreline with high precision. The highest shoreline retreat speed was observed in the western and eastern parts of the area, where they made respectively -2.55 m/year and -1.41 m/year. Positive values of the speed of displacement of the coastline towards the sea up to 0.73 m/year are observed only in the area where the root part of the spit is adjacent to the original loess shore, the location of which corresponds to the zone of change of shore types. With the exception of the transition zone, the average speeds of the coastline separately along the sand spit and separately along the loess slope are -1.27 m/year and -0.62 m/year, respectively. The difference in the shoreline movement speed is explained by the fact that there is a gradual washing out of a large amount of collapsed material at the foot of the loess slope. It takes some time to process this material and this is what reduces the rate of shoreline retreat. The comparison of coastline dynamics indicators obtained from space images of different resolutions was performed for the time periods of almost the same duration: Landsat - 2005-2020 and Maxar - 2005-2021. As there were no Maxar space images available for 2020 calculations of shoreline dynamics indicators based on Maxar space images for 2005-2019 and 2005-2021 were used. Statistical analysis of the results of shoreline dynamics indicators calculation (Table 5.14) based on space images of different resolution shows slight differences in NSM (distance between the oldest and youngest shoreline) and WLR (speed of shoreline movement).

Table 5.14. Statistical characteristics of shoreline dynamics indicators for the coastal area near Lebedivka village according to the data from Landsat (2005-2020), Maxar (2005-2019), Maxar (2005-2021)

Statistical characteristics	Landsat (2005-2020)			Maxar (2005-2019)			Maxar (2005-2021)		
	Shoreline dynamics indicators								
	NSM (m)	SCE (m)	WLR (m/year)	NSM (m)	SCE (m)	WLR (m/year)	NSM (m)	SCE (m)	WLR (m/year)
MEAN	-9.87	18.49	-0.40	-8.63	27.03	-0.91	-7.72	26.78	-0.81
MIN	-27.38	3.64	-1.50	-32.42	14.35	-2.90	-28.53	14.32	-2.55
MAX	18.68	39.68	1.70	25.88	49.96	0.68	12.14	49.96	0.73

Statistical characteristics of the SCE parameter (the longest distance among all shorelines) for Landsat images differ almost one and a half times from those for Maxar images, which is due to the lower resolution of Landsat images. Using correlation analysis of the spatial distribution of the values of the shoreline dynamics indicators for the indicated periods for which space images of different resolutions (Landsat 2005-2020 - Maxar 2005-2019, 2005-2021) were obtained we established the positive correlation between the NSM indicators with coefficients  $R = 0.45$  and  $R = 0.58$ ; between the SCE indicators no correlation was revealed; correlation coefficients  $R$  between the WRL indicators  $R$  were 0.65 and 0.69 (Fig. 5.22–5.24). Taking into account the closeness of statistical characteristics of the shoreline dynamics indicators based on Maxar images and their significant difference from those obtained from Landsat images, it should be assumed that the Maxar images provide more reliable shoreline dynamics indicators.

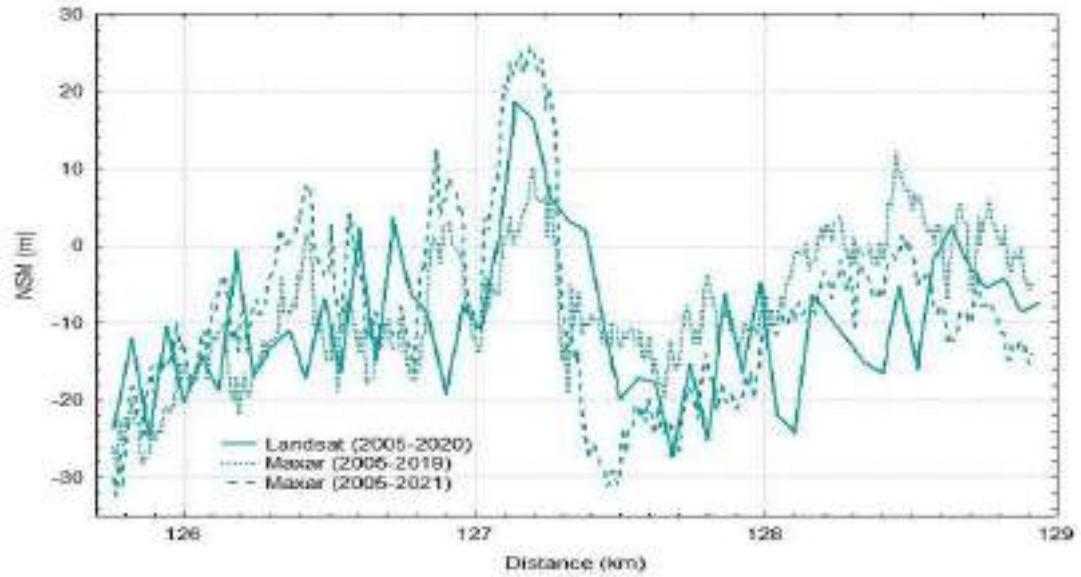


Fig. 5.22. Spatial distribution of the NSM shoreline dynamics indicator for the sea coast in the area of Lebedivka village according to Landsat (2005-2020) and Maxar (2005-2019 and 2005-2021) satellite images

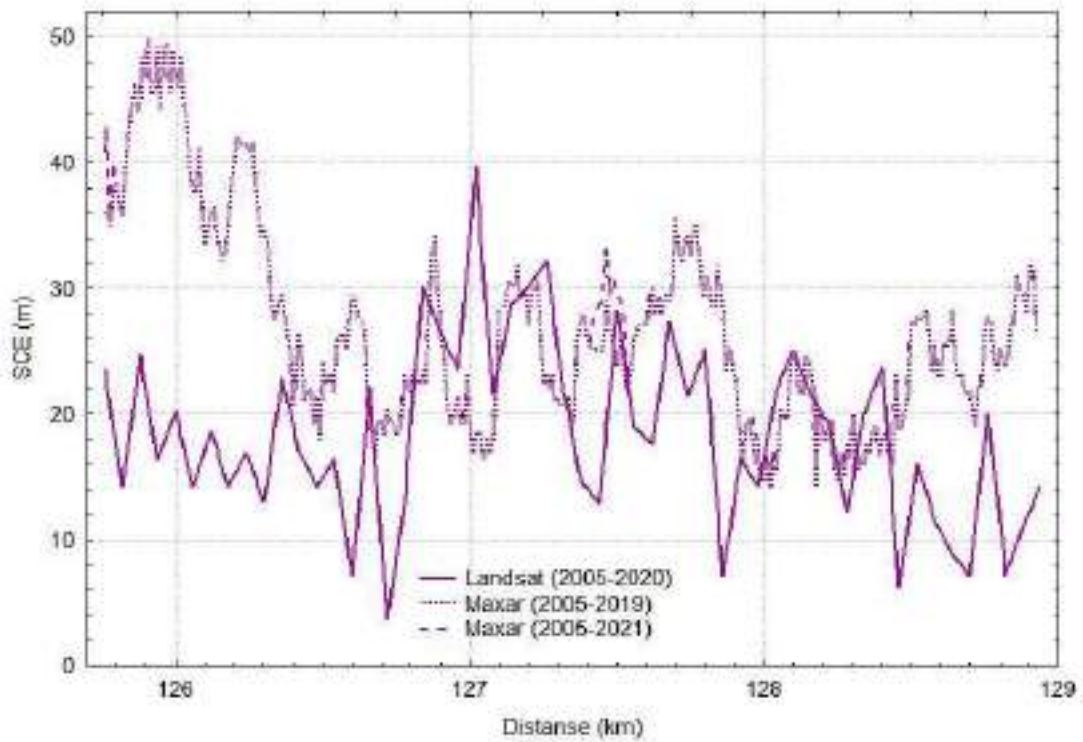


Fig. 5.23. Spatial distribution of the SCE shoreline dynamics indicator for the sea coast in the area of Lebedivka village according to Landsat (2005-2020) and Maxar (2005-2019 and 2005-2021) satellite images.

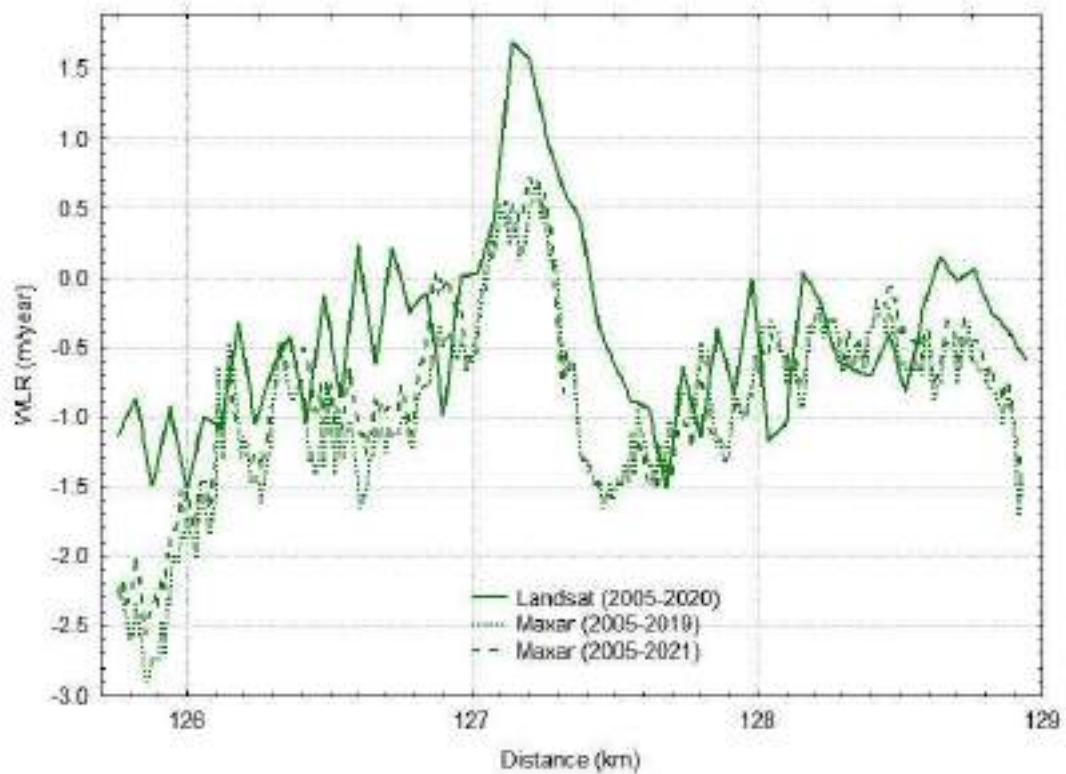


Fig. 5.24. Spatial distribution of the WLR shoreline dynamics indicator for the sea coast in the area of Lebedivka village according to Landsat (2005-2020) and Maxar (2005-2019 and 2005-2021) satellite images.

### 5.5. Subarea UA1- 4 (Budakskyi Estuary – Sukhyi Estuary area)

The Subarea UA1- 4 (Budakskyi Estuary – Sukhyi Estuary area) stretches 50.94 km in the direction from the south-west to the north (Fig. 5.1). The statistical parameters of shoreline change of this area for 1980-2020 were estimated by 817 vertical to the coastline transects. Fig. 5.25 shows the average shoreline change for the total sub-area from 1980 to 2020 in five-year periods. From 1980 to 1985 erosion was observed (in average -5.77 m/year); from 1985 to 2000 accumulation took place with the following rates: 1985-1990 – in average 1.15 m/year, 1990-1995 -1.79 m/year, 1995-2000 – 3.9 m/year (Table 5.15). From 2000 to 2010 erosion processes were observed with average speed of -0.13 m/year and -0.26 m/year for the 5-year periods of 2000-2005 and 2005-2010 respectively. From 2010 to 2020 accumulation was replaced by erosion: in 2010-2015 average rate of accumulation made 1.21 m/year and in 2015-2020 average rate of erosion was -0.71 m/year. The difference between medium positions of the oldest (1980) and the youngest (2020) shoreline is ca. 7.39 m.

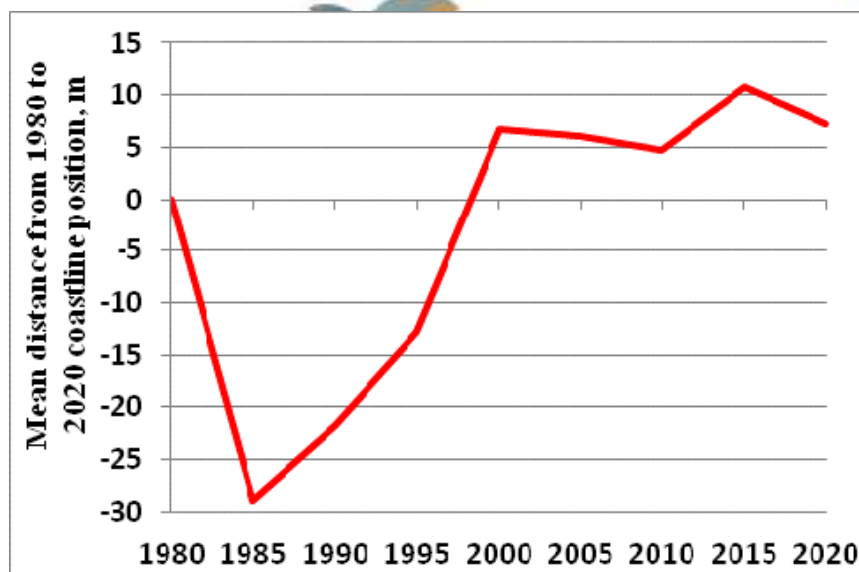


Figure 5.25. Temporal variability of the average shoreline position (m) in the Subarea UA1- 4 (Budakskiy estuary – Sukhiy estuary area) from 1980 to 2020.

Table 5.15. Table of the mean shoreline change rate in periods

Class/time frame	No of Transects	Mean (m/year)	STD Error
1980-1985	817	-5,77	0,27
1985-1990	817	1,45	0,22
1990-1995	817	1,79	0,29
1995-2000	817	3,90	0,22
2000-2005	817	-0,13	0,11
2005-2010	817	-0,26	0,08
2010-2015	817	1,21	0,08
2015-2020	817	-0,71	0,05
1980-2020	817	0,19	0,17

Table 5.16 presents the average, minimum and maximum values of the main statistical parameters (SCE, NSM and WLR) calculated by the vertical to the shoreline transects (Fig. 5.25-5.27).

	SCE (m)	NSM (m)	WLR(m/year)
Average	91,04	7,39	0,24
Min value	13,54	-226,98	-2,93
Max value	389,71	352,04	12,01

The average shoreline change (SCE) estimate in the sub-area is about 91.04 m. The maximal SCE values in the Subarea UA1-4 (Budakskiy Estuary – Sukhiy Estuary area) were observed in the vicinity of Karolino-Bugaz (near the Dniester Estuary) and made from 140.69 m to 380.8 m (transects 1740-1818 or 176.04 – 180.78 km). The second segment with high SCE values (72.28 – 222.59 m) was in the Budakskiy Estuary area (150.84 km – 154.26 km, transects 1320-1377). The third shoreline segment with high SCE values (130.57 – 190.53 m) is from 161.82 km to 162.3 km (transects 1503-1511).

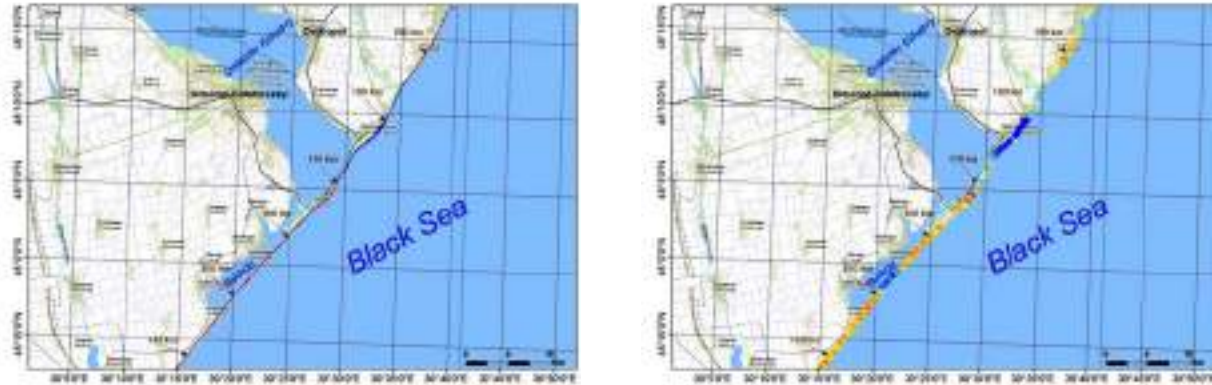


Figure 5.25. Maps of coastal area change in 1980-2020 for subarea UA1- 4 (Budakskiy estuary – Sukhiy estuary). Left – Dynamics of shoreline: **Red** Erosion, **Blue** Accretion. Right – Distribution of WLR (Weighted Linear Regression Rate), m/year: **Red** High Erosion (< -2 m/year), **Orange** Medium Erosion(-2 - -0,5 m/year), **White** Stable Coastline(-0,5 – 0,5 m/year), **Light Blue** Medium Accretion (0,5 -2 m/year), **Dark Blue** High Accretion (>2 m/year).



Figure 5.26. Statistical parameters SCE (left) and NSM (right) by transect along the shoreline for subarea UA1-4 (Budakskiy estuary - Sukhiy estuary) for the period 1980-2020. **Red arrow** km distance; For SCE: **White** 0-20 m, **Light Yellow** 20-50 m, **Yellow** 50-100 m, **Orange** 100-250 m, **Dark Orange** 250-500 m, **Red** 500-1000 m, **Dark Red** >1000 m. For NSM: **Red** < -250 m, **Orange** -250- -100 m, **Yellow** -100 m- -20 m, **White** -20- 20 m, **Light Blue** 20- 100 m, **Dark Blue** 100-250 m, **Dark Blue** >250 m.

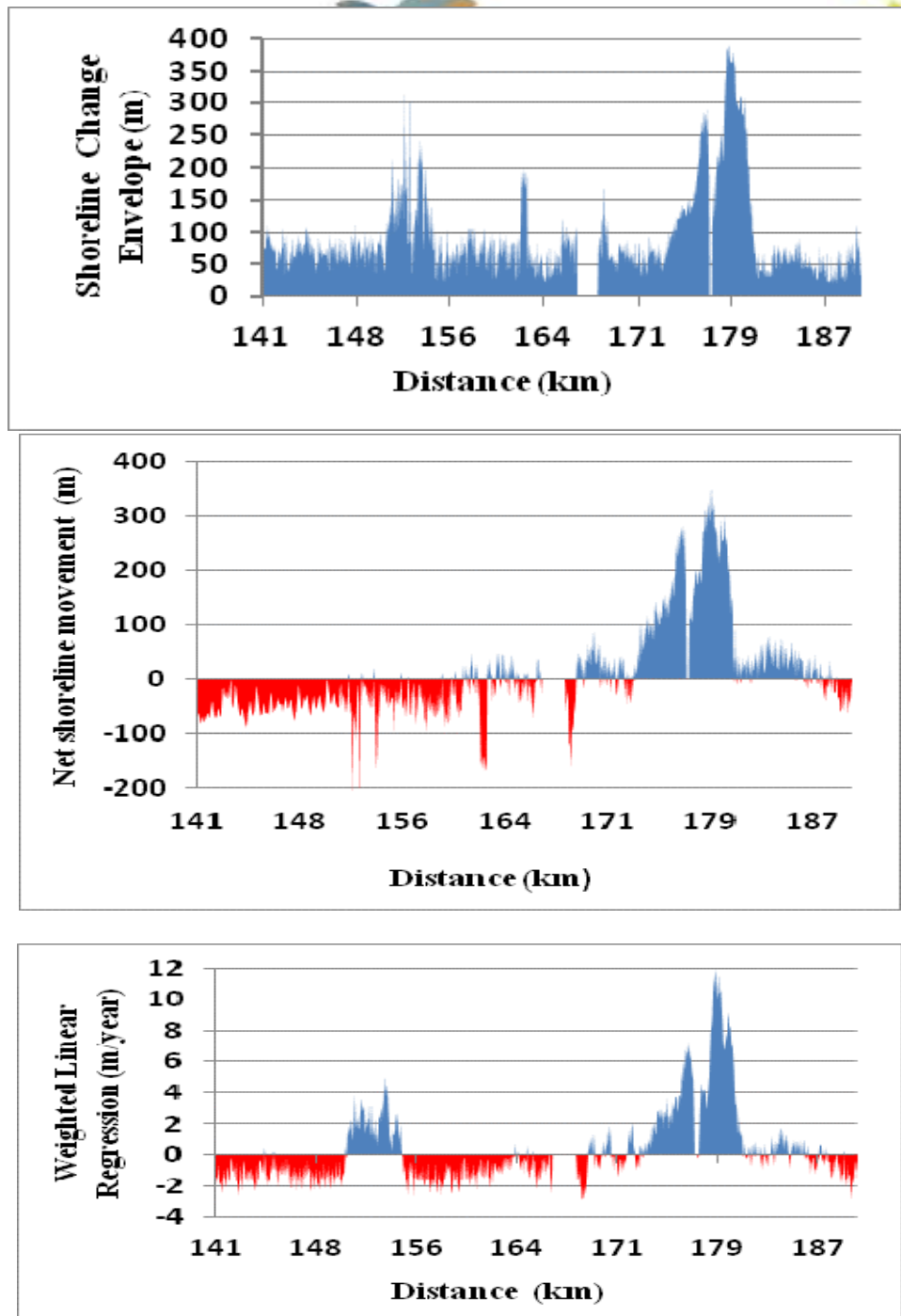


Figure 5.27. Spatial distribution of the estimated statistical parameters (SCE, NSM, and WLR) by transect along the shoreline for the UA1-4 subarea (Budakskiy estuary – Sukhiy estuary)). Red – erosion. Blue – accretion

Through the 40-year period the coastal zone has changed (Net Area Movement  $2.76 \text{ km}^2$ ) as around  $-1,20 \text{ km}^2$  of land retreated (eroded), and almost  $1.56 \text{ km}^2$  accreted (accumulated) because both erosion and accumulation processes are taking place in the area.

Statistical analysis of the shoreline dynamics indicators (Table 5.17, Fig. 5.28), which was performed using the corrected source data for 1985-2020, shows that the highest values of the shoreline movement landward (up to -2.2 m/year) were registered in the vicinity of the western end of the sand spit that separated the Dniester Estuary from the Black Sea (168-169 km). The rate of shoreline retreating in the area of 178<sup>th</sup> km is 0.5 – 0.8 m/year.

Table 5.17. Statistical characteristics of shoreline dynamics in the UA1-4 Subarea.

Statistical characteristics	Shoreline dynamics indicators					
	Initial variant (1980-2020)			Corrected variant (1985-2020)		
	NSM (m)	SCE (m)	WLR (m/year)	NSM (m)	SCE (m)	WLR (m/year)
MEAN	7.39	91.04	0.24	18.34	36.70	0.65
MIN	-226.98	13.54	-2.93	-74.99	1.80	-2.23
MAX	352.04	389.71	12.01	148.69	148.69	4.47

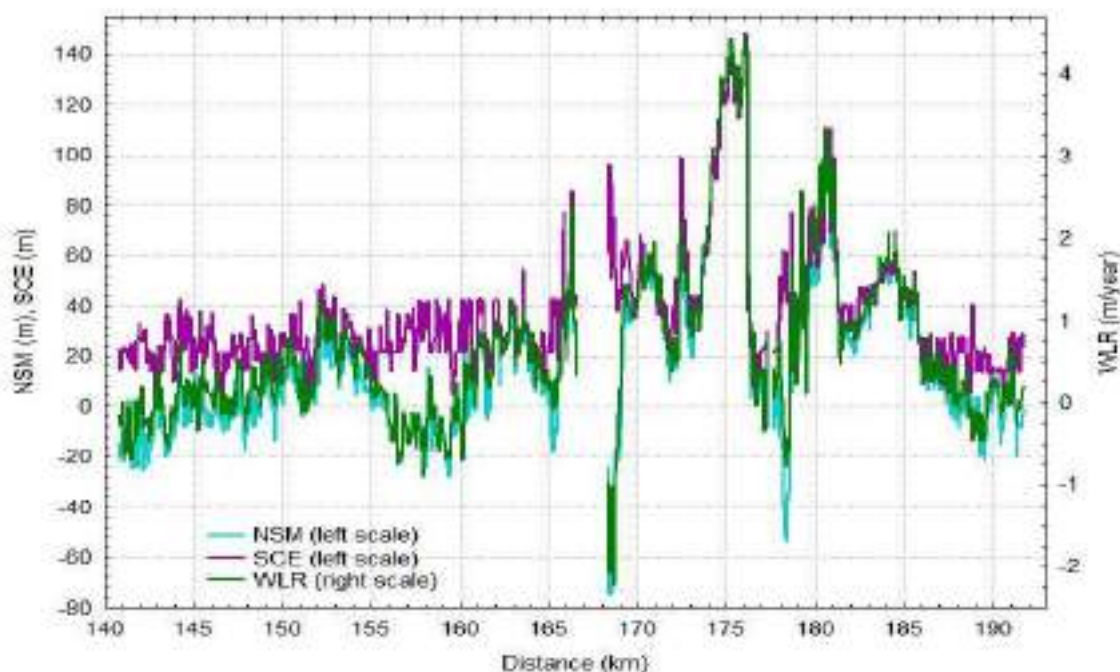


Fig. 5.28. Spatial distribution of the shoreline dynamics indicators in the UA1-4 Subarea.

The most significant shoreline accretion values (up to +4.5 m/year) are observed in the area of 174-176 km in the root part of the eastern sand spit of the Dniester Estuary. In the area of the village Grybivka (181 km) the positive speed of the shoreline movement reach 3.3 m/year. In general, for the entire UA1-4 Subarea the mean shoreline accretion rate makes 0.65 m/year.

Mean SCE value (m) in 1985-2020 (Table 5.17) decreased 2.5 times compared to 1980-2020, while NSM (m) and WLR (m/year) mean values increased 2.5 and 2.7 times respectively.

### 5.6. Subarea UA1-5 (Sukhiy estuary – Great (Velikiy) Adzhalyk estuary (Odessa bay))

The Subarea UA1-5 shoreline stretches 51.42 km and is orientated from south-west to north-east. It embraces the Black Sea coast segment (Fig. 5.1) from the Sukhiy Estuary (village Sanzheyka) to the Velykyi Adzhalyk Estuary (Odessa Bay, village Fontanka). Cities Odessa and Chornomorsk, as well as port facilities, coast protection and landslide protection works are located in the coastal zone of the area, which produces a significant impact on the coastal processes' dynamics, direction and rate of the shoreline movement.

The statistical parameters of the shoreline dynamics from 1980 to 2020 were estimated by 842 vertical to the coastline transects. Figure 5.29 shows the average coastline change of the total subarea from 1980 to 2020 in five-year periods. The strongest erosion processes took place from 1980 to 1985 at the mean rate of -5.11 m/year; than accumulation processes at the mean rate from 0.6 m/year to 3.64 m/year were registered till 2000; from 2000 to 2005 erosion processes resumed with mean rate of -1.33 m/year. During the 10-year period from 2005 to 2015 accumulation processes were observed, their mean rate reached ca. 1.02-1.03 m/year. In the last 5-year period from 2015 to 2020 erosion processes were registered, their mean rate making -0.77 m/year (Table 5.18). It should be noted that for the 40-year period the shoreline position was often changing, however as the result in 2020 the shoreline mean position reached practically the same value as it was back in 1980. The different in mean position between the oldest (1980) and the youngest (2020) shoreline make ca. 0.6 m.

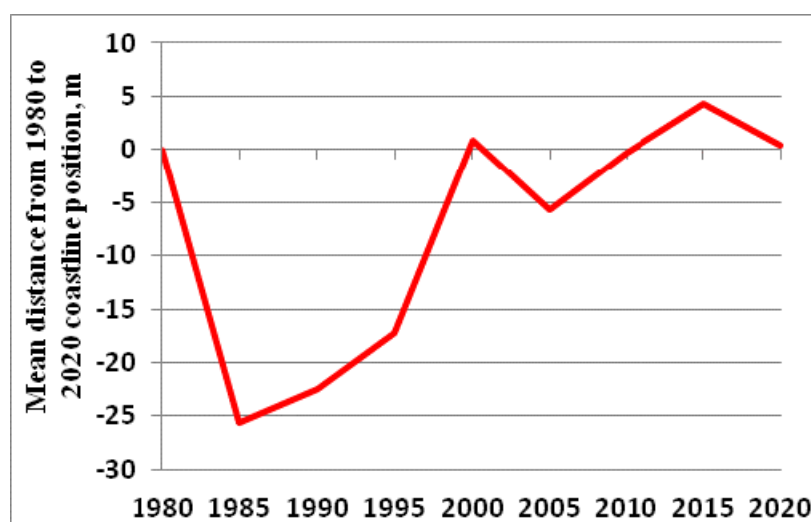


Figure 5.29 . Temporal variability of the average shoreline position (m) in the 3.6 Subarea UA1-5 subarea (Sukhiy estuary – Great Adzhalyk estuary (Odessa bay) from 1980 to 2020.

Table 5.18. Table of the mean shoreline change rate in periods

Class/time frame	No of Transects	Mean (m/year)	STD Error
1980-1985	842	-5,11	0,27
1985-1990	842	0,62	0,69
1990-1995	842	1,03	0,20
1995-2000	842	3,64	0,13
2000-2005	842	-1,33	0,12
2005-2010	842	1,02	0,29
2010-2015	842	1,01	0,37
2015-2020	842	-0,77	0,14
1980-2020	842	0,01	0,28



Table 5.19 presents the average, minimum and maximum values of the main statistical parameters (SCE, NSM, and WLR) calculated by the vertical to the shoreline transects (Fig. 5.30 – 5.32).

Table 5.19. Table with the average, minimum and maximum values of the statistical parameters SCE (m), NSM (m), WLR (m/year) for the Subarea UA1-5 (Sukhiy estuary – Great Adzhalyk estuary (Odessa bay)

	SCE, m	NSM, m	WLR, m/year
Average	88,24	0,60	-0,30
Min value	19,37	-298,85	-8,70
Max value	1254,77	957,11	10,87



Figure 5.30. Maps of coastal area change in 1980-2020 for subarea UA1-5 (Sukhiy estuary – Great Adzhalyk estuary (Odessa bay). Left – Dynamics of shoreline: ■ Erosion, ■ Accretion. Right – Distribution of WLR (Weighted Linear Regression Rate), m/year: — High Erosion (< -2 m/year), — Medium Erosion(-2 - -0,5 m/year), — Stable Coastline(-0,5 – 0,5 m/year), — Medium Accretion(0,5 - 2 m/year), — High Accretion (>2 m/year).

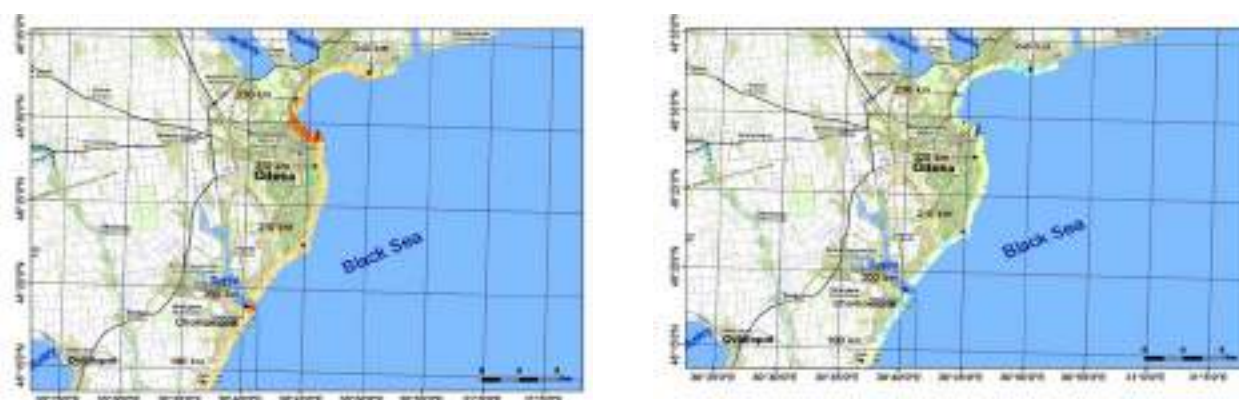


Figure 5.31. Statistical parameters SCE (left) and NSM (right) by transect along the shoreline for 1980-2020 for subarea UA1-5 (Sukhiy estuary – Great Adzhalyk estuary (Odessa bay).

→ km distance. For SCE: — 0- 20 m, — 20-50 m, — 50-100 m, — 100-250 m, — 250-500 m, — 500-1000 m, — >1000 m. For NSM: — < -250 m, — -250- -100 m, — -100 m- -20 m, — -20- 20 m, — 20- 100 m, — 100-250 m, — >250 m.

The average shoreline change (SCE) estimate in the UA1-5 Subarea is about 88.24 m. The SCE maximal values (Fig. 5.32) in the period 1980-2020 were observed in the port area of Odessa (transects 2520-2647, 222.9-230.34 km) and made from 29.35 m to 1254.77 m. High SCE values were also registered in the Sukhyi Estuary area (city Chornomorsk) from 199.56 km to 201.3 km (transects 2131-2160), reaching from 97.71 to 290.87 m (Fig. 5.32).

Through the 40-year period the coastal zone has changed as Net Area Movement (2.07 km<sup>2</sup>), around 0.86 km<sup>2</sup> of land retreated and almost 1.21 km<sup>2</sup> accreted (accumulated) because both erosion and accumulation took place in the subarea.

Statistical analysis of the shoreline dynamics indicators (Table 5.20, Fig. 5.33) performed by us using the corrected source data fro 1985-2020 shows that the highest values of the shoreline movement seaward (5.64 m/year) are registered in the area of the 200<sup>th</sup> km where the western protective spur of the navigable canal leading to Chornomorsk Port is situated as it is intercepting the sediments flow going from the east to the west.

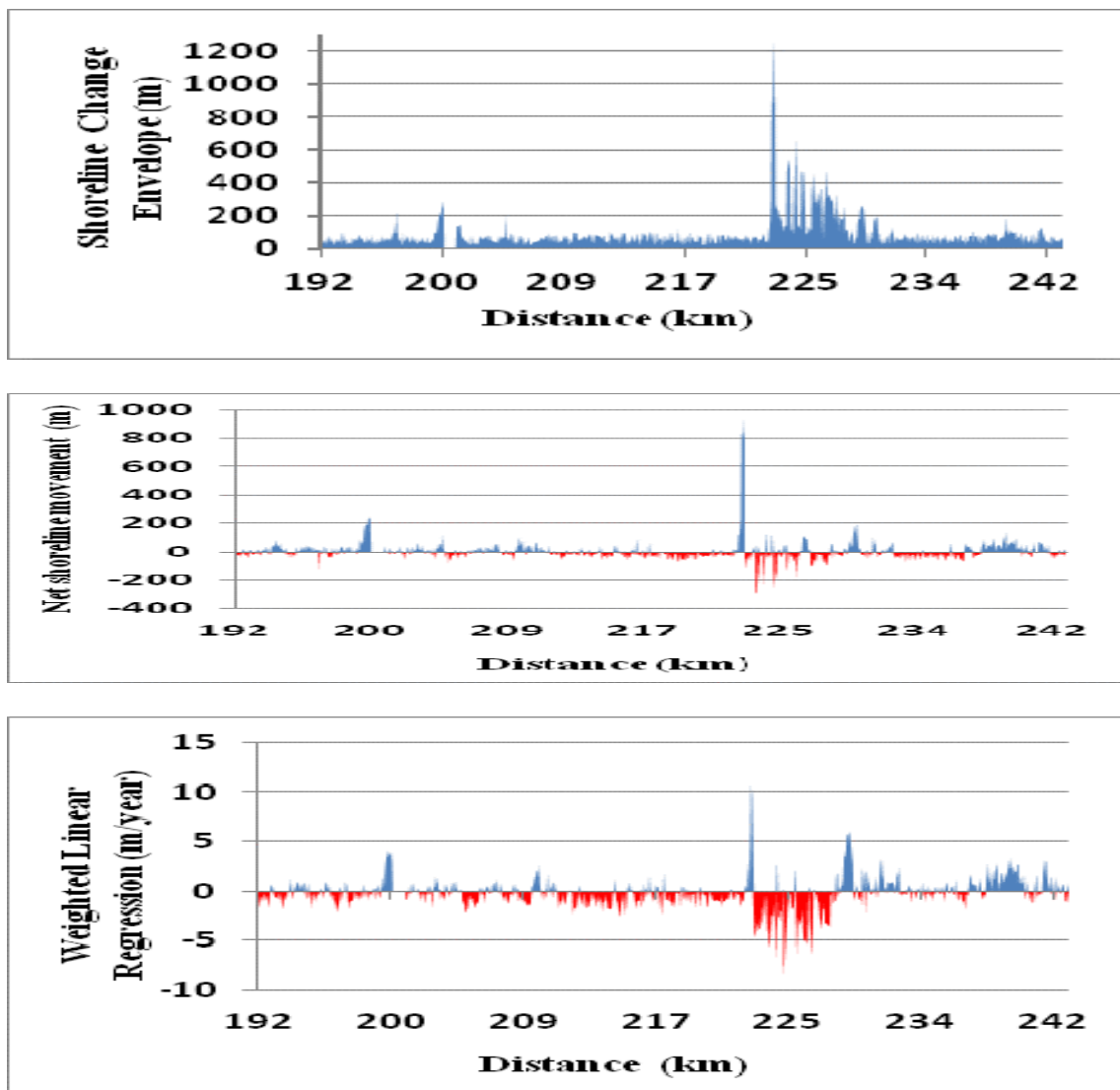


Figure 5.32. Spatial distribution of the statistical parameters (SCE, NSM, and WLR) by transect along the shoreline for the UA1-5 subarea (Sukhyi estuary – Great Adzhalyk estuary (Odessa bay)). Red – erosion. Blue – accretion

Table 5.20. Statistical characteristics of the shoreline dynamics in the UA1-5 Subarea.

Statistical characteristics	Shoreline dynamics indicators					
	Initial variant (1980-2020)			Corrected variant (1985-2020)		
	NSM (m)	SCE (m)	WLR (m/year)	NSM (m)	SCE (m)	WLR (m/year)
MEAN	0.60	88.24	-0.30	22.09	36.13	0.81
MIN	-298.85	19.37	-8.70	-25.54	0.00	-1.04
MAX	957.11	1254.77	10.87	161.70	225.41	5.64

Mean value of the SCE (m) decreased 2.4 times in 1985-2020 (Table 5.20) compared with 1980-2020 and the mean values of NSM (m) and WLR (m/year) increased 36.8 and 2.7 times respectively.

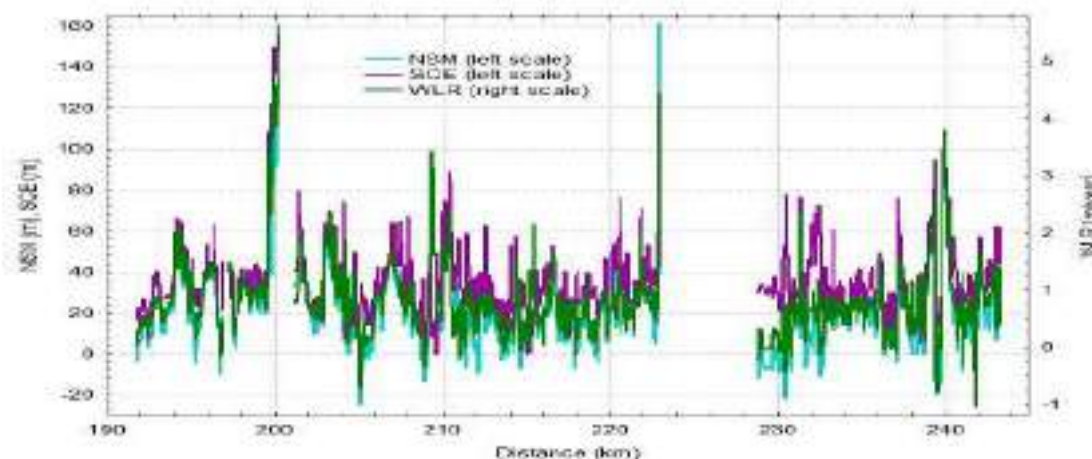


Fig. 5.33. Spatial distribution of the shoreline dynamics indicators in the UA1-5 Subarea.

A similar situation can be observed on the 223 km section, where the average long-term speed of the coastline movement is 2.5 m/year. This is also due to the discharge and natural accumulation of sediments flow from the side of the enclosing pier (the harbour pier, on which the Vorontsovskiy lighthouse is located) of the Odessa Port, where artificial mooring areas with berths have also been created. Significant shoreline accretion rate is observed in the areas of 209-210 km (1.5 - 3.4 m/year), 240 km (2.5 - 3.8 m/year), which can be explained by the influence of coastal protection works. The most significant rates of retreat of the shoreline towards the land are observed in sections 205 km and 239 km (from -0.5 to -0.8 m/year), which shows what was the dynamics before the coastal protection structures were built. Mean value of the SCE (m) decreased in 1985-2020 (Table 5.20) 2.4 times compared to 1980-2020 and the WLR (m/year) mean value changed its sign and increased its absolute value by 2.7 times. This evidences domination of erosion processes in the UA1-5 Subarea.

We have performed pilot assessments of the shoreline dynamics for the Chornomorsk area using the data of high-resolution (VHR) space images for 2019-2021 bought by the project from the Maxar company (Tables 3.6 and 3.7). The shoreline dynamics analysis for Chornomorsk city area (between 196.02 km and 197.4 km) was done using the DSAS, distance between transects was 10 m (Fig. 5.34).



Fig. 5.34. Scheme of the pilot plot in the UA1-5 Subarea, shoreline near city Chornomorsk.

The main characteristic feature of this pilot plot is the abrasion-landslide type of shore in the coastal zone of Chornomorsk where aggravation of situation with landslides is observed for the past decades. The shoreline dynamics indicators were determined from the results of high resolution space images automatic processing for the following dates: 13.07.2019, 28.03.2007, 20.04.2020 and 15.08.2021. Statistical analysis of the shoreline dynamics indicators (Fig. 5.35) shows that the shoreline dynamics rates vary within the range from -5.50 to 4.67 m/year with mean value of -0.46 m/year, which evidences that the shoreline regression is the prevailing tendency i.e. erosion processes dominate.

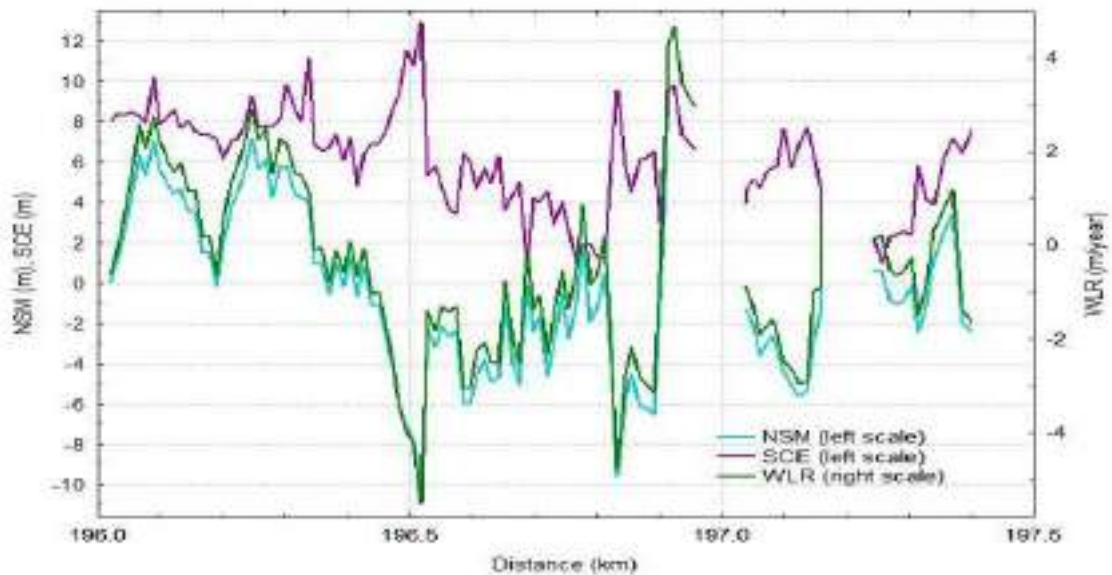


Fig. 5.35. Spatial distribution of the shoreline dynamics near city Chornomorsk according to the data from the high resolution Maxar space images.



The highest rate of shoreline retreat is observed in the central part of the plot in the area of 196.5 km and 196.8 km (-5.57 m/year and -4.76 m/year respectively). Shoreline retreat at the rate of up to -2.95 m/year is also taking place at 197.1 km within the marina area. The examples shown also demonstrate decrease in beaches width due to the active abrasion-landslide processes. The most significant values of the shoreline accretion (up to 4.67 m/year) are observed in the area of 196.9 km where discharge of sediments flow takes place on the southern side of the marina's fending groin i.e. accumulation processes prevail.

## References

- Akpınar, A., Bingölbali, B., Van Vledder, G. [2016]. Wind and wave characteristics in the Black Sea based on the SWAN wave model forced with the CFSR winds. *Ocean Eng.* 126, 276—298, <http://dx.doi.org/10.1016/j.oceaneng.2016.09.026>.
- Akpınar, A., Kömürcü, M.İ. [2012]. Wave energy potential along the south-east coasts of the Black Sea. *Energy*, 42, 289–302.
- Aliyev K.A. [1997]. Water management problems of the Dniester // *Ecological and economical problems of the Dniester: Theses of report at Int. Sc. and Pract. Workshop (18-19 Sept. 1997. Odesa)*, P. 8-11. (In Ukrainian).
- Álvarez Fanjul E, Pascual Collar A, Pérez Gómez B, De Alfonso M, García Sotillo M, Staneva J, Clementi E, Grandi A, Zacharioudaki A, Korres G, Ravdas M, Renshaw R, Tinker J, Raudsepp U, Lagema P, Maljutenko I, Geyer G, Müller M, Çağlar Yumruktepe V. [2019]. Sea level, sea surface temperature and SWH extreme percentiles: combined analysis from model results and in situ observations, Section 2.7, p:31. In: Schuckmann K, Le Traon P-Y, Smith N, Pascual A, Djavidnia S, Gattuso J-P, Grégoire M, Nolan G, et al. Copernicus Marine Service Ocean State Report, Issue 3, *Journal of Operational Oceanography*, 12:sup1, S1-S123, DOI: 10.1080/1755876X.2019.1633075
- Andrianova O.R., Belevich R.R., Peychev V., Skipa M.I. [2017]. Dynamics of shore and level of the Black Sea in the XX and XXI centuries / *Geophysical Journal № 3, V. 39, P 3-14.* (In Russian).
- ArcGIS Desktop [2021]. ArcMap - <https://desktop.arcgis.com/ru/arcmap/> . 24.06.2021
- Arheimer, B., Lindström, G., & Olsson, J. [2011]. A systematic review of sensitivities in the Swedish flood-forecasting system. *Atmospheric Research*, 100 (2-3), 275-284.
- Asch, K. [2003]. The 1:5 Million International Geological Map of Europe and Adjacent Areas: Development and Implementation of a GIS-enabled Concept. *Geologisches Jahrbuch, SA 3, BGR, Hannover (ed.)*, Schweitzerbart (Stuttgart), 190 p., ISBN 978-3-510-95903-7.
- Atlas [2006]. Atlas of the Black Sea and Sea of Azov Nature Protection. Mitin L.I. (ed). Nauka, Saint Petersburg, 436 p. (in Russian).
- Avramets V.M. et al. [2007]. The report on geological survey, scale 1:200 000 in the North-Western part of the Black Sea Shelf. State Geological Survey service, Ukraine. (in Russian)
- Bauer E. [2001]. Interannual changes of the ocean wave variability in the North Atlantic and in the North Sea, *Climate Research*, 18, 63–69.
- Blatov A.S., Bulgakov N.P., Ivanov V.A., Kosarev A.N., Tuzhilkin V.S. [1984]. Variability of the Black Sea hydrophysical fields. L.: Gidrometeoizdat, 340 p. (In Russian).
- Bolshakov V.S. [1970]. Transformation of river waters in the Black Sea. Kyiv: Naukova Dumka, 328 p. (In Russian).
- Bondar C. [1989]. Trends in the evolution of the mean Black Sea level // *Meteorology and hydrology*, 19. No. 2. P. 23-28.
- Buongiorno Nardelli, B., Colella, S. Santoleri, R., Guarracino, M., Kholod, A. [2010]. A re-analysis of Black Sea surface temperature. *Journal of Marine Systems*, 79, Issues 1–2, 50-64, ISSN 0924-7963, <https://doi.org/10.1016/j.jmarsys.2009.07.001>.



- Byelokopytov V.N. [2004]. Thermohaline and hydrological-acoustic structure of the Black Sea waters // Author's abstract of PhD theses (Geography). - MHI NASU, Sevastopol, 24 p. (In Russian).
- Capet, A., Barth, A., Beckers, J. M., & Marilaure, G. [2012]. Interannual variability of Black Sea's hydrodynamics and connection to atmospheric patterns. *Deep Sea Research Part II: Topical Studies in Oceanography*, 77, 128-142. <https://doi.org/10.1016/j.dsr2.2012.04.010>
- Cherkez E. , Shatalin S. , Shmuratko V., Pavlik T. , Medinets V. [2013] . The North-Western Part of the Black Sea Coasts Changes. Abstract Book of the 4-th Bi-annual Black Sea Scientific Conference, (28-31 October, 2013, Constanta, Romania). Constanta, P. 154-155. <http://dspace.onu.edu.ua:8080/handle/123456789/4046> )
- Cherkez E., Pavlik T., Medinets V., Gazyetov Ye, Shatalin S., Shmuratko V. [2014]. Dynamic of coasts line changes in the Black Sea North-Western part for past 30 years. Abstract Book of the PERSEUS Scientific Workshop, (27-30 January, 2014, Athens, Greece). Athens, P. 55.
- Cherkez E., Shatalin S., Shmuratko V., Pavlik T., Medinets V. [2013]. The North-Western part of the Black Sea coasts changes. In abstract book of 4<sup>th</sup> *Black Sea Scientific Conference - Black Sea - Challenges Towards Good Environmental Status*, Odesa, Ukraine, 154-156.
- Cherkez E.A. [1996]. Geological and structural-tectonic factors of landslides formation and development of the North-Western Black Sea coast. In K. Senneset (ed), *Landslides*. Balkema, Rotterdam, 509-513.
- Cherkez E.A., Dragomyretska O.V., Gorokhovich Y. [2006] Landslide protection of the historical heritage in Odesa (Ukraine). *Landslides*, 3(4), 303-309.
- Cherkez E.A., Medinets V.I., Pavlik T.V., Gazyetov Ye.I., Medinets S.V. and Kozlova T.V. [2020] Using of Landsat space images to study the dynamic of coastline changes in the Black Sea north-western part in 1983–2013. In Conference Proceedings, Geoinformatics: Theoretical and Applied Aspects 2020, May 2020, Volume 2020, P.1 – 5. DOI: <https://doi.org/10.3997/2214-4609.2020geo011>
- Cherkez E.A, Kozlova T.V., Shatalin S.N., Medinets V.I., Medinets S.V., Soltys I.E. [2021]. Landslides at the North-Western Black Sea Coast (Ukraine) and the Engineering & Geological Effectiveness of Landslide Prevention Works. In *Third EAGE Workshop on Assessment of Landslide Hazards and impact on communities 2021 (September 2021). European Association of Geoscientists & Engineers.* <https://doi.org/10.3997/2214-4609.202055005> <https://www.earthdoc.org/content/papers/10.3997/2214-4609.202055005>
- Cherkez E. A., Medinets V. I., Pavlik T. V., Gazyetov Ye. I., Medinets S. V. and Kozlova T. V. [2020]. Using of Landsat space images to study the dynamic of coastline changes in the Black Sea north-western part in 1983–2013. *European Association of Geoscientists & Engineers. Conference Proceedings, Geoinformatics: Theoretical and Applied Aspects 2020*, May 2020, Volume 2020, p.1 – 5. DOI: <https://doi.org/10.3997/2214-4609.2020geo011>
- Cherkez, E.A. and Shatalin, S. N. [2012] Regularities of landslides development within the Northern part Black sea Region. In: G.I. Rudko, V.A. Osiyuk (Eds) *Engineering geodynamics of Ukraine and Moldova (landslide geosystems)*, 2, 232–340. (in Russian).
- Cherkez, E.A., Medinets, V.I., Pavlik, T.V. et al. [2020] Using of Landsat space images to study the dynamic of coastline changes in the Black Sea north-western part in 1983–2013. In *Geoinformatics: Theoretical and Applied Aspects 2020* (May 2020). EAGE. <https://doi.org/10.3997/2214-4609.2020geo011>
- Coasts [1991]. / P. A. Kaplin, O. K. Leontyev, S. A. Lukyanova, L. G. Nikiforova. M.: Mysl, 479 p. (In Russian).
- Condego L. [2018]. Semi-Automatic Classification Plugin Documentation Release 6.0.1.1, Feb 10. DOI:[10.13140/RG.2.2.29474.02242/1](https://doi.org/10.13140/RG.2.2.29474.02242/1)
- Data [2018]. Data of Institute of Marine Biology of National Academy of Sciences of Ukraine (IMB). Accessed by: [www.imb.odessa.ua](http://www.imb.odessa.ua).
- Democritus University of Thrace [2021]. <https://duth.gr/> . 24.06.2021
- Deser, C., Alexander, M. A., Xie, S.-P., Phillips, A. S. [2010]. Sea Surface Temperature Variability: Patterns and Mechanisms. *Annual Review of Marine Science* 2010 2:1, 115-143. <https://doi.org/10.1146/annurev-marine-120408-151453>



- Dieng, H. B., Cazenave, A., Meyssignac, B., & Ablain, M. [2017]. New estimate of the current rate of sea level rise from a sea level budget approach, *Geophys. Res. Lett.*, 44. <https://doi.org/10.1002/2017GL073308>.
- Dnieper River Basin Management Plan in Belarus [2018]. Ministry of Natural Resources and Environmental Protection of Republic Belarus, European Union Water Initiative Plus (EUWI+). 111 p. (In Russian).
- Dolan, M. F. J. [2012]. Calculation of slope angle from bathymetry data using GIS - effects of computation algorithms, data resolution and analysis scale, NGU report. Geological Survey of Norway, Trondheim, Norway [accessed Sep 23 2021 at: <https://www.ngu.no/en/publikasjon/calculation-slope-angle-bathymetry-data-using-gis-effects-computation-algorithm-data>].
- Dotsenko, S.A., & Tuchkovenko, Yu.S. [2006]. Odessa region. Hydrology and water circulation. In book: North-Western Part of the Black Sea: Biology and Ecology, (. 445–451). Kyiv: Naukova Dumka [in Russian].
- DSAS [2018]. Digital Shoreline Analysis System (DSAS) Version 5.0 User Guide // Emily A. Himmelstoss, Rachel E. Henderson, Meredith G. Kratzmann, and Amy S. Farris / U.S. Geological Survey, Reston, Virginia. 126 p.: <https://pubs.usgs.gov/of/2018/1179/ofr20181179.pdf>
- DSAS [2021]. USGS Digital Shoreline Analysis System (DSAS) - [https://www.usgs.gov/centers/whcmssc/science/digital-shoreline-analysis-system-dsas?qt-science\\_center\\_objects=0#qt-science\\_center\\_objects](https://www.usgs.gov/centers/whcmssc/science/digital-shoreline-analysis-system-dsas?qt-science_center_objects=0#qt-science_center_objects) . 24.0.2021
- DUTH Report [2022]. DUTH Report on Dynamics of Coastal Line Changes Deliverable D.T1.2.1. PONTOS-GR (Greece) Nestos River, its Delta, and the coastal zone close to the Delta. 100 P.
- EHMS [1982]. Geology of the shelf of the Ukrainian SSR. Environment, history and methodology of studies / Ed. by. Shnyukov E.F. Kyiv: Naukova Dumka, 174 p. (In Russian).
- EOS [2021]. Earth observing system <https://eos.com/find-satellite/sentinel-2/>. 23.11.2021
- Freiberg E., Bellendir E., Golitsyn V., Ablyamitov N., Cherkez E., Tchujko E., Bich G. [2012] The Impact of Structural-Tectonic and Lithogenous Peculiarities of the Rock Mass on the Formation and Development of Geo-Deformation Processes. In *12<sup>th</sup> ISRM Congress - International Society for Rock Mechanics and Rock Engineering*, Beijing, China, 16-21 October 2011, ISRM-12CONGRESS-2011-374.
- Gazyetov Ye., Pavlik T., Medinets V., Cherkez E., Buniak O., Damalas A. [2015] Use of RS/GIS technology for mapping of coastline dynamics and fire r-traces in the Ukraine. In abstract book of *3<sup>rd</sup> International Conference on Remote Sensing and Geoinfromation of Environment RSCy2015*, Paphos, Cyprus, 16-19 March, 42.
- Gazyetov Ye.I., Dyatlov S.Ye. [2021]. Long-term salinity tendencies in coastal waters of Odessa region, Black Sea North-Western part. *Marine Ecological Journal*, v. 1. P. 23-33. Accessed by: <http://mej.od.ua/index.php/mej/article/view/340>
- Gazyetov, Ye. I. Andrianova, O. R., Medinets, V. I., Belevich, R. R., Morozov, V.N. [2015]. Assessment of the Danube River Influence on Some Hydrological Characteristics of the Northwestern Black Sea in 2004-2013, *Odessa National University Herald*, vol. 20, No. 4, P. 22-34.
- GCOS. Global Climate Observing System. [2010]. Update of the Implementation Plan for the Global Observing System for Climate in Support of the UNFCCC (GCO-138).
- GEBCO [2020]. Grid - General Bathymetric Chart of the Oceans (GEBCO) Portal. [accessed Nov 25 2021 at: <https://www.gebco.net/>]
- GEBCO [2020]. Grid map. Historical GEBCO data sets. Historical bathymetric grids. [https://www.gebco.net/data\\_and\\_products/gridded\\_bathymetry\\_data/gebco\\_2020/](https://www.gebco.net/data_and_products/gridded_bathymetry_data/gebco_2020/) or [https://www.gebco.net/data\\_and\\_products/historical\\_data\\_sets/#gebco\\_2020](https://www.gebco.net/data_and_products/historical_data_sets/#gebco_2020)
- Ginzburg, A. I.; Kostianoy, A. G.; Sheremet, N. A. [2004]. Seasonal and interannual variability of the Black Sea surface temperature as revealed from satellite data (1982–2000), *Journal of Marine Systems*, 52, 33-50. <https://doi.org/10.1016/j.jmarsys.2004.05.002>.
- González-Marco D, Sierra J P, Ybarra O F, Sánchez-Arcilla A. [2008]. Implications of long waves in harbor management: The Gijón port case study. *Ocean & Coastal Management*, 51, 180-201. doi:10.1016/j.ocecoaman.2007.04.001.



- Goryachkin Yu.N., Ivanov V.A. [1996]. Modern changes of the Black Sea level // *Water Resources*. 23, No.2. P. 246-248. (In Russian).
- Goryachkin Yu.N., Ivanov V.A. [2006]. Level of the Black Sea: past, present and future. Sevastopol : EKOSI-Gidrofizika, 210 p. (In Russian).
- Gregorio, A. D., Jansen, L. J. M. [2000]. Land cover classification system (LCSS): classification concepts and user manual for software, v. 1.0. FAO Land and Water Development Division, ISBN 92-5-104216-0 [accessed Sep 23 2021 at: <http://www.fao.org/3/x0596e/x0596e00.htm>]
- Grychulevych L. [2020] Annual report on the matters of water resources management in the Lower Danube sub-basin. Odesa: Basin Department of Water Resources Management in the Black Sea Area and the Lower Danube. 54 p. Accessed by: <https://oouvr.gov.ua/wp-content/uploads/2020/10/Річний-звіт-суббасейну-Нижнього-Дунаю.pdf> (In Ukrainian).
- Hansom, J. D. , Switser, A. D. and Pile, J. [2015]. Extreme waves: causes, characteristics, and impact on coastal environments and society. In: *Coastal and Marine Hazards, Risks, and Disasters*. Eds.: Ellis, J. T. and Sherman, D. J. Elsevier: Amsterdam, P. 307-334. ISBN 9780123964830 <https://doi.org/10.1016/B978-0-12-396483-0.00011-X>
- Hartmann DL, Klein Tank AMG, Rusticucci M, Alexander LV, Brönnimann S, Charabi Y, Dentener FJ, Dlugokencky EJ, Easterling DR, Kaplan A, Soden BJ, Thorne PW, Wild M, Zhai PM. [2013]. Observations: Atmosphere and Surface. In: *Climate Change 2013: The Physical Science Basis. Contribution of Working Group I to the Fifth Assessment Report of the Intergovernmental Panel on Climate Change*. Cambridge University Press, Cambridge, United Kingdom and New York, NY, USA.
- Hewit J E, Cummings V J, Elis J I, Funnell G, Norkko A, Talley T S, Thrush S.F. [2003]. The role of waves in the colonisation of terrestrial sediments deposited in the marine environment. *Journal of Experimental marine Biology and Ecology*, 290, 19-47, doi:10.1016/S0022-0981(03)00051-0.
- Himmelstoss, E.A., Henderson, R.E., Kratzmann, M.G., and Farris, A.S. [2021]. Digital Shoreline Analysis System (DSAS) version 5.1 user guide: U.S. Geological Survey Open-File Report 2021–1091, 104 p. <https://doi.org/10.3133/ofr20211091> <https://www.usgs.gov/centers/whcmssc/science/digital-shoreline-analysis-system-dsas>, <https://pubs.er.usgs.gov/publication/ofr20211091>
- Himmelstoss, E.A., Henderson, R.E., Kratzmann, M.G., and Farris, A.S. [2018]. Digital Shoreline Analysis System (DSAS) version 5.0 user guide: U.S. Geological Survey Open-File Report 2018–1179, 110 p., <https://doi.org/10.3133/ofr20181179>.
- Hydrological studies (Chapter 2) [2006]. // *Northwestern part of the Black Sea: Biology and ecology*. Kyiv: Naukova Dumka. P. 25–31. (In Russian).
- Hydrometeorology and hydrochemistry of seas of the USSR [1991]. / Ed. by F.S. Terziev. SPb.: Gidrometeoizdat. V. 4. Hydrometeorological conditions; Issue. 1. Black Sea. 430 p. (In Russian)
- HYPE [2021]. Swedish Hydrometeorological Institute HYPE database. Accessed by: <https://hypeweb.smhi.se>, 2021.
- Ignatov V.I. [2010]. Current knowledge on the coastal relief and the bottom of the Black Sea // *Herald of Moscow University. Series 5. Geography*. № 1. p. 56-63. (In Russian).
- Ilyin Yu. et al. [2012]. Hydrometeorological conditions of the Ukrainian seas. Vol. 2. The Black Sea, 421 p.
- IPCC [2019]. IPCC Special Report on the Ocean and Cryosphere in a Changing Climate /Pörtner, D.C. Roberts, V. Masson-Delmotte, P. Zhai, M. Tignor, E. Poloczanska, K. Mintenbeck, A. Alegría, M. Nicolai, A. Okem, J. Petzold, B. Rama, N.M. Weyer (eds.). In press.
- IPCC [2021]. *Climate Change 2021: The Physical Science Basis. Contribution of Working Group I to the Sixth Assessment Report of the Intergovernmental Panel on Climate Change* /V., P. Zhai, A. Pirani, S.L. Connors, C. Péan, S. Berger, N. Caud, Y. Chen, L. Goldfarb, M.I. Gomis, M. Huang, K. Leitzell, E. Lonnoy, J.B.R. Matthews, T.K. Maycock, T. Waterfield, O. Yelekçi, R. Yu, and B. Zhou (eds.). Cambridge University Press. In Press.





- Konikov E.G., Likhodedova O.G. [2010]. Global and regional factors of the Black Sea level variations as the basis for coastal zone geodynamic model // *Geology and Minerals of the World Ocean*. № 1. P. 84-93. (In Russian).
- Korak Saha; Zhao, Xuepeng; Zhang, Huai-min; Casey, Kenneth S.; Zhang, Dexin; Baker-Yeboah, Sheekela; Kilpatrick, Katherine A.; Evans, Robert H.; Ryan, Thomas; Relph, John M. [2018]. AVHRR Pathfinder version 5.3 level 3 collated (L3C) global 4km sea surface temperature for 1981-Present. NOAA National Centers for Environmental Information. Dataset. <https://doi.org/10.7289/v52j68xx>
- Korotaev, G. K., Saenko, O. A., & Koblinsky, C. J. [2001]. Satellite altimetry observations of the Black Sea level, *Journal of Geophysical Research*, 106, 917-933.
- Korotaev, G., Oguz, T., Nikiforov, A., Koblinsky, C. [2003]. Seasonal, interannual, and mesoscale variability of the Black Sea upper layer circulation derived from altimeter data, *Journal of Geophysical Research*, vol. 108, No. C4, 3122, doi:10.1029/2002JC001508.
- Krivoguz D., Semenova A., Mal'ko S. [2021]. Spatial analysis of seasonal patterns in sea surface temperature and salinity distribution in the Black Sea (1992-2017) / *IOP Conference Series: Earth and Environmental Science*, Volume 937, 032013. doi:10.1088/1755-1315/937/3/032013).
- Kubryakov A.A. and S.V. Stanichny. [2011]. Mean dynamic topography of the Black Sea, computed from altimetry, drifter measurements and hydrology data // *Ocean Science*. No7. P.745-753.
- Lappo S.S., Reva Yu.A. [1997]. Comparative analysis of long-period level variability in the Black and Caspian Seas // *Meteorology and hydrology*. No. 12. P. 63–75. (In Russian).
- Legeais J-F, K. von Schuckmann, A. Melet, A. Storto and B. Meyssignac [2018]. Sea Level, in Copernicus Marine Service Ocean State Report, Issue 2, *J Oper Oceanogr*, 11, S1, s13-s16, DOI: 10.1080/1755876X.2018.1489208.
- Lenôtre N., Thierry P., Batkowski D., Vermeersch F. [2004] The Coastal Erosion Layer. BRGM Report of EuroSION Project. 102 p. [accessed Dec 22 2021]. Available from: [https://www.google.com/url?sa=t&rct=j&q=&esrc=s&source=web&cd=&cad=rja&uact=8&ved=2ahUKEwiBkoTB\\_Pb0AhUWSPEDHQgRBpEQFnoECAkQAQ&url=https%3A%2F%2Fwww.eea.europa.eu%2Fdata-and-maps%2Fdata%2Fgeomorphology-geology-erosion-trends-and-coastal-defence-works%2Fcoastal-erosion-layer%2Fcoastal-erosion-layer%2Fdownload&usq=AOvVaw0IA-0JznrEQ4jrnBKBpEs8](https://www.google.com/url?sa=t&rct=j&q=&esrc=s&source=web&cd=&cad=rja&uact=8&ved=2ahUKEwiBkoTB_Pb0AhUWSPEDHQgRBpEQFnoECAkQAQ&url=https%3A%2F%2Fwww.eea.europa.eu%2Fdata-and-maps%2Fdata%2Fgeomorphology-geology-erosion-trends-and-coastal-defence-works%2Fcoastal-erosion-layer%2Fcoastal-erosion-layer%2Fdownload&usq=AOvVaw0IA-0JznrEQ4jrnBKBpEs8)
- Lindström, G., Pers, C., Rosberg, J., Strömquist, J., & Arheimer, B. [2010]. Development and testing of the HYPE (Hydrological Predictions for the Environment) water quality model for different spatial scales. *Hydrology research*, 41(3-4), 295-319.
- Longinov V.V. [1963]. Coastal zone dynamics of tideless seas. M.: Publisher of the USSR Acad. of Sci., 379 p. (In Russian).
- Luijendijk A., Hagenaars G., Ranasinghe R., Baart F., Donchyts G., Aarninkhof, S. [2018] The State of the World's Beaches. *Scientific Reports*, 8, 6641.
- McFeeters, S. K. [1996]. The use of the Normalized Difference Water Index (NDWI) in the delineation of open water features. *International Journal of Remote Sensing* 17(7), 1425-1432. DOI:10.1080/01431169608948714
- McFeeters, S. K. [1996]. The use of the Normalized Difference Water Index (NDWI) in the delineation of open water features. *International Journal of Remote Sensing* 17(7), 1425-1432. DOI:10.1080/01431169608948714
- Merchant, C. J., Embury, O., Bulgin, C. E., Block, T., Corlett, G. K., Fiedler, E., ... & Eastwood, S. [2019]. Satellite-based time-series of sea-surface temperature since 1981 for climate applications. *Scientific data*, 6(1), 1-18.
- MIW [2000]. Main indicators of water use in Ukraine for 1999. Kyiv, Issue 19. (In Ukrainian).
- MIW [2003]. Main indicators of water use in Ukraine for 2002. Kyiv, Issue 22. (In Ukrainian).
- Mulet S, Nardelli BB, Good S, Pisano A, Greiner E, Monier M. [2018]. Ocean temperature and salinity. In: Copernicus Marine Service Ocean State Report, Issue 2, *Journal of Operational Oceanography*, 11:sup1, Chap. 1.1, s5–s13, DOI: <https://doi.org/10.1080/1755876X.2018.1489208>



- Mulet, S., Buongiorno Nardelli, B., Good, S., Pisano, A., Greiner, E., Monier, M., Autret, E., Axell, L., Boberg, F., Ciliberti, S., Drévilion, M., Droghei, R., Embury, O., Gourrion, J., Høyer, J., Juza, M., Kennedy, J., Lemieux-Dudon, B., Peneva, E., Reid, R., Simoncelli, S., Storto, A., Tinker, J., Von Schuckmann, K., Wakelin, S. L. [2018]. Ocean temperature and salinity. In: Copernicus Marine Service Ocean State Report, Issue 2, Journal of Operational Oceanography, 11:sup1, s5–s13, DOI: 10.1080/1755876X.2018.1489208
- NC [1999]. Natural conditions of the Danube offshore area and the Zmiinyi Island: current state of the ecosystem / Ed. by V.A. Ivanov, S.V. Goshovskiy. Sevastopol: Marine hydrophysical institute of the NAS of Ukraine. 268 p. (In Russian).
- NR [2002]. The State of the Black Sea environment. National Report of Ukraine. 1996-2000. Odessa: Astroprint, 80 p. [in Ukrainian]
- Oguz, T., Latun, V. S., Latif, M. A., Vladimirov, V. V., Sur, H. I., Makarov, A. A., Ozsoy, E., Kotovshchikov, B. B., Ereemeev, V., & Unluata, U. [1993] Circulation in the surface and intermediate layers of the Black Sea, Deep Sea Res., Part I, 40, 1597-1612.
- PCC [2013]. PCC 5th Assessment Report. The physical Science Basis. Contribution of Working Group I to the Fifth Assessment Report of the Intergovernmental Panel on Climate Change.
- PE [2021]. Planet Explorer <https://www.planet.com/explorer/>. 24.06.2021
- Peltier R. [2004]. Global glacial isostasy and the surface of the ice-age Earth: The ICE-5G (VM2) model and GRACE. Annual Review of Earth and Planetary Sciences (32:111-149).
- Pérez Gómez B., De Alfonso M., Zacharioudaki A., Pérez González I., Álvarez Fanjul E., Müller M., Marcos M., Manzano F., Korres G., Ravdas M., Tamm S. [2018]. Sea level, SST and waves: extremes variability. In: Copernicus Marine Service Ocean State Report, Issue 2, Journal of Operational Oceanography, 11:sup1, Chap. 3.1, s79–s88, DOI: <https://doi.org/10.1080/1755876X.2018.1489208>
- Pérez-Gómez B, Álvarez-Fanjul E, She J, Pérez-González I, Manzano F. [2016]. Extreme sea level events, Section 4.4, p:300. In: Von Schuckmann K, Le Traon PY, Alvarez-Fanjul E, Axell L, Balmaseda M, Breivik LA, Brewin RJW, Bricaud C, Drevillon M, Drillet Y, Dubois C, Embury O, Etienne H, García-Sotillo M, Garric G, Gasparin F, Gutknecht E, Guinehut S, Hernandez F, Juza M, Karlson B, Korres G, Legeais JF, Levier B, Lien VS, Morrow R, Notarstefano G, Parent L, Pascual A, Pérez-Gómez B, Perruche C, Pinardi N, Pisano A, Poulain PM, Pujol IM, Raj RP, Raudsepp U, Roquet H, Samuelsen A, Sathyendranath S, She J, Simoncelli S, Solidoro C, Tinker J, Tintoré J, Viktorsson L, Ablain M, Almroth-Rosell E, Bonaduce A, Clementi E, Cossarini G, Dagneaux Q, Desportes C, Dye S, Fratianni C, Good S, Greiner E, Gourrion J, Hamon M, Holt J, Hyder P, Kennedy J, Manzano-Muñoz F, Melet A, Meyssignac B, Mulet S, Nardelli BB, O’Dea E, Olason E, Paulmier A, Pérez-González I, Reid R, Racault MF, Raitos DE, Ramos A, Sykes P, Szekely T, Verbrugge N. The Copernicus Marine Environment Monitoring Service Ocean State Report, Journal of Operational Oceanography. 9 (sup2): 235-320. <http://dx.doi.org/10.1080/1755876X.2016.1273446>
- Pezzulli, S., Stephenson, D. B., Hannachi, A. [2005]. The Variability of Seasonality. J. Climate. 18:71–88. doi:10.1175/JCLI-3256.1.
- Podoplelov O.N., Karpov V.A., Ivanov V.G. et al. [1973–1975]. Report on geological survey 1:50,000 within northwestern part of the Black Sea. Krymgeologya, Odessa, Ukraine. (in Russian)
- Podrugina T.M. [1972]. To the matter of the Black Sea average levels variability // Transactions of Lab. of Southern Seas, State Oceanographic Institute. Issue 9. P. 3-10. (In Russian).
- Prandi, P., Meyssignac, B., Ablain, M. et al. [2021]. Local sea level trends, accelerations and uncertainties over 1993–2019. Sci Data 8, 1. <https://doi.org/10.1038/s41597-020-00786-7>
- Rokitskiy V.E. et al. [2020] Report on about the results of prospecting works for the gold in terigenous deposits of the North-Western Shelf of the Black Sea. [accessed Nov 28 2021]. Available from: [https://data.geus.dk/egdi/?mapname=egdi\\_emodnet\\_geology&showCustomLayers=true#baslay=baseMap\\_EEA\\_baseMapGEUS&optlay=&extent=5403820,2335640,5673580,2464480&layers=emodnet\\_mineral\\_o](https://data.geus.dk/egdi/?mapname=egdi_emodnet_geology&showCustomLayers=true#baslay=baseMap_EEA_baseMapGEUS&optlay=&extent=5403820,2335640,5673580,2464480&layers=emodnet_mineral_occurrences/)  
[ccurrences/](https://data.geus.dk/egdi/?mapname=egdi_emodnet_geology&showCustomLayers=true#baslay=baseMap_EEA_baseMapGEUS&optlay=&extent=5403820,2335640,5673580,2464480&layers=emodnet_mineral_occurrences/)



- Rokitskiy V.E. et al. [2020] Report on about the results of prospecting works for the gold in terigenous deposits of the North-Western Shelf of the Black Sea. [accessed Nov 28 2021]. Available from: [https://data.geus.dk/egdi/?mapname=egdi\\_emodnet\\_geology&showCustomLayers=true#baslay=baseMap\\_EEA\\_baseMapGEUS&optlay=&extent=5403820,2335640,5673580,2464480&layers=emodnet\\_mineral\\_o](https://data.geus.dk/egdi/?mapname=egdi_emodnet_geology&showCustomLayers=true#baslay=baseMap_EEA_baseMapGEUS&optlay=&extent=5403820,2335640,5673580,2464480&layers=emodnet_mineral_occurrences/)  
[ccurrences/](https://data.geus.dk/egdi/?mapname=egdi_emodnet_geology&showCustomLayers=true#baslay=baseMap_EEA_baseMapGEUS&optlay=&extent=5403820,2335640,5673580,2464480&layers=emodnet_mineral_o)
- Ropot V.M., Lupashku T.G., Sandy M.A. et al. [1997]. Hydrochemistry of the Dniester, problems of the Dniester water quality and use // Ecological and economical problems of the Dniester: Theses of report at Int. Sc. and Pract. Workshop (18-19 Sept. 1997. Odesa). P. 54-56. (In Russian).
- Roquet, H., Pisano, A., Embury, O. [2016]. Sea surface temperature. In: von Schuckmann et al. The Copernicus Marine Environment Monitoring Service Ocean State Report, Jour. Operational Ocean., vol. 9, suppl. 2. doi:10.1080/1755876X.2016.1273446.
- Rotar M.F. [1975]. Some regularities of exogenous processes development on the northwestern Black Sea coast // Geology of coast and bottom of the Black and Azov Seas within the Ukrainian SSR. Issue. 8. P. 97-108. (In Ukrainian).
- Safranov T.A, Chugay A.V., Cherkez E.A., Pedan G.S. et al. [2017] State and Quality of Environment in the Coastal Zone of the North-Western Black Sea. FOB Panov A.M., Chuguev, 300 p. (in Ukrainian).
- Sakalli A, Baştusta N. [2018]. Sea surface temperature change in the Black Sea under climate change: A simulation of the sea surface temperature up to 2100. International Journal of Climatology, 38(13), 4687-4698. <https://doi.org/10.1002/joc.5688>
- Savina H, Lefevre J-M, Josse P, Dandin P. [2003]. Definition of warning criteria. Proceedings of MAXWAVE Final Meeting, October 8-11, Geneva, Switzerland.
- Sen, P. K. [1968]. Estimates of the regression coefficient based on Kendall's tau. J Am Statist Assoc. 63:1379–1389.
- Shcherbakov F. A., Morgunov Yu. G. [1975]. The latest tectonics of the shelf of the North-Western part of the Black Sea / In book "Problems of shelf geology", Moscow: Science, 294 p. [in Russian]
- Shmuratko V.I. [2016]. Northwestern Black Sea shelf in Holocene: monograph / Odesa, ONU, 128 p. (In Russian).
- Shuiskiy Yu.D. [1989]. Exogenous processes in accumulative coasts development in the northwestern Black Sea [Text] / Yu. D. Shuiskiy, G. V. Vykhoanets. Moscow : Nedra, 198 p. (In Russian).
- Shuiskiy Yu.D. [2000]. Types of coasts of the World Ocean. Monograph. Odesa: Astroprint. 480 p. (In Ukrainian).
- Shuiskiy Yu.D. [2013]. Main issues of studies of the nature in the coastal zone of Ukrainian seas // Environmental Safety of Coastal and Shelf Zone and Integrated Management of Shelf Resources. Issue. 27. P. 341-352. (In Russian).
- Shuiskiy Yu.D., Rotar M.F. [1975] Abrasion and its Role in Accumulation of Sediments on the North-Western Coast of the Black Sea. In Geology of Coast and Bottom of the Black and Azov Seas within Ukrainian SSR, Issue 8, 58-66. (in Russian).
- Shuiskiy Yu.D., Vykhoanets G.V. [1989] Exogenic Processes of Accumulative Coast Development in the Black Sea North-Western Part. Nedra, Moscow, 198 p. (in Russian).
- Shuiskiy Yu.D., Vykhoanets G.V. [2009]. Maps of coast types and average abrasion and accumulation speed in 1960 – 1994 // Oceanographic Atlas of the Black and Azov Seas. – K: SD «Derzhgidrografiya». P.43-47. 356 p. (In Ukrainian).
- Sibirchenko M.G., Karpov V.A., Ivanov V.G. [1983]. Report on Lithological Study of the Black Sea Shelf for the Preparation of Geological-Lithological Map 1:200,000. Krymgeologia, Odessa, Ukraine, 150 p. (in Russian).
- Staneva J, Behrens A., Gayer G, Aouf A., [2019b]. Synergy between CMEMS products and newly available data from SENTINEL, Section 3.3, In: Schuckmann K, et al. 2019. Copernicus Marine Service Ocean State Report, Issue 3, Journal of Operational Oceanography, doi: 10.1080/1755876X.2019.1633075.
- Staneva, J. Behrens, A., Gayer G, Ricker M. [2019a]. Black sea CMEMS MYP QUID Report



- Staneva, J., Behrens, A. and Groll, N. [2014] Recent Advances in Wave Modelling, *Die Küste* 81/2014, 233 – 254
- Tătuți F., Pîrvan M., Popa M., Aydogan B., Ayat B., Görmüş T., Korzinin D., Văidianu N., Vespremeanu-Stroe A., Zăinescu F., Kuznetsov S., Preoteasa L., Shtremel M., Saprykina Y. [2019] The Black Sea coastline erosion: Index-based sensitivity assessment and management-related issues. *Ocean and Coastal Management*, 81, 104949.
- The state and quality of the natural environment of the coastal zone of the North-Western Black Sea Coast [2017] col. avt .; and. T.A. Safranov, A.V. Chugai, E.A. Cherkez, G.S. Pedan and others. for order. T.A. Safranov, A.V. Chugai. Chuguyev: FOB Panov AM, 300 p.
- Thieler, E. R., Himmelstoss, E. A., Zichichi, J. L., & Ergul, A. [2009]. The Digital Shoreline Analysis System (DSAS) version 4.0-an ArcGIS extension for calculating shoreline change (No. 2008-1278). US Geological Survey.
- Thieler, E. R., Himmelstoss, E. A., Zichichi, J. L., & Ergul, A. [2009]. The Digital Shoreline Analysis System (DSAS) version 4.0-an ArcGIS extension for calculating shoreline change (No. 2008-1278). US Geological Survey. <https://doi.org/10.3133/ofr20081278>,
- UNECE [2005]. Transboundary Diagnostic Study for the Dniester River Basin. Report on the Project «Transboundary Cooperation and Sustainable Management of the Dniester River Basin»: United Nations Economic Commission for Europe (UNECE) and Organization for Security and Co-operation in Europe (OSCE), 73 p. Accessed by: <https://www.osce.org/files/f/documents/4/4/38321.pdf> , 2021.
- USGS [2021a] – science for a changing world. Landsat 3. - [https://www.usgs.gov/core-science-systems/nli/landsat/landsat-3?qt-science\\_support\\_page\\_related\\_con=0#qt-science\\_support\\_page\\_related\\_con](https://www.usgs.gov/core-science-systems/nli/landsat/landsat-3?qt-science_support_page_related_con=0#qt-science_support_page_related_con) . 23.11.2021
- USGS [2021b] – science for a changing world. Landsat 4,5. - [https://www.usgs.gov/centers/eros/science/usgs-eros-archive-landsat-archives-landsat-4-5-thematic-mapper-tm-level-1-data?qt-science\\_center\\_objects=0#qt-science\\_center\\_objects](https://www.usgs.gov/centers/eros/science/usgs-eros-archive-landsat-archives-landsat-4-5-thematic-mapper-tm-level-1-data?qt-science_center_objects=0#qt-science_center_objects) . 23.11.2021
- USGS [2021c] – science for a changing world. Landsat 4. - [https://www.usgs.gov/core-science-systems/nli/landsat/landsat-4?qt-science\\_support\\_page\\_related\\_con=0#qt-science\\_support\\_page\\_related\\_con](https://www.usgs.gov/core-science-systems/nli/landsat/landsat-4?qt-science_support_page_related_con=0#qt-science_support_page_related_con) . 23.11.2021
- USGS [2021d] – science for a changing world. Landsat 5. - [https://www.usgs.gov/core-science-systems/nli/landsat/landsat-5?qt-science\\_support\\_page\\_related\\_con=0#qt-science\\_support\\_page\\_related\\_con](https://www.usgs.gov/core-science-systems/nli/landsat/landsat-5?qt-science_support_page_related_con=0#qt-science_support_page_related_con) . 23.11.2021
- USGS [2021e] – science for a changing world. Landsat 7. - [https://www.usgs.gov/core-science-systems/nli/landsat/landsat-7?qt-science\\_support\\_page\\_related\\_con=0#qt-science\\_support\\_page\\_related\\_con](https://www.usgs.gov/core-science-systems/nli/landsat/landsat-7?qt-science_support_page_related_con=0#qt-science_support_page_related_con) . 23.11.2021
- USGS 2 [2021]. USGS – science for a changing world - [https://www.usgs.gov/centers/eros/science/usgs-eros-archive-landsat-archives-landsat-4-5-thematic-mapper-tm-level-1-data?qt-science\\_center\\_objects=0#qt-science\\_center\\_objects](https://www.usgs.gov/centers/eros/science/usgs-eros-archive-landsat-archives-landsat-4-5-thematic-mapper-tm-level-1-data?qt-science_center_objects=0#qt-science_center_objects) . 23.11.2021
- USGS 3 [2021]. USGS – science for a changing world - [https://www.usgs.gov/core-science-systems/nli/landsat/landsat-5?qt-science\\_support\\_page\\_related\\_con=0#qt-science\\_support\\_page\\_related\\_con](https://www.usgs.gov/core-science-systems/nli/landsat/landsat-5?qt-science_support_page_related_con=0#qt-science_support_page_related_con) . 23.11.2021
- USGS 4 [2021]. USGS – science for a changing world - [https://www.usgs.gov/core-science-systems/nli/landsat/landsat-4?qt-science\\_support\\_page\\_related\\_con=0#qt-science\\_support\\_page\\_related\\_con](https://www.usgs.gov/core-science-systems/nli/landsat/landsat-4?qt-science_support_page_related_con=0#qt-science_support_page_related_con) . 23.11.2021
- USGS 5 [2021]. USGS – science for a changing world - [https://www.usgs.gov/core-science-systems/nli/landsat/landsat-7?qt-science\\_support\\_page\\_related\\_con=0#qt-science\\_support\\_page\\_related\\_con](https://www.usgs.gov/core-science-systems/nli/landsat/landsat-7?qt-science_support_page_related_con=0#qt-science_support_page_related_con) . 23.11.2021



- USGS Digital Shoreline Analysis System (DSAS) [2021] - [https://www.usgs.gov/centers/whcmssc/science/digital-shoreline-analysis-system-dsas?qt-science\\_center\\_objects=0#qt-science\\_center\\_objects](https://www.usgs.gov/centers/whcmssc/science/digital-shoreline-analysis-system-dsas?qt-science_center_objects=0#qt-science_center_objects) . 24.0.2021
- USGS Earth Explorer [2021] - <https://earthexplorer.usgs.gov/> .24.06.2021
- Vextractor [2021]. Raster to vector conversion tool -<https://www.vextrasoftware.com/>. 24.06.2021
- Vinogradov, K.A. Ed. [1967]. Biology of the north-western part of the Black Sea. Kiev: Naukova dumka Publ. 268pp. (in Russian)
- Vykhovanets G. V., Pankratenkova D. O. [2018]. Impact of anthropogenic factor on the contemporary state of accumulative relief forms in the northwestern Black Sea / ONU Herald. Series: Geography and Geology. V. 23, Issue. 1. P 11-29. (In Ukrainian).
- Zachopoulos K. [2020]. Training in shoreline change methodology. PONTOS training. 08-09 December 2020 - <https://drive.google.com/drive/folders/1-UDFyuT5maCPwQO6JUAuiciIrNI2E0O4>
- Zaitsev Yu et al. [2006]. North-western Black Sea: biology and ecology. Project. / Edited by: Yu.P.Zaitsev, B.G.Aleksandrov, G.G.Minicheva. Kiev, Naukova Dumka. (In Russian).
- Zelinskiy I.P., Korzhenevskiy B.A., Cherkez E.A. et al. [1993] Landslides of the Black Sea North-Western Coast, their studying and forecasting. Naukova Dumka, Kyiv, 228 p. (in Russian).
- Zenkovich V.P. [1958]. Coasts of the Black and Azov Seas. – M.: Geografiz, 373 p. (In Russian).
- Zenkovich V.P. [1960]. Morphology and dynamics of the Soviet Black Sea coasts. M.: Publisher of the USSR Acad. of Sci. V. 2. 215 p. (In Russian).